National Library of Canada
Acquisitions and Bibliographic Services
395 Wellington Street
Ottawa ON K1A 0N4
Canada

Bibliothèque nationale du Canada
Acquisitions et services bibliographiques
395, rue Wellington
Ottawa ON K1A 0N4
Canada

Your file Votre référence

Our file Notre référence

The author has granted a non-exclusive licence allowing the National Library of Canada to reproduce, loan, distribute or sell copies of this thesis in microform, paper or electronic formats.

L'auteur a accordé une licence non exclusive permettant à la Bibliothèque nationale du Canada de reproduire, prêter, distribuer ou vendre des copies de cette thèse sous la forme de microfiche/film, de reproduction sur papier ou sur format électronique.

The author retains ownership of the copyright in this thesis. Neither the thesis nor substantial extracts from it may be printed or otherwise reproduced without the author's permission.

L'auteur conserve la propriété du droit d'auteur qui protège cette thèse. Ni la thèse ni des extraits substantiels de celle-ci ne doivent être imprimés ou autrement reproduits sans son autorisation.

0-612-60293-1

Canada

UNIVERSITY OF ALBERTA

LIBRARY RELEASE FORM

NAME OF AUTHOR: Jianjun Jason Gu
TITLE OF THESIS: DESIGN, SENSING AND CONTROL OF A ROBOTIC PROSTHETIC EYE FOR NATURAL EYE MOVEMENT

DEGREE: Doctor of Philosophy
YEAR THIS DEGREE GRANTED: 2001

Permission is hereby granted to the UNIVERSITY OF ALBERTA LIBRARY to reproduce single copies of this thesis and to lend or sell such copies for private, scholarly or scientific research purposes only.

The author reserves all other publication rights and other rights in association with the copyright of the thesis, and except as hereinbefore provided neither the thesis nor any substantial portion thereof may be printed or otherwise reproduced in any material form whatever without the author's prior written permission.

(Signed) 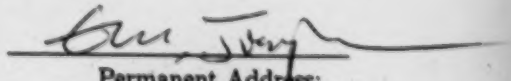

Permanent Address:
520k, Michener Park
Edmonton, Alberta
CANADA

Date: Jan 21st 2001

UNIVERSITY OF ALBERTA

FACULTY OF GRADUATE STUDIES AND RESEARCH

The undersigned certify that they have read, and recommend to the Faculty of Graduate Studies and Research for acceptance, a thesis entitled **DESIGN, SENSING AND CONTROL OF A ROBOTIC PROSTHETIC EYE FOR NATURAL EYE MOVEMENT** submitted by **Jianjun Jason Gu** in partial fulfillment of the requirements for the degree of Doctor of Philosophy.

Dr. Max Meng (Co-Supervisor)

Dr. Albert Cook (Co-Supervisor)

Dr. Tongwen Chen

Dr. Qing Zhao

Dr. Gary Faulkner

Dr. Hong Zhang

Dr. Wu-sheng Lu, External Examiner

Date: Jan. 29, 2001

Dedication

To my parents,

Who have provided me with the foundation

To my wife,

Who has shared my happiness and sadness

To my daughter,

Who brings the joys to our world

Abstract

Loss of an eye is a tragedy for a person, who may suffer psychologically and physically. This thesis is concerned with the design, sensing and control of a robotic prosthetic eye that moves horizontally in synchronization with the movement of the natural eye.

Two generations of robotic prosthetic eye models have been developed. The first generation model uses external infrared sensor array mounted on the frame of a pair of eye glasses to detect the natural eye movement and to feed the control system to drive the artificial eye to move with the natural eye. The second generation model removes the impractical usage of the eye glass frame mounted external sensors and instead uses the human brain EOG (electrooculargraph) signal picked up by electrodes placed on the sides of a person's head to carry out the same eye movement detection and control tasks as mentioned above.

Theoretical issues on sensor reliability, sensor failure detection and recovery, and signal processing techniques used in sensor data fusion are studied using statistical methods and artificial neural network based techniques.

In addition, practical control system design and implementation using micro controllers are studied and implemented to carry out the natural eye movement detection and artificial robotic eye control tasks. Simulation and experimental studies

are performed and the results are included to demonstrate the effectiveness of the thesis research project reported in this document.

Acknowledgements

I owe gratitude to many people for helping me complete this document and the work associated with it. I want to express my heartfelt gratitude to my supervisors - Dr. Max Meng and Dr. Albert Cook for their excellent and enthusiastic guidance during my thesis research. They have been a tremendous source of support during my stay here. Dr. Meng has provided me with the intellectual environment and theoretical guidance that have made the experience pleasurable. Dr. Cook provided me his technical guidance in biomedical engineering. Mere words cannot express the indebtedness and gratitude that I owe them.

I will thank Dr. Tongwen Chen, Dr. Gary Faulkner, Dr. Hong Zhang and Dr. Qing Zhao for their time and assistance while serving on my thesis committee. I also thank Dr. Wu-Sheng Lu for serving as the external examiner and offering expert suggestions.

Financial support from Dr. Meng and Dr. Cook in the form of research grant, and from the Department of Electrical and Computer Engineering in the form of Teaching Assistantship are also gratefully acknowledged.

I will thank Kees den Hartigh and Shaju Zacharia, for providing a second-to-none computing environment and thank Michelle Lock, Leena Vanhala, Carla De-Jager, Maureen Lebrecht and Carla Zittlau for their help with administrative matters.

I am also very grateful to those fellow students, who volunteered as subjects, who were always willing to offer their time and ideas. Special thanks go to Terry Blois and Narc who had spent hours to test the circuit with me during the data collection phases of this research.

A big thanks to my lab mates: Cheng Chen, Mike Yu Chen, Dave Erickson, Yan Liu, Peter Xiaoping Liu, James Andrew Smith, Dr. Dalong Wang, and others for providing an intellectually stimulating environment.

My friends Bob Cook and Phyllis, my former classmates Xiaoming Sheng and Donguang Li and their family have been very helpful at some crucial times - to them goes heartfelt thanks from me and my wife Lan.

Finally I would like to express my deep gratitude to my wonderful wife Lan for her longtime support and understanding, and sacrifice, and brother in-law Bin for his being very helpful. Last but not least, I will thank my daughter for bringing me lots of fun and happiness to my life.

Contents

1 Introduction 1

1.1 Overview of Eye Movement and Detection 2

1.1.1 Classification of the Eye Movement and Eye Blink 3

1.1.2 The Sensing Technologies of Eye Movement and Eye Blink . . 7

1.2 Objectives of the Thesis 25

1.2.1 Design Specifications 25

1.2.2 System Design and Implementation 26

1.2.3 Application Aspect 29

1.3 Contribution of This Thesis 29

1.3.1 Pioneering Robotic Eye System and Its Social Effect 29

1.3.2 The Online Calibration System 30

1.3.3 Real-time Eye Movement Detection and Analysis System . . . 30

1.3.4 Multisensor Fusion, Sensor Failure Detection and Fault Data Recovery 31

1.3.5 Motion Control of Robot Manipulators 31

1.4 Thesis Structure 31

2 A Simulation Study on Robotic Eye System 34

2.1 Introduction 34

2.1.1 History of the Artificial Eye 34

2.1.2 Previous Work 35

2.2 The Experimental System 36

2.3 Fusion Method 36

2.3.1 Dynamic Timing Window 39

2.3.2 Dynamic Polynomial Approach 40

2.3.3 Distance 41

2.3.4 Minimum Distance 42

2.3.5 Matching Detection 42

2.3.6 Model Matching 43

2.3.7 Simulations 44

2.4 Proposed Method 48

2.5 Conclusion 50

3 Neural Network Based Sensor Fusion and Fault Detection and Recovery in Robotic Eye System 51

3.1 Introduction 51

3.2 Background 52

3.3 Neural Network Approach 53

3.3.1 Two Layer Neural Network 53

3.3.2 Learning of Neural Network 54

3.3.3 Sensor Fusion and Sensor Failure Detection 56

3.4 Experimental Study 56

3.4.1 Sensor Data Space Creation 56
3.4.2 Experimental Results for Fusion 58
3.4.3 Experimental Results for Fault Free Sensor Data 58
3.4.4 Experimental Results for Soft Sensor Failure 59
3.4.5 Experimental Results for Hard Sensor Failure 59
3.4.6 Experimental Results for Failure Detection and Recovery . . . 61
3.5 Conclusion 63

4 Electrooculography Based Robotic Eye System 64
4.1 Introduction 64
4.2 Background 65
4.3 The Experimental Components 66
4.3.1 Motor 66
4.3.2 ECG (Electrocardiography) Electrode
Biomedical Sensor 67
4.3.3 Artificial Eye Model 67
4.4 Using EOG to Detect the Eye Horizontal Movement 69
4.5 Experimental Results for EOG Eye Movement Detection 70
4.5.1 Health Research Ethics Approval 70
4.5.2 Sensor Placement 71
4.5.3 Two Eye and One Eye EOG Signal 73
4.6 Experimental Study with the Eye Movement and Motor Control . . . 76
4.7 Conclusions 81

5 Reliability of Multiple Sensors in Robotic Eye System 82
5.1 Introduction 82

5.2 Background 83
5.3 The Reliability Model of Multiple Types of Sensors 85
5.3.1 Cost Constraints in Redundancy Systems 87
5.3.2 Optimization Methods 88
5.4 Numerical Experiment 91
5.5 Conclusion 95

6 Using Multivariate Statistical Sensor Fusion Techniques in Robotic Eye System 97
6.1 Introduction 97
6.2 Background 98
6.3 Principal Component Analysis 99
6.3.1 Identifying the Optimal Dimension n 102
6.3.2 Online Monitoring 102
6.4 Sensor Fusion 104
6.5 Sensor Fault Detection 105
6.6 Fault Sensor Isolation 105
6.7 Error Data Recovering 107
6.7.1 LMS Method For The Sensor Data Estimation 107
6.7.2 Minimum Error Variance Method 107
6.8 Application of the Eye Movement Detection 110
6.8.1 System Under Normal Operation 111
6.8.2 System With Sensor Fault 114
6.8.3 Fault Sensor Recovery 117
6.9 Conclusion 118

7 Using FIR Median Hybrid Filters on Study of Eye Movements in Robotic Eye System 119

7.1 Introduction 119

7.2 Background 120

7.3 Median Filters and Improved Median Filters 122

7.3.1 Median Filters 122

7.3.2 FIR Median Hybrid Filter 122

7.3.3 Least Square Optimal Approach 123

7.3.4 Residual Smoothing 125

7.3.5 Linear-nonlinear Combinational Filters 126

7.4 Properties of the Median Filters 127

7.5 Experimental Study with the EOG 129

7.5.1 Using EOG to Detect the Eye Horizontal Movement 129

7.5.2 Using the Median Filter to Remove the Eye Blink from the Corrupted Signal 131

7.6 Conclusion 131

8 Fundamental Study of Robotic Motion Control for Robotic Eye System 133

8.1 Introduction 134

8.2 Partially Unknown Robot Manipulator Control 135

8.2.1 Model for Motion Control of Robot Manipulators 135

8.3 Simulation Study 136

8.3.1 Trajectory Generation 136

8.3.2 Using the Proposed Neural Network Controller to Control the Robot Under Uncertainty 137

8.3.3 The Comparison of Joint Dynamics With Other Controller . . 138
8.4 Conclusion 142

9 Conclusion and Future Work 143
9.1 Conclusion 143
9.2 Future Work 146

Bibliography 148

Appendix

List of Figures

Figure

1.1 The Patient Lost One of His Eyes (left) and Has It Replaced by the Ocular Implant(right) 1

1.2 Functional Arrangement of the Imaging Lenses 11

1.3 Eye Landmarks 16

1.4 Application of Eye Movements Detection Using CCD Image Sensor . 17

1.5 Video Camera Based Overview of Eye Movement Measurement System 18

1.6 ERICA Block Diagram 19

1.7 Schematic Diagram of the System 20

1.8 System Representation of Fatigue Measurement System 21

1.9 Arrangment of MI Element on the Glasses Frame 25

2.1 Use Sensor Array to Detect an Object 38

2.2 Modeling Matching Block Diagram 43

2.3 The Relationship Between the Number of the Sensors and the Minimum Distance in the Space 45

2.4 Modeling Matching 45

2.5 The Relationship Between Threshold and Error 46

2.6 Dynamic Polynomial Fit and Estimation 47
2.7 Block Diagram of the Control System 48
2.8 Eye Pit Model with Eyes 49
2.9 Eye Pit with Eyeglass and Eyes 49

3.1 Two Layer Neural Network 54
3.2 Supervised Learning 55
3.3 Fusion and Sensor Failure Detection 55
3.4 The Artificial Eye Model 56
3.5 The Eye Movement Record in Tracking Target 58
3.6 The Fusion Block Diagram 59
3.7 Fusion with Fault Free 60
3.8 Fusion with Soft Sensor Failure 60
3.9 Hard Sensor Failure without Failure Detection and Recovery 61
3.10 Failure Detection and Recovery 62

4.1 Light Servo Motor 66
4.2 ECG Electrodes 68
4.3 Artificial Eye Model 68
4.4 The Configurations of the Electrodes 72
4.5 The Baseline of EOG to Detect Eye Movement with Different Electrode Configurations 74
4.6 Using EOG to Detect One Eye and Two Eye Movement 75
4.7 Experimental Study with Subject 1 2 3 77
4.8 Experimental Study with Subject 4 5 6 78
4.9 Experimental Study with Subject 7 8 9 79

4.10 The Natural Eye Calibration Set Up 79
4.11 The Calibration Curve of EOG to Detect Eye Movement 80
4.12 The Eye Movement Detection and Ocular System Set Up 81

5.1 Relationship Between Number of Sensors and the Reliability 84
5.2 Three Types of Sensor Example 90
5.3 Relationship Between the Reliability and the Average Probability of Success 94
5.4 Linear Recursive Curve Fit 94
5.5 Q-Q Plot for Data in figure 3.4 96

6.1 Loading and Score Plot for Normal System 112
6.2 SPE Test 112
6.3 Loading and Score Plot Under Sensor Fault 115
6.4 SPE Test Under Sensor Fault 115
6.5 Use Residual Structure to Isolate the Fault 116
6.6 SPE Test Under Hard Sensor Failure 117

7.1 General Structure of the FMH Filter 123
7.2 The Block Diagram of the Estimator 124
7.3 Linear-Nonlinear Combinational Filters 126
7.4 Output Variance Versus Filter window Length 128
7.5 Use Linear-Nonlinear Combinational Filters to Filter the Signal with and without Noise 128
7.6 Electrode Configuration 130
7.7 The Block Diagram of EOG Based Eye Movement Detection System . 130
7.8 Using the Median Filter to Remove the Eye Blink 131

8.1 A Typical Robot Control System with Uncertainties 134
8.2 Cartesian Space and Joint Space 137
8.3 The Error Dynamics of Off-Line Training 138
8.4 The Trajectory and Error Dynamics Using Neural Network Controller. The Left Panel Shows the Simulated Trajectory in Comparison with the Desired Trajectory. The Error Dynamics is shown in the Right Panel. 139
8.5 The Error Dynamics of Joint Angles Using a PD Controller 140
8.6 The Error Dynamics of Joint Angles Using a Computed Torque Controller with Exact Model (Left Panel) and Model Mismatch (Right Panel). 141
8.7 The Error Dynamics of Joint Angles Using an Adaptive Controller . . 142

List of Tables

Table

1.1 Table of Specification 26

2.1 Table of Relationship Between the Order of Polynomial and the Estimated Error 46

4.1 The Variance of the Data from Each Set of Configuration 73

5.1 The New Search Method 90

5.2 Table of Sensor Cost and Possibility of Success 91

5.3 Sensor Configuration Under Cost Limit 92

5.4 Difference Among the Methods 92

5.5 Efficiency of the Method 93

6.1 Eigenvalues of the Correlation Matrix 111

6.2 Desired Isolation Structure 113

6.3 Structure of the Faulty Sensors 114

6.4 Comparison Between Two Methods 118

Chapter 1

Introduction

The main objective of the thesis is to study the fundamental theory, practical implementation, and biological suitability associated with the design of an assistive device that will help patients who have eye-implants to have natural eye movement.

Figure 1.1: The Patient Lost One of His Eyes (left) and Has It Replaced by the Ocular Implant(right) (copyright of this figure was obtained from COMPRU)

A person with one eye lost, due to various causes, may suffer severely psychologically as well as physically. Patients with such problems may unwillingly withdraw

from society to avoid embarrassment and social inconvenience. Fortunately, COMPRU (Craniofacial Osseointegration and Maxillofacial Prosthetic Rehabilitation Unit) at Misericordia Hospital, in Edmonton, Alberta, Canada, can help the patients with ocular implants, as shown in figure 1 where that the patient lost an eye was pictured with and without an ocular implant. The prosthesis has been created by COMPRU to replace the lost eye. The prosthesis is an artificial eye, which appears natural. But it is static. The purpose of this thesis is to help these patients to have a natural movement of their artificial eye. In the proposed experimental device, a cosmetically artificial eye will be mounted onto a tiny servomotor. The sensor device detects the movement of the real eye and uses the real eye movement signal to control the artificial eye movement [1, 2]. This system is called a robotic eye system. The first step in this project is to detect the natural eye movement. In the next section, the eye movement detection techniques are thoroughly reviewed. The advantages and disadvantages of each detection method are presented. From these techniques, the most suitable sensing techniques for the robotic eye system are identified.

1.1 Overview of Eye Movement and Detection

From as early as the 1950's, many researchers have investigated the eye movements. Researchers and practitioners in psychology, education, clinical and basic medicine, and ophthalmology used measurement of human eye blink and eye movement. Application areas include human factors research, human performance evaluation, and human-machine interface [3]. Young [4, 5] described the major types of eye movement recording techniques and analyzed the advantages and disadvantages of each method. Recently, researchers are paying more attention to human-machine

interface design. Many novel devices and systems have been developed to help people who have disabilities. Due to the increasing frequency of traffic accidents and asthenopia (eyestrain) from the prolonged eye use, many researchers are interested in eye blink rate detection. The typical blinking speed is 12cm/sec. By analyzing the blink rate and the environment, it is possible to determine whether a person is tired and, if so, to provide a warning signal. This technique can also be used to monitor the physiological state of pilots. To understand various types of eye sensing methods, we need to understand all types of eye movements. Knowledge of the various types of eye movements will help to understand the eye movement sensing techniques.

1.1.1 Classification of the Eye Movement and Eye Blink

Types of eye movements are summarized by Young [4]. There are saccadic eye movements, pursuit or slow-tracking movements, compensatory eye movements, vergence eye movements, miniature eye movements, optokinetic nystagmus eye movements and torsional eye movements. Movements of the human eye can be divided into five categories: movements associated with the vestibule-ocular reflex, optokinetic movements, saccades, vergence movements, and miniature eye movements [6].

1.1.1.1 Vestibulo-Ocular Reflex

Vestibulo-ocular reflex eye movements occur in response to stimulation of the vestibular system [7, 8]. These movements are divided into two classes: static and dynamic responses to vestibular stimulation.

Static responses are produced by linear accelerations of the head. The static reflexes are very weak in humans. They can be observed in response to rotations about an anterior-posterior axis. The eyes respond to this stimulus by tilting their

anterior-posterior axes to maintain their former orientation in space with respect to the world coordinates. These eye movements are very small. The static vestibule-ocular reflex usually does not exceed 7 degrees of rotation.

Dynamic responses are produced by rotational accelerations of the head about a vertical axis. Movements of the eyes occur much more readily to rotation of the head than to static responses. While the head is rotating, the eyes rotate in the opposite direction, keeping the image of the outside world stationary on the retina. If the rotation is large enough the eye will exhibit nystagmus. That is, the eye alternates between rotating in a slow phase in the opposite direction of the head and rotating in a quick phase in an anti-compensatory direction to fixate on a new point in the visual field [6].

1.1.1.2 Vergence

Vergence eye movements are movements of the two eyes in opposite directions in order to fuse the image of near or far objects [9]. These movements reach maximum velocities of 10 degrees/sec over the range of nearly 15-degree.

The angle between the pupil centers and the object being observed depends on the distance to the object being viewed. To bring the object to the fovea of both eyes, the angle between the lines of sight become smaller for objects that are far away and larger for objects that are nearer. The distance from the eyes to an object is judged by the subject using a number of factors such as the amount of accommodation required for focusing, the disparity of images on the retina, and the known size of the object. The ability to control vergence eye movements varies from one person to another [7].

1.1.1.3 Visual Tracking

Visual tracking refers to the movements of the eyes that are made under visual guidance, and that hold an object of regard, and follow it when it moves [6, 10]. Visual tracking is also called tracking movements, optokinetic movements, slow pursuit or smooth pursuit. If the entire visual field is in motion, optokinetic nystagmus can be induced and is characterized by a slow phase to fixate on a point in the field and a fast phase to bring a new point of fixation to the fovea. Optokinetic movements and optokinetic nystagmus can be induced in both the horizontal and vertical dimensions. Smooth pursuit is distinct in origin from movements of the eye associated with the vestibulo-ocular reflex, but in most cases, it cannot be induced in the absence of an appropriate stimulus. It is not effective in tracking a target moving at greater than 30 degrees per second or oscillating faster than 1 cycle per second [7].

Optkinetic nystagmus, also known as "train nystagmus" is a characteristic saw tooth pattern of eye motion elicited by a moving visual field containing repeated patterns. Vestibular nystagmus is an oscillatory motion of the eye, similar in appearance to optokinetic nystagmus containing a slow phase and a fast saccadic-like return. Spontaneous nystagmus, or gaze nystagmus, is an abnormal nystagmus associated with a number of neurological disorders.

1.1.1.4 Saccades

Saccades are the fast movements of the eye that bring a new portion of the visual field to the fovea region [6, 11]. Saccadic eye movements are induced while reading or scanning a computer screen. They are voluntary in nature, but some involuntary movements of the eye are similar to saccades. Most naturally occurring saccades are smaller than 15 degrees [6]. Angular velocities during saccades can reach 1000

degrees per second during larger saccades. Large saccades are often accompanied by smaller and corrective saccades to compensate for inaccuracies in the ending point of the saccade. Saccades also occur to correct for the sluggish response of optokinetic movements to sudden changes in stimulus velocity, and bring the visual field back to the fovea.

Saccadic eye movements include the "jump and rest" fixation movements observed in scanning a visual scene or reading. They are characterized by very high initial acceleration and final deceleration (up to 40,000 deg/sec^2) and a peak velocity as high as 400 to 600 degrees/sec. The duration of the saccadic eye movement varies with its magnitude from 30 to 120 milliseconds. Pursuit, or slow-tracking movements are used to track slowly moving visual targets in the range of 1 to 30 degrees/sec. These movements are independent of the saccadic eye movements. Compensatory eye movements are smooth movements, closely related to pursuit movements, which compensate for active or passive motion of the head.

1.1.1.5 Miniature Eye Movements

According to Carpenter [6, 12], there are three types of miniature movements of the eye: tremor, drift and micro-saccades. Tremor has a bandwidth of around ninety-Hertz. It is centered between 150 and 200 Hertz and its magnitudes are generally below 25 seconds of arc. Drift has a velocity of around 1 minute of arc per second and amplitudes of 2 to 5 minutes of arc. Drift is normally terminated by a micro-saccade. Micro-saccades differ from saccades in that they are smaller (around 10 minutes of arc) and slower (around 10 degrees per second), and tend to be more random in direction and amplitude. Miniature eye movement or fixation movements are normally less than 1 degree in amplitude and occur during attempted steady fixation on a target.

And perception of an object on which the subject is fixating depends on the motion of the retinal image induced by these movements.

1.1.1.6 Eye Blink Movement

Eye blink is classified as endogenous eye blink, reflex eye blink, and voluntary eye blink [58]. The endogenous eye blink is defined as a cortically controlled response. It is distinguishable from other blinks by the absence of an identifiable eliciting stimulus. The reflex blink is a protective response that is induced to stimuli potentially injurious to the organism. The voluntary eye blink responds to an identifiable stimulus, either self-initiated or at the request of an experimenter. The spontaneous eye blink is one of physiological indices, which reflects human psychological process such as intention, concentration, anxiety, or arousal level [13].

1.1.2 The Sensing Technologies of Eye Movement and Eye Blink

For eye movement sensing, the following methods are used: electrodes, magnetic induction, optical sensing, photoelectric methods, infrared oculography(IROG), and video imaging.

1.1.2.1 Electrodes

There are many methods that do not measure the mechanical movement of the eyeball itself; rather they measure the induced potential, which cause the eye movement. These methods include the electro-oculograph signal sensing, electroretinogram sensing, electromyogram sensing, CRP signals detection and EMF detection.

The electro-oculograph (EOG) is a classical method used to detect horizontal and vertical eye movements [14, 15, 16, 17]. In the 1990's many researchers used the

EOG to detect eye movement [18, 174, 165, 190, 184, 182, 20, 21]. The method is briefly described as follows. Three surface electrodes are attached to each subject for this purpose, two at each outer edge of the eyes and one at the middle of the forehead. The EOG signal is amplified and recorded onto a magnetic tape for further processing by a mini-computer [14]. The eye movement recorded with the electro-oculogram has an accuracy of 1-degree [16].

In the EOG, a pair of electrodes is mounted above and below the eye, in close proximity to the eye. The electrodes are used to detect a voltage difference, which is proportional to the eye position relative to the electrodes. This pair measures the vertical eye position. Another set of electrodes is mounted to the left and right temples to measure horizontal motion. Detectable signal levels are about 500 microvolts for a 50-degree eye movement. There are several sources of noise, including neuro-muscular, encephalographic, and blink artifacts, as well as power line pickup. Proper placement of the electrodes is necessary in order to minimize cross coupling between vertical and horizontal signals and to obtain a consistent scale factor.

In electroretinogram [22, 23, 24, 25], miniature silver-silver chloride electrodes are applied to the skin surface near both canthi of one eye. The response recorded on the skin is identical in shape and latency to the electroretinogram recorded at the cornea. The amplitude of the surface-recorded ERG is about six percent of the corneal ERG. When the light stimulus is held constant, the peak-to-peak amplitude of the surface-recorded ERG b-wave is found to be: 1) Linearly proportional to the angular deviation of the eye about a vertical axis, and 2) Constant over time when the eye position is constant. The signal amplitude is about twenty microvolts; the electronic noise level is about 0.3 microvolts. A calibration curve must be obtained for the object. Nonlinearity of this curve is no longer a problem, since an inexpensive

microprocessor can easily convert the measured voltage amplitude to gaze angle using table look-up procedures.

The electromyogram (EMG) is used to record eye blinks bilaterally with two pairs of surface electromyogram (EMG) electrodes [26, 19, 27, 28, 29]. Electrodes are placed on the lower eyelids, over the palpebral part of the orbicularis oculi muscles. EMG activity from the orbicularis oculi of both eyes is recorded on the two channels of a portable biomedical tape recorder. The tapes are played back and analyzed. Long-term recording of normal human eye blink behavior (up to 14h continuously) showed a number of periodic trends in blink rate. Mean rates varied from 2 to 50 blinks/min and periods ranged from 10min to 2.5h.

Martin and others [30] described a passive, two-axis oculomotor detector to determine the eye position by measuring the charge distribution generated by the corneo-retinal potential (CRP) of the eye.

Two electrodes are placed near the eye in the horizontal plane, to detect the voltage, which results from the induced electromotive force (EMF) [31], in the eye orbit. The measured voltage is a function of the position of the eye in the horizontal plane. After amplification, the voltage is sampled by an A/D converter and then processed by software. The aim of their project is to help people who have disabilities, particularly those who have difficulties in speech due to brain damage, to express elementary needs, or to reach a suitable level of interaction with human or material environment. The accuracy of the detection is not available from the paper. But the detection can be used to activate the menu on the screen of a computer.

1.1.2.2 Magnetic Proximity Sensing

A small copper coil, incorporated into a contact lens, is worn by the subject who then sits in a magnetic field [32]. The current induced in the coil due to the angle with the field gives its orientation, and hence the use of a number of orthogonal fields will give positional information. Remmel gives the details about the electromagnetic eye movement monitor. Compared to electro-oculography, infrared reflection and pupil tracking; this monitor has very low noise, very low drift, good frequency response, and good linearity. With only three adjustments, the gain and horizontal and vertical angle offsets, this eye movement monitor offers unprecedented simplicity, resolution, and stability at an affordable cost. While this method offers highly accurate positional and temporal information, its disadvantages include the inflexibility of the experimental set-up, and the discomfort to the subject due to its invasive nature (allowing only around 30 minutes of recording time per session, and with some subjects reporting eye infections). Three Japanese researchers used this method to track eye movement in their stereoscopic display system project [33].

1.1.2.3 Optical Sensing

In optical sensing, one or two small infrared sources, together with detectors, are positioned close to the eye (e.g. on a spectacle frame). The sources are situated so that they shine on either side of the iris, on the boundary of the iris and the sclera (the white of the eye). The method works due to the different reflective properties of the iris compared with the sclera. When the eye moves to one side, less infrared light is reflected back to the detector on one side of the eye than the other. The signals can thus be calibrated for eye-movement. The advantage of the method is that it is relatively inexpensive. A major disadvantage of this method is that while reasonable

accuracy can be achieved in the horizontal direction, performance is severely compromised in the vertical direction. Set-up and alignment of the IR sources and detectors can also be a problem.

Fiber optic eye position sensing enables both horizontal and vertical eye position to be determined with respect to a pair of eye glass frames placed on a subject [36, 37, 34].

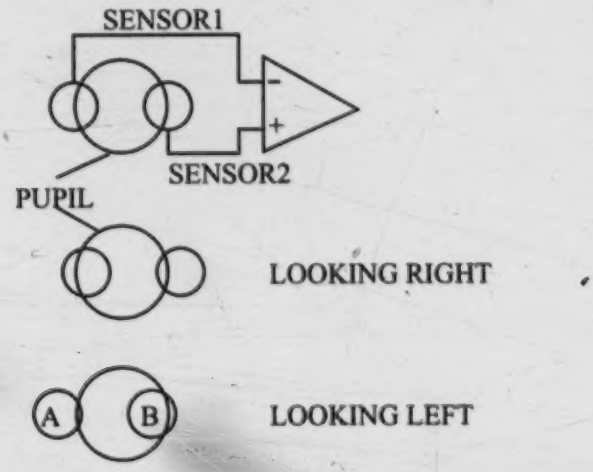

Figure 1.2: Functional Arrangement of the Imaging Lenses (from [35])

The imaging lenses are mounted on a pair of eyeglass frames around the field of vision. This allows normal eye movement and unobstructed vision. The optical sensors detect light reflected from left and right of the iris and send this light through optical fibers to remote detectors. The instrument can achieve accuracy of better than half a degree in the horizontal direction and three degree in the vertical direction. To accomplish this, two portions of the eye (A and B) are imaged as shown in the figure 1.2, and the reflected light from each is monitored [35]. When the subject looks straight ahead, the imaged areas of the iris and sclera (A and B) are equal.

When the subject looks right, the area of A will decrease and that of B will increase. The converse is true for looking left. The relationship between the amount of reflected light gathered by the imaging lenses and the degree to which the eye moves to either side is linear. By acquiring analog signals of the reflected light reaching the sensors, horizontal position of the subject's eye can be determined [36, 37]. The calibration of the eye position sensor is accomplished in a short time simply by aligning the imaging lenses. The fiber optic method has been used to study saccadic suppression, eye movement prediction, and visual acuity in a dynamic rather than static environment [38].

1.1.2.4 Photoelectric Methods

The photoelectric technique is applied to limbus. It is also called the limbus reflection technique. The limbus is defined as an annular transitional zone, approximately 1mm wide, between the cornea and the bulbar conjunctiva and sclera. It is highly vascular and involved in the metabolism of the cornea. The ratio between the dark iris and bright sclera observed on the left and right sides of the eye may either be measured directly with photo-sensors or directly on the image of the eye. The ratio is directly related to the horizontal position of the eye. The best wavelength for making the distinction between iris and sclera depends on the iris color [39]. In limbus reflection, a spot of light is imaged on the limbus, and the scattered light from it is detected by a nearby photocell. The amount of light reflected varies as described above, and this information is used to shift the position of the spot's source so that the limbus is continually tracked during eye-movements. The position of the source thus gives the relative position of the gaze. Though spatial accuracy is high, disadvantages include movements of the head being interpreted as eye-movements,

and the necessity for low ambient illumination.

Recording of eye movements requires mechanical and electronic stability, easy and nontraumatic application, non-contact with the eye, low cost, linear properties, a sufficiently wide dynamic measuring range and high spatial resolution. Limbus reflection methods seem to meet all the mentioned criteria [4]. They do not require a device touching the eye. In this method, infrared light emitting diodes and infrared sensitive detectors are positioned in front of the eye so that their 'receptive' fields match the iris/sclera transition, both on the nasal and on the temporal side. Upon horizontal rotation of the eye, for example in the case of abduction, the nasal detector detects iris reflection, while the temporally placed detector measures a decreased iris reflection. Subtraction of the nasal and temporal detector signals gives eye position with respect to head position [40]. The advantage of using two sensors instead of one is discussed by Matsuoka [41]. A sensor array is used to detect the eye movements by Reulen et al.[40]. Maximum IR-light emission of the LEDs is at a wavelength of 950nm. The detector array, with the same dimensions as the emitter array, is positioned above the LED array. In this arrangement, a given portion of radiant infrared-red light is constrained within a narrow beam-width, which covers a selected reflector area.

Practical realizations employ a pair of emitter/detector systems directed at opposite sides of the eye and amplify the difference between the detected signals as the eye moves. The use of a pair of emitter/detectors has been shown to improve the linearity of the system. Vertical eye movement can be measured if desired, by employing an additional pair of emitter/detectors mounted so that the line joining midpoints of the infrared beams is at right angles to the line joining the horizontal pair.

The advantages of the limbus reflection systems are that they are inexpensive, easy to use, not significantly interfering with the subject's field of vision and useful for measuring a wide range of horizontal eye movements. The disadvantage of the limbus reflection methods is that the head movement has a large effect on the output signal; it has been shown that a head movement of 1mm produces a signal equivalent to a horizontal movement of 12 degrees.

For the recording of purely horizontal or vertical eye movements, this system matches or nearly matches the magnetic induction (MI) systems as far as linearity, resolution and other basic properties are concerned. For the recording of oblique or torsional eye movements, the MI systems are superior. However, the invasive nature of the MI methods as well as other drawbacks (limited time of use, eye irritation, requires corneal anesthetic) make these methods far from ideal for clinical application. The work reported in [39] shows that the limbus reflection technique is capable of measuring horizontal eye movement with a resolution of better than 1 min of arc. Two papers use the limbus reflection technique to do research work in the area of eye movement [42, 43].

1.1.2.5 Video Imaging

Monitoring eye movement using video cameras has the advantage of not being intrusive, being inexpensive, and automated. The eye is imaged using CCD (Charged couple devices) cameras. Often, these cameras are sensitive to infrared light, and image by detecting illumination from banks of IR LEDs situated close to the subject's eyes. A computer then scans the image, and the boundary of the pupil is determined. This can be performed using either a threshold technique (picking up the difference in intensity of the image over the iris and the darker pupil, and then calculating the

best-fit circle for a number of these points) or a more complicated pattern recognition technique. More sophisticated systems will also pick up the reflection of a point of light on the cornea, and use this to adjust for inaccuracies brought about by small head movements. This method is able to track all eye movement parameters that are visible on the image, including pupil size and horizontal and vertical movements. The images may be videotaped for later re-analysis.

A video-based Eye-tracking system and a software package are used for the acquisition, analysis and plotting of eye movement [44]. There are many researchers using the image sensing methods to detect eye movements.

A miniature color field camera and very compact eye-movement sensors are attached to a translucent reinforced plastic goggle affording a wide view and excellent safety [45]. This device is developed to analyze the displacement of human lines-of-sight. Movements of the eyeballs are detected and converted into direct voltages corresponding to the rotation of eyeball in horizontal and vertical directions. In using the eye pointer, just as any other device of a similar nature, there is always a need to ensure first that the observer's line-of-sight and the location of the mark indicating the position of that line-of-sight on the eye pointer agree with each other. The calibration procedure is simple and effective. Asking the observer to gaze at a fixed point on a board, the researchers can perform the calibration. Then the position of the eyeballs at the time of gaze is computed. This calibration method can eliminate the trapezoidal and U-shaped distortions. Using a similar calibration method, a television camera senses the two-dimensional eye movement for tele-operator control [46].

As shown in figure 1.3, the human eye is potentially an ideal input device for tele-operator pointing and control applications due to the innate ability of the oculo-motor system to rapidly shift the eye's line of gaze in response to the operator's area

of interest. Calculating the visual point of regard as the tele-operator scans a video display and feeding back onto the display a reticule slaved to eye movements may allow an operator with minimal hand/eye coordination skills to designate potential targets within RPV imagery simply by looking at the desired target of interest. A

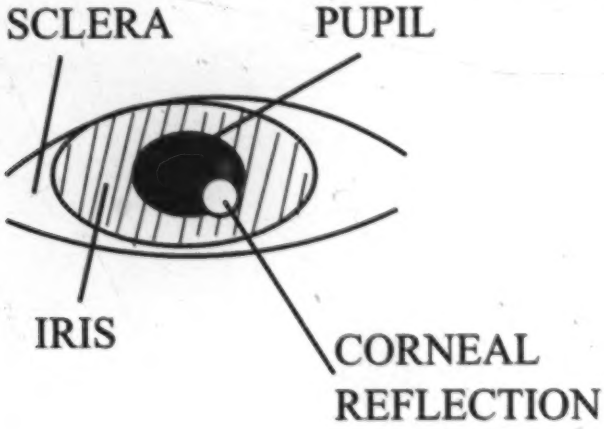

Figure 1.3: Eye Landmarks (from [47])

low-cost, automated, non-intrusive measurement and analysis system is designed for eye dynamics using a PC-based video image processor. Using the video recordings of the human face, the system is capable of measuring the time profiles of the duration, rate and velocity of eye blinks by automatically tracking the pupil, iris and the eyelid and measuring their positions and openings [47].

Blink frequencies, duration and latencies have been related to vigilance, drowsiness, and mental workload. An eye gaze system is designed for measuring eye blinks [48]. The Eye gaze system is a tool for measuring, recording, playing back, and analyzing what a person is doing with his eyes. A video camera located below the computer screen or below the workspace, if a computer monitor is not used, continu-

ally observes the participant's eye. Specialized image-processing software determines the eye orientation and projects the participant's gaze point. The system imposes no mechanical constraints on the participant, but requires a calibration procedure for each participant that takes less than 10 seconds [48].

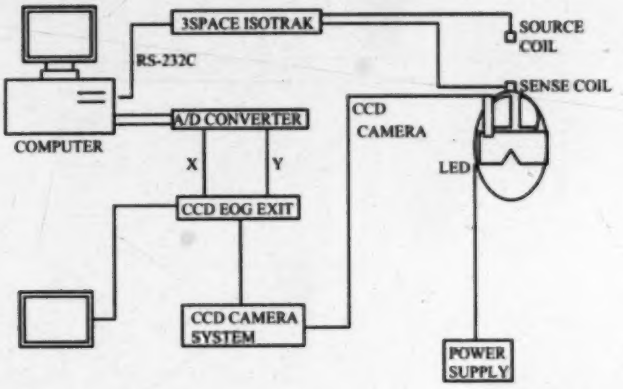

Figure 1.4: Application of Eye Movement Detection Using CCD Image Sensor (from [49])

Figure 1.4 shows the apparatus composed of a CCD camera system, 3SPACE ISOTRAK, a personal computer, a headgear and a mask. The left figure shows the system diagram and the right side shows the application of the headgear and the mask. Calibration is not described in the paper. But if the mask is fixed on the head, the calibration procedure becomes easy. CCD image array sensor technology are applied to eye movement measurement [49]. Figure 1.5 shows the measurement system. The whole system includes a video camera, support hardware, video and signal processing electronics, an IBM compatible computer, data acquisition and signal processing software, and a light emitting diode target display. The error for the eye position estimate is less than 0.05 degree.

A computer-based video eye tracker to measure the eye movement in real-time

has been developed [50]. When viewed along the axis of gaze, the pupil is essentially a circle. If the subject then looks away from the axis (rotate the angle by theta), the pupil appears to the camera as an ellipse whose minor-axis along the direction of eye movement is equal to the major axis times the cosine of deflection angle. The new method measures the aspect ratio of the elliptical pupil, and the angle of inclination of the major axis. From these measurements, the axis of gaze in the coordinate system can be determined.

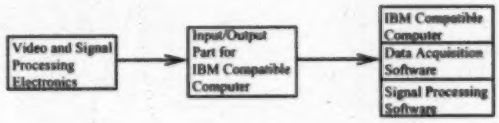
Video and Signal Processing Electronics
Input/Output Part for IBM Compatible Computer
IBM Compatible Computer
Data Acquisition Software
Signal Processing Software

Figure 1.5: Video Camera Based Overview of Eye Movement Measurement System (from [50])

An efficient approach for real-time eye feature tracking from a sequence of eye images has been proposed [3]. First a dynamic model for eye feature tracking is formulated, which relates the measurements from the eye model to the tracking parameters. The center of the iris is chosen as the tracking parameter vector and the gray level center of the eye is chosen as the measurement vector. A discrete Kalman filter is then constructed for the recursive estimation of the eye features, while taking into account of the measurement noise. The whole eye window is 75 pixels by 45 pixels and the tracking accuracy is approximately 0.25 pixels. The Kalman filter method [51] and statistical algorithm [52] are used to track eye movements. A maximum likelihood estimation technique tracks the location and size of pupil in a video image to find horizontal and vertical eye position. Many researchers use the video based eye movement measurement technique [53, 54, 55, 56].

Erica shown in figure 1.6 is a prosthetic device called the eye-gaze-response

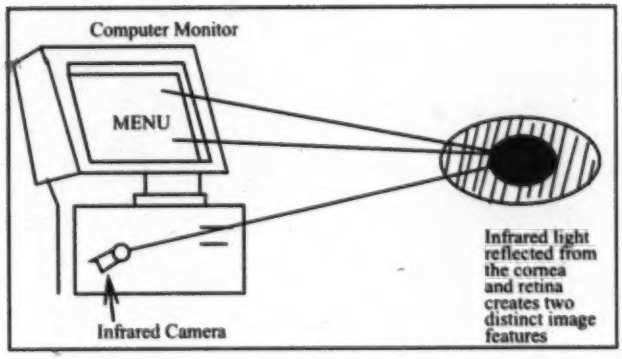
Computer Monitor
MENU
Infrared light reflected from the cornea and retina creates two distinct image features
Infrared Camera

Figure 1.6: ERICA Block Diagram (from [57])

interface computer aid [57] (It is equipped with eye imaging hardware and software, which automatically recorded a digital portrait of the user's eye. From the features of the current eye portrait, the interface calculates the approximate location of the user's eye gaze on the computer screen. Six or nine menu options are displayed on the computer monitor. The user made a selection by staring at the desired option for a short time that is pre-set to two or three seconds. In this way, the user could interact with the computer, run application software, and manage peripheral devices. The limit of this system is the small number of the menu on the screen, which is not large enough to present a full keyboard. Also head movement will cause the computer to lose the image of the eye. EHCI (eye-controlled human/computer interface) is an improved system [58]. It uses the line-of sight (LOS) and an intentional blink to invoke commands. Figure 1.7 shows the system diagram.

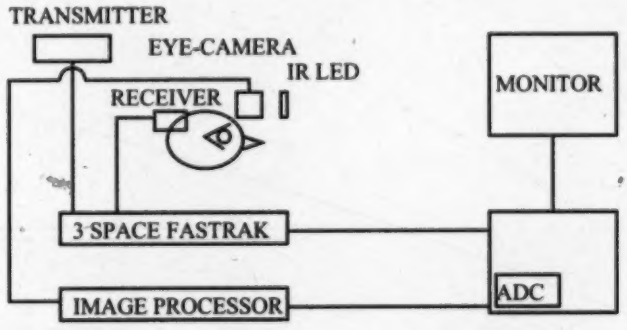

Figure 1.7: Schematic Diagram of the System (from [58])

A human must periodically blink to keep his/her eyes moist. Blinking is involuntary and fast. Eye blinking also provides very valuable information about the physical, physiological, and emotional aspects of the person [59, 60, 61]. Also there is a correlative relationship between eye blinking and head nodding, which throws

further light on the physical condition of the person such as the alertness, tiredness and fatigue [62]. Two parameters of the eye blink, blink rate and blink duration are used to assess workload [63]. The highest average blink rate is about 21 blinks per minute, the lowest approximately 7 per minute. A statistical study can be found in [64]. Vincent [65] designed a system to collect data on the subjects' eye blink, heart rate, head movement, etc to analyze on set of fatigue. The system diagram is in figure 1.8.

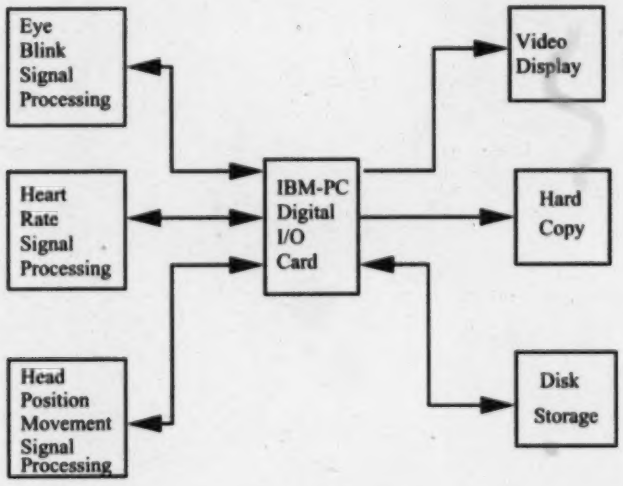

Figure 1.8: System Representation of Fatigue Measurement System (from [65])

Following are some references that deal with the eye blink.

1.1.2.6 Using Image Processing

Nakano et al [66] measure blinks using image processing and apply it to detect driver's drowsiness. Many traffic accidents are caused by drowsiness while driving. The purpose of research is to detect a driver's blinking using facial images obtained

by a TV camera and to estimate the driver's arousal level to prevent the occurrence of an accident due to drowsiness. The method can obtain the facial images, using infrared light sources, which are not affected much by the change of the ambient light by day and by night.

Tock [67] described a computer vision system for tracking the eyes of a car driver in order to measure the eyelid separation. This measurement is used as part of a larger system designed to detect when a car driver is becoming drowsy. The system runs unattended in a car. It does not interfere with the driver's normal driving actions and requires no cooperation from the driver. A color CCD camera is mounted behind the steering wheel of a car. It is connected to a Sun SparcStation 2 with a Datacell S2200 24-bit real time color frame grabber. The system is able to compute eyelid separation at frame rates, so that it can be recorded synchronously with the output of other in-vehicle sensors. The output from the system is a continuous measurement of eyelid separation. The same approach can be found in [68]. A small CCD camera is mounted in the vehicle instrument panel to capture images of the subject's face while driving. The system analyzes facial images of the driver to determine blinking behavior, which it uses as a measure of driver alertness. An accurate real-time drowsiness detector prototype is manufactured and tested in an actual vehicle. The testing shows that long blink duration becomes more frequent as the subject feels drowsy.

1.1.2.7 Using EEG Signals to Detect Eye Blinks

Gupta and Varner [69, 70] concentrated on real-time removal of eye-blink and eyeball movement artifacts from the forehead EEG recordings. A fixed band pass FIR filter is used to remove slow baseline drift. The average human eye blink rate is about 12 blinks/min. The eye blink signal can be obtained by using a low pass filter.

The center frequency is set to the eye blink frequency, about 10hz. Some experiments with eye blink movement have been carried out in the Advanced Research Control and Robotics lab at the Faculty of Rehabilitation Medicine of University of Alberta. The eye movements include eye open, eye close, blink both eyes with fast speed, blink both eyes with normal speed, and blink both eyes with slow speed. During the experiment the EEG signal from the subject was recorded. The low pass filter was used to process the raw data, and then band pass filter from 5hz to 10hz was used to obtain the eye movement data.

1.1.2.8 Eye Blink being Used in Human/Computer Interface

This system is setup for the people who have motor disabilities and have limited methods of adaptive control and means of communication and control, the majority of whom also suffer vocal impairments. Phillips and others developed switch to enable a severely physically limited person to access and operate a computer through switch closure [71]. The patient can use eye blink to activate the switch. Even more, Murphy [72] successfully developed a system called the blink-writer for patients with amyotrophic lateral sclerosis (ALS), those with strokes, and high spinal cord injury, and for a patient who was paralyzed as a result of having contracted bulbar polio. ALS causes a progressive degeneration of the nervous system, from which the patient gradually loses the ability for all voluntary muscular movement. However, some of the functions remain, such as cognitive, emotional and intellectual functioning. Sometimes these patients are referred to as "locked in". The blink-writer system overcomes these problems by automating the alphabet board process. The menu scheme and item scanning method used in blink-writer form the basis of the functional interface with the patient. Items are alternately highlighted on the screen and then the

highlight is extinguished. While an item is being highlighted, the system looks for a response from the patient. If none occurs within the preset time, the system moves to the next item in the sequence. In this way the patient can communicate with the outside world. The blink-writer has proven very effective in re-establishing limited communication capabilities for patients with severe neurological impairment, and also in giving them some control over their environment.

1.1.2.9 Magnetic Eyelid Movement Sensor

Takagi et al [73] constructed a displacement sensor for detection of eyelid movement, using amorphous wire magneto-inductive (MI) elements. The elements are formed from tension-annealed zero-magnetostriction amorphous wires. The MI effect and the symmetrical MI characteristics of the element are used to form thin sensor heads without coils. An amorphous displacement sensor in non-contact detection of the minute mechanical vibrations of both eyelids has been used. The minute magnets (three mm in diameter, 1mm thick) are fastened to the eyelids using double-backed tape, and a magnetic sensor head is fixed to the glass frame worn by the subject. Figure 1.9 shows the arrangement. Changes in magnetic field due to magnet displacement during eyelid vibrations are then detected from a distance of 10 mm or so by magnetic field sensors fastened to the nonmagnetic frame of glasses worn by the subject.

Jaschinski et al [74] investigated the possible effects of temporally modulated light stimulation near the critical fusion frequency (CFF) when subjects observe a cathode ray tube (CRT) operated at different refresh rates. In this experiment, a photodiode is mounted on the monitor that displayed the image of the eye next to the pupil at a position where the iris is imaged. Whenever the eyes close, the bright

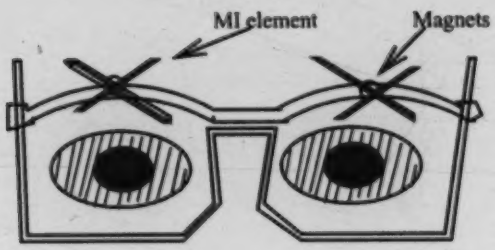

Figure 1.9: Arrangment of MI Element on the Glasses Frame (from [73])

image of the lid produced a signal in the photodiode, which is sampled at 20ms intervals. Based on the data, the duration of the eye blinks and the interval between blinks is evaluated. In order not to influence their spontaneous blinking, subjects are not informed that eye blinks are measured. The eye blink duration of individuals is from 71ms to 225ms, and the eye blink interval of individuals is from 1.55s to 11.01s.

1.2 Objectives of the Thesis

The thesis is to design an assistive device that will help patients with eye implants to have natural eye movement. The first part is the determination of design specifications. The second part is the system design and implementation. This includes the sensor and motor, the system setup and the system on-line calibration. The third part is the application of the system.

1.2.1 Design Specifications

The purpose of this thesis is to have the same movement in the artificial eye as in the natural eye. With the unaided eye, only large movements can be observed. Rotations of the eye through 1-degree are not noticeable [156]. That means the error

between the real eye position and the artificial eye position should be less than or equal to 1 degree. The resolution of the sensor used to measure the portion of the real eye and the artificial eye should also be less than one degree. The resolution of the motor movement should also be one degree. Different eye movements have different speeds. For visual tracking, the eye movement speed is less than 30 degrees per second, which means that the speed of the motor should be faster than 30 degrees per second to drive the artificial eye to move simultaneously with the real eye.

Specification Table	
Position error between two eyes	Less than 1-degree
Speed of motor	Less than 30 degrees/seconds
Resolution of the motor	Less than 1 degree

Table 1.1: Table of Specification

1.2.2 System Design and Implementation

The design phase includes the sensor and motor specification, the wireless communication between the sensor and the motor controller, the control algorithm, the final system experiment and the online calibration.

1.2.2.1 Sensor

What kinds of sensors to use to sense the eye movement is a key issue. From the review described before, we know that there are many classical methods and some advanced new techniques.

The constraint of the project limits the size of the sensor. By detailed review of the available sensing technologies, we finally decide to start with a tiny infrared sensor array, which is the first generation of our model. The subject may use eyeglass,

so some small devices and circuits may attach to the frame of the eyeglass without being noticed. The small sensors mounted on the eyeglasses will detect the movement of the real eye and the movement signal can be used to control the artificial eye movement. The eyeglass introduces the unstable factor of the system in the sense that the resolution will dramatically drop when there is a shift between the eyeglass and the head of the subject.

The standard clinical method of recording eye movements, such as electro-oculography and other electrode methods, has been used for a long time. Although it suffers from low resolution, drift and noise, the digital signal processing and other filter method can be used to overcome this drawback and this method can be used chronically. So the second-generation model of the robotic eye will be based on biomedical electrode sensing method.

1.2.2.2 Motor

The motor has to be put inside the eye socket. So we have to choose smaller and lighter ones. The light servo 3.5 motor from Germany we are currently using is the smallest and lightest motor we have found. It only weights 3.5 grams. The speed of the motor is very high. It only takes 0.2 second for the actuator to move from one end to the other end, on the other side, the gear will rotate about $14 \times 360 = 5040$ degrees. So the angular velocity of the motor is about $5040/0.2 = 2.5 \times 10000$ degree/seconds. The speed is higher than 1000 degree per second, so it is fast enough to simulate the eye movement.

1.2.2.3 Control Diagram and Algorithm

In order to design the system and minimize the circuit, the motor drive and control components are integrated into the eye socket model and miniaturized programmable electronics are required. We will use miniaturized CMOS micro-controllers called Pico micro-controller for the control part. This micro-controller is now available in surface technology and is one of the smallest controllers. Most of the Pico controllers have functions such as analogue data acquisition, counter/timers, real-time clocks, RS-232 micro-programmable serial communication and on-board storage in PROM.

The eye movement signals will be the input signal for our control loop. Because the artificial eye will be mounted to the motor, we can determine the artificial eye position signal from the motor. This will be the feedback signal of the control loop. The Pico controller is the kernel of the circuit. We can also connect it to the computer to do the simulation and analysis. The control program will be written and built into the memory of the Pico controller. We will start with the classical control algorithm such as PI, PD and PID to control the motor. Advanced control algorithms will also be developed and compared with each other.

1.2.2.4 Online Calibration of the Eye Movement

When we design an instrument, it must be calibrated. For the data obtained during an experimental procedure to be representative of the events being quantified, the measurement instrument must be calibrated and tested. To explore and quantify the performance of a measurement instrument, a known input must be applied to the measurement instrument, and then an output is measured. A transfer function can be derived for the measurement instrument. We need to calibrate our robotic

eye system. For horizontal eye movement detection, the user is asked to gaze at a fixed point on a board in front of him, then the position of the eyeballs at the time of gaze is computed. If we want higher resolution, then more points will be used for the patient to gaze at. In this way we can find the relationship between the eye position and the output signal. The relationship usually is not a linear curve. However this non-linearity of this curve is not a problem, since an inexpensive Pico microprocessor can easily convert the measured voltage amplitude to gaze angle using table look-up procedures or some other algorithms.

1.2.3 Application Aspect

When the whole system is ready, we will do the experiment with the real eye. Ethics approval will be obtained prior to the participation of any human subjects. The sensor will detect the subject's eye movement. The movement signal will be simulated on the screen. At the same time, the signal will be used to control the artificial eye model, so that the artificial eye and the real eye will move simultaneously.

The last stage of the project is to minimize the system size and mount the whole system into the patient's injured eye socket and do the experiment. During my Ph.D. study, we probably cannot do this. But I am sure that the advanced technology and the effort of the researchers will make the dream come into reality.

1.3 Contribution of This Thesis

1.3.1 Pioneering Robotic Eye System and Its Social Effect

Although there are many papers in the literature that describe the movement of the eye, they are all about the real eye. No paper describes the movement of an ocular

implant. This research will fill a major gap in this area. This is a piece of pioneering that develops a miniature robotic device to enable natural movement of an artificial eye implant using highly integrated circuit design and micro size components with efficient multi-sensor fusion and control algorithms. This project has attracted broad public attention recently. It was published on Robotics and Autonomous Systems magazine in 1999. It was reported in the July 29, 2000 issue of the New Scientist Magazine and the U of A Express News. It was featured on the front page of the Aug. 9th's 2000 the Globe and Mail, and on Aug. 9th 2000 evening TV news programs of CBC News iTV News, A-Channel News, CTV/CFRN News, and other TV and radio stations. Worldwide newspapers and media cited Reuters report on the study.

1.3.2 The Online Calibration System

Many researchers developed systems to detect the eye movement. For the system they designed, they have to do the calibration before they can use it. The calibration procedure is off-line. But in our research, we have to design an online calibration procedure, so that whenever the sensor slips or there is a reference change between the sensor and the eye, the system can automatically calibrate.

1.3.3 Real-time Eye Movement Detection and Analysis System

A real-time eye movement detection and analysis system is set up for the real eye movement detection and ocular implant control.

During the experiment, the real eye movement of the subject can be detected and the signal is sent to the micro controller to control the artificial eyeball to move simultaneously. The real eye movement signal, and the artificial eye movement signal will be transmitted to the computer through the RS232 port. All signals can be

displayed and analyzed by the computer. In this way we can detect the real eye movement and simulate the movements on the screen simultaneously.

1.3.4 Multisensor Fusion, Sensor Failure Detection and Fault Data Recovery

Sensor fusion is a key issue in many systems, especially in robotic systems. In this thesis a neural network based fusion method for sensor fusion of infrared reflection data to estimate the position of the eye is proposed. From the simulation, it can be observed that this network performs well in the situation when sensor noise and sensor failure occur.

1.3.5 Motion Control of Robot Manipulators

In this thesis a neural network controller is developed. It takes advantage of the manipulator regressor and the recursive error back propagation learning algorithm, it can dynamically control the robot to follow a desired trajectory.

The proposed neural network controller can be built into the robotic eye system to do the control.

1.4 Thesis Structure

The organization of this thesis is as follows.

Chapter 1 is an overview of existing eye movement detection technologies. This chapter derives the design objectives.

Chapter 2 develops an autonomous ocular motor system, so that the artificial eye can have more natural movement. Fusion method is proposed for eye movement

detection. First the eye movement is recorded and stored as sensed data space. Then during the experiment, the eye movement signal is obtained through the sensor array and through the matching rule and the eye position is obtained. The main part of this chapter deals with the experimental system, fusion technologies, and preliminary results.

Chapter 3 presents a neural network based approach for sensor fusion. An artificial neural network can learn the characteristics of a non-linear, non-modeled system through training samples. Then during the real application, the sensor signal can be used to feed the network and obtain the desired output. This approach has been used in the thesis to detect the eye movement.

Chapter 4 describes intelligent sensor and control system, the robotic eye system, which comprises biomedical electrodes and a micro controller. The system is intended to provide a rehabilitation ocular implant device that could be useful to some people with ocular implant. With the proposed device, the ocular implant can have the same natural movement as the normal eye. The basis for this system is the use of bioelectrical signals from the user's body. The system can acquire the dynamical eye orientation, which is sent to the micro controller to control the artificial eye to have the same orientation. The system is set up to carry out experimental study. Different configurations of the electrodes are explored and the best configuration is used to sense the eye movement and controls the artificial ocular. The ethics approval was obtained and the pilot study has demonstrated its potential for clinical applications.

Chapter 5 describes an approach that uses search algorithms to maximize sensor system reliability and minimize the sensor cost. Many search algorithms are used to determine the optimized solution. These include tabu search, genetic search, and simulated annealing. An improved search algorithm is also developed for this purpose.

The new algorithm is very efficient and can guarantee the optimal solution. Numeric examples are also included in this chapter.

In chapter 6, principal component analysis is used to monitor the eye movement sensor data and detect the sensor failure. Incidence matrix is used to isolate the fault sensor. LMS and minimum variance methods are used to recover the fault sensor data. Simulation studies using the recorded eye movement data are also included in the chapter.

Chapter 7 describes an approach of using FIR Median Hybrid Filters for the analysis of eye tracking movements. The filter can remove the eye blink artifact from the eye movement signal. The method based on electrooculograph (EOG) to determine the eye position is used. Because the EOG signal is always corrupted by the eye blink artifact, and the artifact must be filtered out. For this purpose, the FIR Median Hybrid Filter is studied in the chapter, and its properties are explored with examples. Finally the filter is used to deal with the real eye blink corrupted EOG signal. Examples are given of analysis procedure for eye tracking or a random moving target. The method proved to be highly reliable.

Chapter 8 addresses several techniques to control robot manipulators uncertainties. First a neural network is proposed to control the robot to follow the generated path. This network model is able to compensate the structured and unstructured dynamic uncertainties of the robot by using both on-line and off-line training. PD controller computed torque controller and adaptive controller with and without exact model are used to control the robot and compared with the proposed method. A simulation study is also included.

Chapter 9 wrap up with the conclusions and future directions.

Chapter 2

A Simulation Study on Robotic Eye System

2.1 Introduction

In this chapter, a simulation study on robotic eye system is described. Infrared sensor array is used to detect the eye movement. First the eye movement is detected by the sensor array and the sensor data is recorded and stored as sensor data space. Then during the simulation, the eye movement signal is obtained through the proposed fusion method. The simulation results and preliminary experimental results concerning the robotic prosthetic eye system are presented.

2.1.1 History of the Artificial Eye

There is a long history of artificial eyes, from antiquity to present [75, 76, 77]. Before the nineteenth century, artificial eyes were made of metal. They were expensive, heavy and painful to wear. Metal eyes were replaced by glass eyes at

the beginning of the nineteenth century. Ocular prostheses were created to replace the lost eye. Physically artificial eye appears natural, but it is static. Patients are generally not satisfied with a static artificial eye. Rather, they want the artificial eye to move like the natural eye. Several research groups have addressed this problem [78, 79, 80]. The most successful method was the hydroxyapatite orbital implant after enucleation. This method was designed to improve the motility of the prosthesis of the patients who had undergone enucleation. All the patients who had the mobile implant had better cosmetic results than those with static implants, and the small-degree motility of the prosthesis was excellent. Large-degree movement was not good, however.

2.1.2 Previous Work

The eye can rotate around any axis. A three-dimensional model can be used to describe the movement of the eye. The eye rotates from side to side around the x-axis. Rotation around the horizontal y-axis leads to eye movements that are directed upward or downward. Torsional eye movement occurs around the z-axis.

Three antagonistic pairs of muscles control natural eye movement: the lateral and medial recti, the superior and inferior oblique, and the superior and inferior recti.

Although all of the extra ocular muscles contribute to some degree to all eye movement by contracting or relaxing, only two muscles in any one plane determine each movement. For example, the lateral and medial recti are chiefly responsible for moving the eyes horizontally. Both the superior and inferior oblique and the superior and inferior recti can move the eye vertically as well as torsionally [81].

To provide the artificial eye with the same functionality as the natural eye, we mounted the artificial eye onto a tiny small servomotor. The aim of this chapter is to

describe the sensing of natural eye movement and control of the motor to drive the artificial eye simultaneously.

2.2 The Experimental System

A small servomotor was used to drive the artificial eye. A servomotor is controlled by pulse-modulated signal. The width of the pulse signifies to what position the shaft should turn.

The small infrared emitter array, which can easily be fitted to the eyeglass frame, is used. The emitter sends out an infrared light to illuminate the eye, and the reflected infrared light is detected by the detector array. Using the fusion algorithm described in the next section, the eye movement signal can be obtained.

2.3 Fusion Method

Due to the advantages of multiple sensor fusion in automatic target recognition, autonomous robot navigation, and automatic manufacturing, research on multisensor fusion has received increasing attention for the past years [82, 83, 84]. The fusion of a multisensor system involves more complicated algorithms in comparison with the single sensor. First, the sensors, which have been employed in a multisensor environment, include various types of sensors, such as video camera, tactile sensor, range finder, sonar, and torque sensor. To develop a coherent and efficient treatment of the information provided by many sensors and to allow for the sensor system reconfiguration are very important. Second, a number of fusion strategies, ranging from simple set intersection, logical operations, heuristic production rules, to more complex meth-

ods involving nonlinear least square fitting and maximum likelihood estimates, have been employed to combine the sensor outputs [84]. Finally, the multisensor system may introduce redundancy, which can be used to tolerate sensor failures and recover faulty sensor data [85].

The fusion algorithms and theories developed earlier can be roughly divided into three categories: statistical fusion algorithms [86, 87], neural network and fuzzy set based fusion [88, 89], and information theoretic fusion algorithms [90, 91]. Statistical fusion policies need the a priori knowledge about the observation process to make inference about identity. Algorithms of this type were developed using Bayesian theorem, Dempster-Shafer evidence theory, and adaptive decision theory. Neural network and fuzzy set based fusion policies are distribution free and no prior knowledge about the statistical distributions of the classes in the data source is needed in order to apply these methods for fusion. Information theoretic fusion policies make use of a transformation or mapping between parametric data and a resultant identity declaration. The techniques include expert systems, rule based and adaptive learning. Each of the above methods has been successful in dealing with certain problems associated with multisensor robot systems. But these methods have been developed based on some assumptions such as the representative training samples for the neural network and fuzzy set based fusion algorithm, model specification of data classes for the statistical fusion algorithms [92], and the knowledge about the information theoretic fusion algorithms.

In this chapter, a modeling sensor fusion approach is presented using the sensor array [93]. A linear array of photo diodes is used to receive the reflected lights from an object. Assume that the sensor data is binary. If a photo diode receives a reflection, its output is 1, otherwise the output is 0. Then we will have reflected data vector

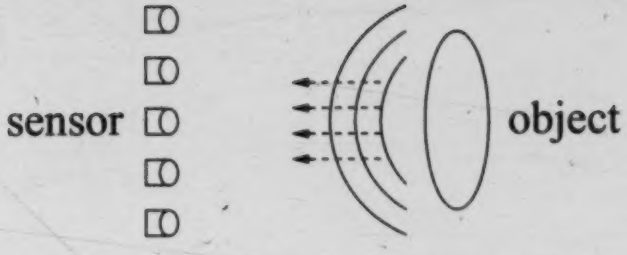

Figure 2.1: Use Sensor Array to Detect an Object

$V = [V_1, V_2, V_3, \ldots, V_m]$, where m is the dimension of the sensor.

$$V_i = \begin{cases} 0 & \text{non reflection} \\ 1 & \text{otherwise} \end{cases} \tag{2.1}$$

With this approach, the shape of the object cannot be obtained, but the information as whether the space is occupied by the object or not is gathered. This single algorithm can be used to detect an object. If the sensor is sonar, then the data can be used detect the distance between the sensor and the target. Let us assume that range data values are between 0 and 255. Then the reflected data structure is the same, except the value is different:

$$V_i = \begin{cases} 0 & \text{non reflection} \\ d_i & 0 < d_i < 255 \end{cases} \tag{2.2}$$

If the sensor is an infrared sensor, then it not only represents the distance between the object and the sensor, but also includes information about the surface color of the object. This property will be explored to detect the eye movement. The linear sensor array is used to detect infrared reflection from the eye. There are many methods for detecting the movement of an eye. The survey of eye movement recording methods can be found in Young's review [4]. The sensor measurement in this case is

different from an autonomous mobile robot. The mobile robot will always confront an uncertain environment. In the present case, the sensor here is always facing the natural eye, except when the eye is moving. For each specified position of the eye, there will be a corresponding output of the linear sensor array. In this way different eye positions are used to train the sensor. Eventually, a data space of eye position and the sensor data space will be obtained, using a matching method to find their relationship.

2.3.1 Dynamic Timing Window

When dealing with sensor data, the validation should be known and the next data point can be estimated. To determine sensor error and estimate the next sensor data point, a dynamic timing window is introduced. If the object property being observed is varying with respect to time, then the sensor data is also varying with respect to time. Current data and previous data are used to estimate the next data the sensor will get. In this way a dynamic timing window is introduced. Assume there are m sensors. Each sensor S_i, for $i = 1, 2, \ldots, m$ gives an output sample y_i. A timing window with n successive samples is used for each sensor, as shown below.

$$\begin{matrix} y_{11} & y_{12} & \cdots & y_{1n} \\ y_{21} & y_{22} & \cdots & y_{2n} \\ \vdots & \vdots & \vdots & \vdots \\ y_{m1} & y_{m2} & \cdots & y_{mn} \end{matrix} \tag{2.3}$$

Each column is the data for m sensors at the same sample time, and each row is the data for same sensor at successive sample times. How to use this $m \times n$ data to estimate the $(n+1)^{th}$ data for each sensor will be discussed in next the section.

2.3.2 Dynamic Polynomial Approach

When the sensor is used to explore the property of the object, the information obtained must be maximized. The object's property is changing with respect to time. A higher sample rate will be used to detect the object, so that the object property change is insignificant during the time interval. In this way, the data for each sensor is very smooth and can be approximated by a polynomial equation. Normally a polynomial equation can be expressed as follows:

$$f(t) = a_0 + a_1 t + a_2 t^2 + \ldots + a_n t^n \tag{2.4}$$

Where t is time, and $[a_0\ a_1\ \ldots\ a_n]$ denotes the coefficient vector. To determine the coefficients, $n+1$ equations are required. That means that if there are n equations, the $(n-1)$th order polynomial can be used to fit the data. Take the first row in the timing matrix $[y_{11}, y_{12}, \ldots, y_{1n}]$, assuming that the data are sampled at time $[t_1, t_2, \ldots, t_n]$ respectively. A least mean square algorithm is used to fit in the polynomial. For each time point t_i, there is the $f_i(t_i)$, and the sampled data y_{1i}. The mean square error for this curve fitting E_1 is

$$E_1 = \frac{1}{n-1} \sum_{i=1}^{n-1} [\sum_{j=0}^{n} a_j t^j - y_{1i}]^2 \tag{2.5}$$

Partial differentiation of E_1 with respect to $[a_0, a_1, \ldots, a_n]$ respectively, gives the n linear equations with the coefficients $[a_0, a_1, \ldots, a_n]$.

$$\begin{pmatrix} \sum_{i=1}^{n-1} 1 & \sum_{i=1}^{n-1} t_i & \cdots & \sum_{i=1}^{n-1} t_i^{n-1} \\ \sum_{i=1}^{n-1} t_i & \sum_{i=1}^{n-1} t_i^2 & \cdots & \sum_{i=1}^{n-1} t_i^n \\ \vdots & \vdots & \vdots & \vdots \\ \sum_{i=1}^{n-1} t_i^{n-1} & \sum_{i=1}^{n-1} t_i^n & \cdots & \sum_{i=1}^{n-1} t_i^{2n-2} \end{pmatrix} \begin{pmatrix} a_0 \\ a_1 \\ \vdots \\ a_{n-1} \end{pmatrix}$$

$$= \begin{pmatrix} \sum_{i=1}^{n-1} y_{1i} \\ \sum_{i=1}^{n-1} y_{1i} t_i \\ \vdots \\ \sum_{i=1}^{n-1} y_{1i} t_i^{n-1} \end{pmatrix} \tag{2.6}$$

2.3.3 Distance

Luo et al. [94, 96, 95] used the distance matrix to determine the corresponding relationships of the sensors to each other. Here a distance vector is introduced to determine the relationships of the next sensor data to the current one. The definition following is:

Assume vector

$$V_1 = [v_{11}, v_{12}, \ldots, v_{1m}], \tag{2.7}$$

and

$$V_2 = [v_{21}, v_{22}, \ldots, v_{2m}], \tag{2.8}$$

then the distance between these two vectors is defined as,

$$\begin{aligned} & d_{12} \\ & = (V_1 - V_2)^2 \\ & = \sum_{i=1}^{m} (v_{1i} - v_{2i})^2 \end{aligned} \tag{2.9}$$

2.3.4 Minimum Distance

For a data space which has n distinct vectors, there will be $n \times (n-1)$ distance vectors. A very important variable is the minimum of them. The definition is:

Assume space $S = [V_1, V_2, \ldots, V_n]$, V_i and V_j are two different vectors among the space. Then the distance between these two vectors is defined as, d_{ij}, according to the definition in (2.9)

The minimum is defined as:

$$d_{min} = min(d_{ij}), i, j = 1, 2, \ldots, n \text{ and } i \neq j \tag{2.10}$$

2.3.5 Matching Detection

The matching rule is shown in the following equation. First a threshold is chosen and then the distance between two vectors is calculated. Finally the distance is compared with the threshold. If the distance is less than the threshold, the two

vectors are said to be matching; otherwise, the two vectors are said to be not matching.

$$\begin{cases} D_i <= D_{tm} & \text{matching} \\ \\ D_i > D_{tm} & \text{no matching} \end{cases} \tag{2.11}$$

Where D_i stands for the distance between two vectors and D_tm stands for threshold constant.

2.3.6 Model Matching

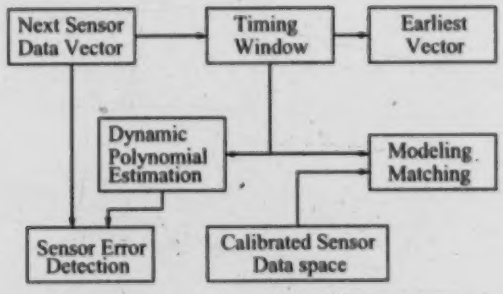

Figure 2.2: Modeling Matching Block Diagram

In our model matching approach, the timing window, the least-squares estimation of the parameters in the polynomial model, and the above matching rules are combined. As shown in the block diagram in figure 2.2, the timing window is always changing. The next sensor data vector comes into the timing window, as the earliest ones are popped out. The polynomial estimation is used to predict the next data, to detect the sensor error and correct it. The model-matching block uses the newest data vector data from the timing window to match the data in the calibrated sensor data space, and generates out an output close to the desired value.

2.3.7 Simulations

2.3.7.1 Initial Sensor Data Space Creation

A linear sensor array is used to detect the infrared reflection from the eye. Assume the real ideal model of eye. For each position of the eye, there is a corresponding output of the sensor. In this way the eye position data space and the sensor data space are generated. The minimum distance among the sensor data space is found and used as a criteria for matching purposes. So if the threshold is less than the minimum distance, it is guaranteed that there will not be more than two vectors matching the same vector. So the output is unique. Figure 2.3 shows the relationship between the number of sensors and the minimum distance in the sensor space. From simulation study, we found that with more sensors, the distance in the space data will be larger, and accordingly the space for the threshold will be larger. It can tolerate larger error. That is one of the reasons why multiple sensors are used.

2.3.7.2 Simulation Results for Matching

Figure 2.4 shows the simulation result for the matching. A sinusoidal eye target tracking signal is used here as the eye movement signal. The circle and the dot stand for the ideal position and real position respectively. The thresholds chosen for matching are 2 and 3 respectively. When the threshold equals to 2. Two vectors cannot find their matches. The reason is that the threshold is too small, and the error of the vector has some effect on it too. For threshold equals to 3, the match is good. The error amplitude is less than 1.5 degree..

Figure 2.5 shows the relationship between the threshold and the error. It is easy to see that if the threshold is too small, there will be only fewer matches and the error

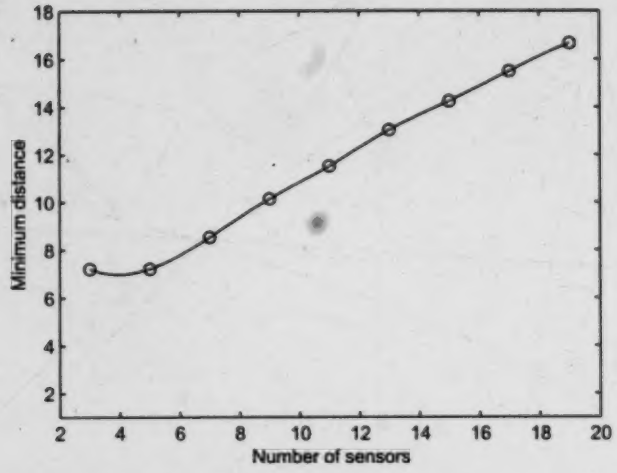

Figure 2.3: The Relationship Between the Number of the Sensors and the Minimum Distance in the Space

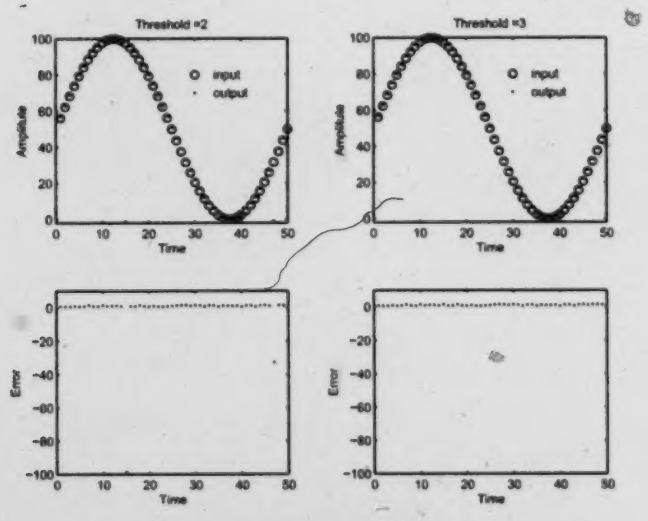

Figure 2.4: Modeling Matching

will be very large. If the threshold is too large, it will also induce wrong vectors. From the curve, an optimal threshold can be found for this situation. An optimal match will be achieved for this threshold. In this case the number of the sensors is 7.

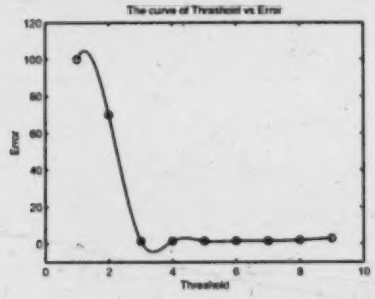

Figure 2.5: The Relationship Between Threshold and Error

2.3.7.3 Dynamic Estimation

Figure 2.6 shows the output of the sensor and estimated sensor output and the corresponding error. The circle and the dot stand for the ideal ones and estimated ones respectively. It is easy to see that recursive polynomial fit works very well for this case. With a polynomial of higher order, improved performance is achieved, as shown in table 2.1 (order means the order of the polynomial).

order	Error	
3	-0.1	0.1
4	-0.015	0.015
5	-1.5×10^{-3}	1.5×10^{-3}
6	-2×10^{-4}	2×10^{-4}
7	-2.5×10^{-5}	-2.5×10^{-5}

Table 2.1: Table of Relationship Between the Order of Polynomial and the Estimated Error

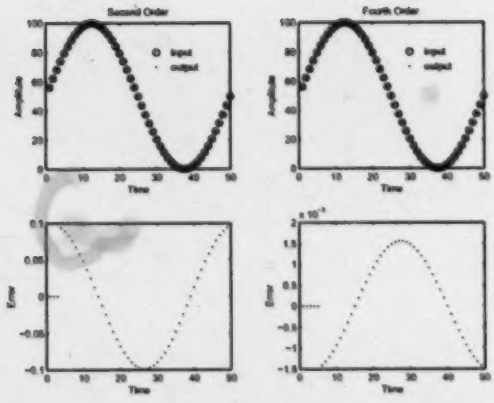

Figure 2.6: Dynamic Polynomial Fit and Estimation

2.4 Proposed Method

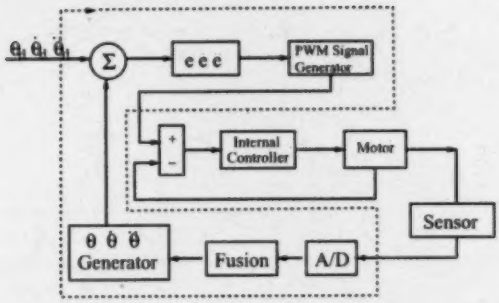

Figure 2.7: Block Diagram of the Control System

The aim of the project is to detect natural eye movement, and use the detected signal to control the movement of an artificial eye. A block diagram of the control system is shown in figure 2.7. The infrared sensor acquired the desired position angle of the natural eye. The desired angle, angular velocity and angular acceleration were generated as the input signals. In figure 2.7 the part enclosed by dashed line describes the micro controller. It obtains the feedback information from the motor and transfers the angle information signals. The error signal was formed to generate the PWM (pulse Width Modulation) signal for motor control. The motor then drives the ocular implant to the desired position. An eye pit model was used in the experiment. The pits of the model are in the same size as that of the real eye.

An eyeglass frame was mounted on the eye pit model. Two artificial eyeballs were mounted into the eye pits. One eyeball was used to simulate the real eye (right part of figure 2.8).

One eye ball can be rotated manually. The other eyeball was mounted on a motor, and then mounted into the eye pit (see the left part of figure 2.8). This eye

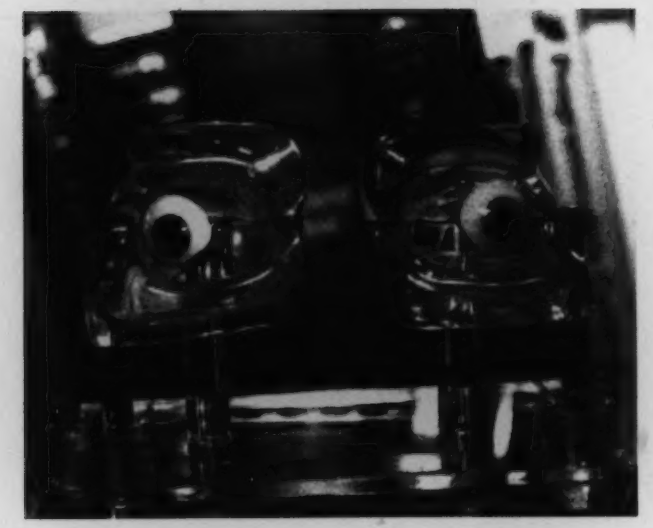

Figure 2.8: Eye Pit Model with Eyes

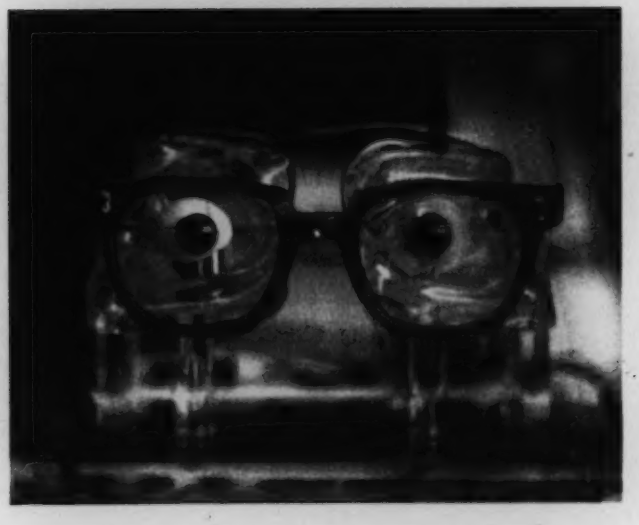

Figure 2.9: Eye Pit with Eyeglass and Eyes

simulates the artificial eye. The infrared emitter and detector were mounted onto the upper front eyeglass frame in front of the natural eye simulation (figure 2.9).

During the experiment, the simulated natural eye was rotated manually horizontally from one extreme to the other. The detector sensed the eye position signal. The eye signal was coded and transferred to the PWM signal. The motor drives the artificial eyeball to the desired position through a built-in control unit.

2.5 Conclusion

This chapter describes a simulation study of sensing the eye movement as well as a prototype of an assistive device, for detecting natural eye movement and driving the artificial eye to follow the natural eye movement. A laboratory prototype has been proposed.

Chapter 3

Neural Network Based Sensor Fusion and Fault Detection and Recovery in Robotic Eye System

3.1 Introduction

This chapter describes an approach of using the Artificial Neural Network to do the sensor fusion to detect the eye movement in the Robotic Eye System.

Two types of neural networks were used for the sensor fusion and sensor fault detection and recovery respectively. Usually the sensor fusion relies on the model of the system, however, sometimes it was not possible to get the accurate model of the system, or one or several of the parameters of the system may be unknown or partially known. In addition, there may be measurement in accuracies associated with the sensors. In this case, conventional method may not have good performance. An artificial neural network can learn the characteristic of a non-linear, non-modeled

system through training samples. Then during the real application, the sensor signal can be used to feed the network and obtain the desired output. Using the micro sensor array to detect the eye movement carried out experimental study. The sensor data was amplified, digitized and then sent to the computer. Two-layer neural networks were trained by the data samples. First trained network was used to do the sensor fusion, and the second two neural networks were used to detect the sensor failure and recover the faulty data. Soft sensor failure and hard sensor failure experimental studies were included. Main part of this chapter deals with the network training method and experimental studies.

3.2 Background

Multisensor integration and fusion have got much attention in recent years [164]. Bayesian method was one of the classic methods that have been used in sensor fusion. This method had its shorting comings. It lacked flexibility and could not discriminate uncertainty and ignorance. Dempster-shafer theory was used to overcome this shortcoming, which could be found in [168, 173]. It provided a way for information fusion where uncertain elements existed. Instead of placing an exact probability on a given event as Bayesian theory did, upper and lower probabilities were used as likelihood bounds. It was used for image processing and signal classification. Based on Bayesian theory and Dempster-shafer theory, Wang [189] presented a new strategy for statistical decision and evidence combination, which was called double bound testing (DBT). It increased the flexibility of decision. All of the above methods were statically based fusion algorithms, which have been successfully applied to the multiple sensor fusion in some applications. However, statistically based fusion algorithms policies need the

a priori knowledge about the observation process to make inference about identity, which sometimes was difficult to obtain. To compensate for this drawback, neural network and fuzzy set based fusion policies were distribution free and no prior knowledge was needed about the statistical distributions of the classes in the data source in order to apply these methods for fusion.

Fuzzy set and neural network were also used in sensor fusion [188, 155, 191, 171, ?, 170]. Fuzzy approach [188] was used for classification. Neural network was used to do motion detection [155], object detection [191], speech perception [170], and signal processing [161]. Lee [171] presented perception-action network. The net embedded feasible system behaviors in various level of abstraction, so that the system can re-plan and control its behaviors towards the set goals.

This chapter presents a neural network based approach for sensor fusion [167, 166]. An artificial neural network can learn the characteristics of a non-linear, non-modeled system through training samples. Then during the real application, the sensor signal can be used to feed the network and obtain the desired output.

3.3 Neural Network Approach

3.3.1 Two Layer Neural Network

An artificial neural network can learn the characteristic of a non-linear, non-modeled system through training samples. Assume there were n inputs $X = [x_1, x_2, \ldots, x_n]$, and m outputs $Y = [y_1, y_2, \ldots, y_m]$. They were related by a nonlinear unknown function $Y = F(X)$. A neural network sketched in figure 3.1 was able to learn the relationship between X, and Y.

This was a two layer neural network. Input layer was a hidden layer, and all

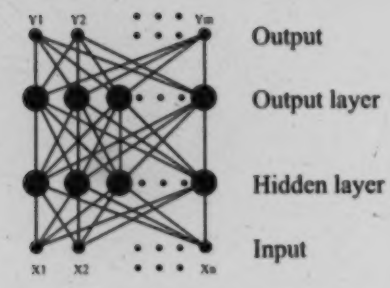

Figure 3.1: Two Layer Neural Network

the neurons were fed with the sensor measurement x_i. i from 1 to n.

The hidden neurons have activation function F_{in} and biases B_{in}.

Output layer was the second layer, and all the neurons of this layer were fed with the output of hidden layer. The output neurons have activation function F_{out} and biases B_{out}.

A set of weights was connected to each layer. Let W_{in} be hidden layer and W_{out} output layer.

In this network, the output of Y can be expressed as

$$Y = F_{out}(W_{out} * (F_{in}(W_{in} * X) + B_{in})) + B_{out} \tag{3.1}$$

3.3.2 Learning of Neural Network

Supervised learning method was used for this two-layer network. The output of the network was compared to the desired output. The error was used to adjust the weight and the bias. In this way, the network can be trained by minimizing this error term. The block diagram of the learning method was shown in figure 3.2.

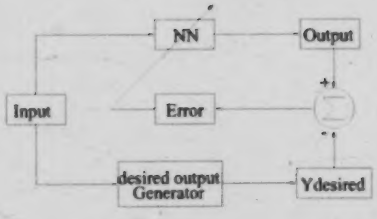

Figure 3.2: Supervised Learning

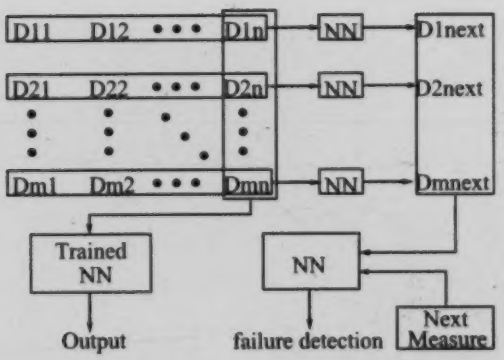

Figure 3.3: Fusion and Sensor Failure Detection

3.3.3 Sensor Fusion and Sensor Failure Detection

Figure 3.3 was the block diagram for sensor fusion and detection. D_{ij} was jth data of sensor i. Each row data was the successive data from same sensor and each column data was the data from the entire sensor at the same time. Each row data and the time interval were fed into the neural network to obtain the weight, and the estimated sensor output can be acquired. The last column was the newest data, which was used as input for the trained neural network to do the fusion.

3.4 Experimental Study

3.4.1 Sensor Data Space Creation

Figure 3.4: The Artificial Eye Model

Multiple sensors were used to detect the eye movement [122]. A nine cells pair infrared sensor arrays were used to detect the eye movement. Here in this chapter, only three cells sensor array was used for the detection. The experimental study was first carried out using the artificial eye modal, as shown in figure 3.4. Two artificial

eyeballs were mounted inside the eye socket model, which have same volume of the real eye pit. Two eyeballs were linked to the servomotors, which was controlled by a micro controller. The micro controller drives the servomotor to move the eyeball using a predefined eye movement signal. The infrared emitter will send out the infrared light to illuminate the artificial eye, and the infrared detector will receive the reflected infrared light. The relationship between the infrared array output and the eye position was non linear. Training the neural network could complete the nonlinear mapping between the input and the output, which was divided into the following three steps:

- Calibration

  First step was to let the eye move following the predefined eye movement signal, and record the infrared sensor output simultaneously. Do this calibration procedure many times until the number of times was large enough, to minimize the expected square error.

- Training

  Using the recorded sensor output as input for the multi-layer neural network, the predefined eye movement signal as output to train the supervised network. The weight and the bias of the network were obtained as the information for the mapping between the sensors and the eye position.

- Experiment

  During the experiment, feed the recorded sensor output to the neural network, the output of the network was the eye movement signal.

As shown in figure 3.5, the artificial eyeball movement range was 40 degrees, from minus 20 degrees to plus 20 degree. The servomotor drives the artificial eyeball

from the left end to the right end at the slow speed. The resolution was 1 degree for the time being. And then the infrared sensor recorded the data and sent it to the computer for analysis. The three cells sensor array data was shown on the left side panel of the figure 3.5. Using the three steps described above, the trained neural network was obtained.

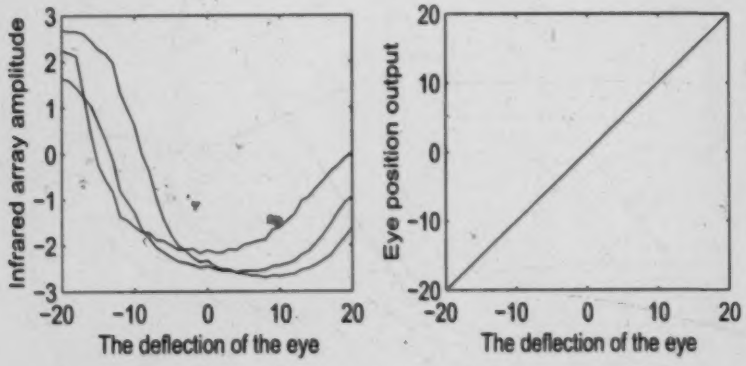

Figure 3.5: The Eye Movement Record in Tracking Target

3.4.2 Experimental Results for Fusion

To do the experiment for the fusion, periodical eye movement signal was sent to the controller to drive the artificial eyeball. The recorded sensor array data with noise was fed into the trained neural network to get the fusion output. Figure 3.6 shows the process.

3.4.3 Experimental Results for Fault Free Sensor Data

Matlab was used to do the neural network training and the simulation. Figure 3.7 shows the experimental result for fusion. Left side of the panel of figure 3.7

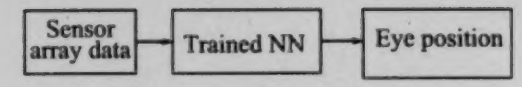

Figure 3.6: The Fusion Block Diagram

shows the infrared array data. From the figure, we can see that the artificial eye moves back and forth three times during the experimental study. The right side of the panel of figure 3.7 shows the eye position output. The result verifies the fusion algorithm.

3.4.4 Experimental Results for Soft Sensor Failure

Soft sensor failure means that the sensors were still working, however, there will be some noise in the sensor data, such as the bias, drifting, and precision degradation. The amplitude of the sensor noise was very low. The network can tolerate this. Figure 3.8 shows the experimental results with soft sensor failure. In the experiment, the random noise was added to the sensor output. The noise amplitude was from 1 percent of the maximum sensor output amplitude to 10 percent of the maximum amplitude. The relationship between the noise amplitude in percentage and the position error in degree was shown in the figure.

3.4.5 Experimental Results for Hard Sensor Failure

Hard sensor failure means that the sensor does not work at all. Usually in electronics it can be defined as the stuck-at sensor failure, where the sensor was stuck at one extreme of its signal range. In practice, this is likely to be an open (stuck-at 0) sensor or a short circuit (stuck-at 1) sensor. Figure 3.9 shows results when sensor cell one, cell two and cell three stuck at 0 respectively. It was clear that using the

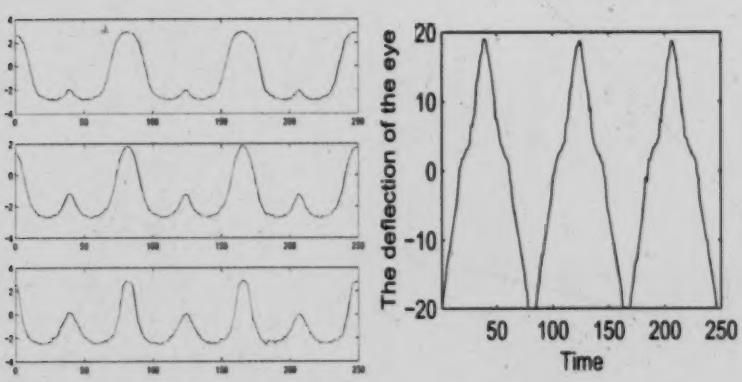

Figure 3.7: Fusion with Fault Free

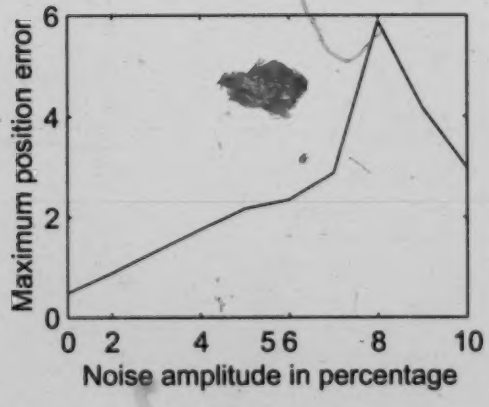

Figure 3.8: Fusion with Soft Sensor Failure

trained network without failure detection and recovery, the result was totally out of order.

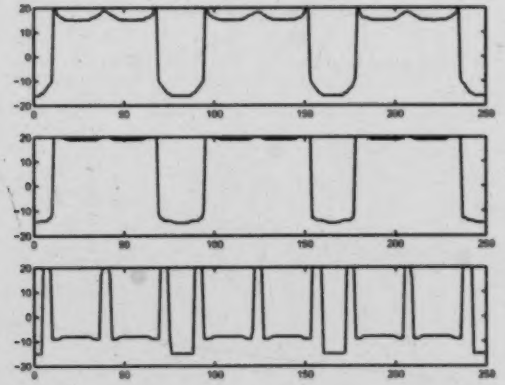

Figure 3.9: Hard Sensor Failure without Failure Detection and Recovery

3.4.6 Experimental Results for Failure Detection and Recovery

To deal with the sensor failure, two types of neural networks have been generated. The training steps of the neural networks was described as follows:

- Sample selection

  Select a set of data samples for normally working sensors and a failed sensor, whose readings were to be recovered.

- Training for failure detection network

  Using the normally working sensor data and the data of faulty sensor data as input for the multi-layer neural network, the maximum and minimum value were assigned as output for those two types of data respectively to train the supervised network.

- Training for failure recovery network

  Using the normally working sensor output as input for the multi-layer neural network, the failed sensors' data as output to train the supervised network. The weight and the bias of the network were obtained as the information for the mapping between the normal sensors and the abnormal sensors.

- Completion

  Try to add the sets of normal sensors versus abnormal sensors data sample. The thorough exploration of the data will enable the network to deal with different sensor failure configuration.

Using the trained neural network, the previous hard failure problem can be solved easily. As shown in figure 3.10, the left side was the detection result. The threshold distinguishes the normal sensor data and the abnormal sensor data. The right half panel shows the recovered eye position signal.

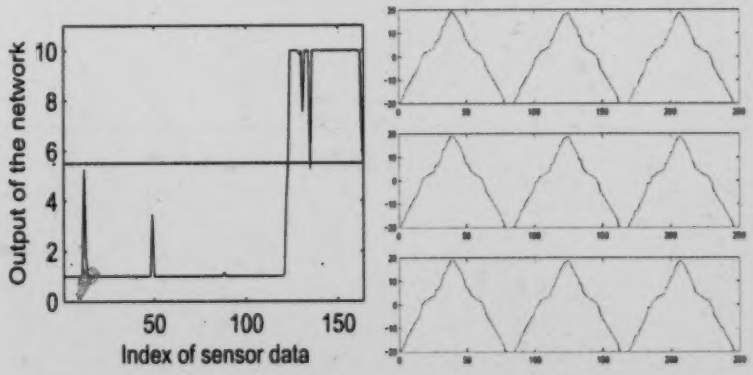

Figure 3.10: Failure Detection and Recovery

3.5 Conclusion

Sensor fusion was a key issue in many systems, mainly in robotics related systems. This chapter proposes a neural network method for sensor fusion of infrared reflection data to estimate the position of the eye for the Robotic Eye System. From the experiment, it was easy to find out that this network performs well under the situation of noise and sensor fault.. This approach needs to be further validated by the experiment through real eye movement experiment. Future work will be the experimentation and extension of this method to related field.

Chapter 4

Electrooculography Based Robotic Eye System

4.1 Introduction

This chapter describes the intelligent sensor and control system, robotic eye system bench model, which comprises biomedical electrodes and a micro controller. The system was intended to provide a rehabilitation ocular implant device that could be useful to some people who have ocular implants. With the proposed device, the ocular implant can have the same natural movement as the normal eye. The basis for this system was the use of bioelectrical signals from the user's body. The system can acquire the dynamical eye orientation, which was sent to the micro controller to control the artificial eye to have the same orientation. The bioelectrical sensors, micro servomotor, and artificial eye model were setup to investigate the eye movement detection and control methods. This chapter starts with the review of EOG method. Then the system was set up to carry out experimental study. Different configuration

of the electrodes was explored and the best configuration was used to sense the eye movement and controls the artificial ocular. The pilot study has demonstrated its potential for clinical applications.

4.2 Background

The aim of the study is to identify the natural eye movement and then to control the motor to drive the artificial eye to the desired position. The first step is to detect eye movement from the natural eye.

The EOG (Electrooculography) method is investigated in this chapter. It was widely used in ophthalmic research and clinical laboratories because it provides a non-invasive method for recording full range of eye movements. The EOG was useful in ophthalmology for diagnosis and prognosis of several diseases such as best's disease [97], and multiple sclerosis [98]. It can be used for diagnosis and prognosis of several eye ailments caused due to primary depigmentation such as those associated with myopia, siderosis or chloroquine intoxication, retinopathies due to hypertension or diabetes [99]. Besides the clinical research and laboratories use, the EOG was also broadly used as assistive technologies, such as the HMI (Human machine Interface) [100], which provides a pointing device that could be useful to the people with physical disabilities; and for the determination of eye position in fast jet flight [101].

From the above studies, we found out the EOG is simple to use, the electronic parts can be very small, and it can be used as long term monitoring. These entire characteristics are required for the purpose of our project. Therefore, it was selected as our eye motion sensor.

The organization of the chapter is given as follows. Section 2 describes the

all the components needed for the experimental system. Section 3 discusses the methodology and the mechanism of EOG. Section 4 presents the experimental study with EOG. Section 5 addresses the issue on the system integration and control. The last section concludes the chapter.

4.3 The Experimental Components

4.3.1 Motor

A small servomotor was used to drive the artificial eye. The motor shown in figure 4.1 is the one of the lightest normal servo, weighting only 3.5 grams. With a 5 volt power supply, the motor has sufficient torque to drive the artificial eyeball mounted onto the motor shaft. A servomotor was controlled by a pulse-modulated signal. The width of the pulse was the code that signifies to what position the shaft should turn.

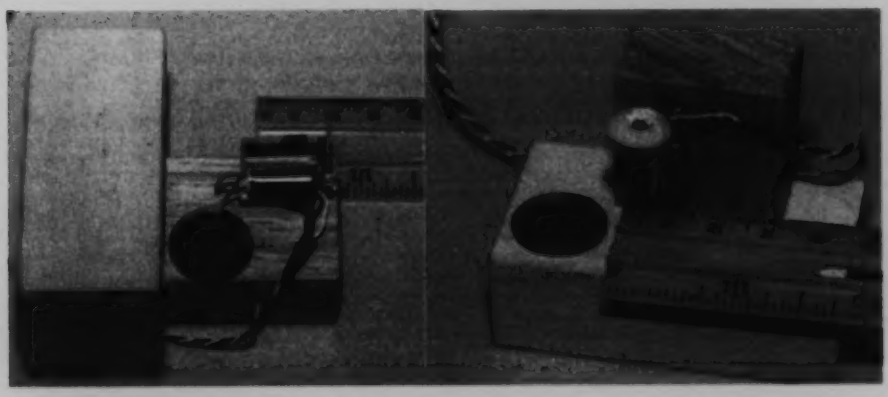

Figure 4.1 Light Servo Motor

Choosing a sensor for natural eye position is a challenge. Many kinds of sensors

have been tried. Large sensors are not practical for this application.

4.3.2 ECG (Electrocardiography) Electrode Biomedical Sensor

The electrode shown in figure 4.2 is ECG silver/silver chloride electrode, which is used to detect the ECG. The disposable electrode is about 1 centimeter in diameter and attached to the rectangular disposable sponge pads. The tip of 30-inch lead wire was attached to the electrode, as shown in figure. It can also be used to detect the EOG. The EOG measures the electrical potential of the eyes. The human eye is a dipole. The EOG signal can be used to measure the positions of the eyes with respect to the head. The electrical axis of the eye corresponds to its visual axis. Determining orientation of the dipole will determine the orientation of the eye (Davison, H, 1980). EOG can record the eye movements over 70°, with a typical accuracy of approximately $\pm 1.5^{o}$ to $\pm 2^{o}$. However, greater resolution is possible by averaging equivalent responses.

4.3.3 Artificial Eye Model

An eye pit model was used in the experiment as shown in figure 4.3. The size of the pit of the model is the same size as the natural eye pit. Eyeballs were mounted on to the servomotors.

Figure 4.2: EOG Electrode

Figure 4.3: Artificial Eye Model

4.4 Using EOG to Detect the Eye Horizontal Movement

EOG is one of the methods that have received much attention recently. EOG measures the induced potential, which causes the eye movement, rather than measure the mechanical movement of the eyeball itself.

Two small (6-8mm in diameter) electrodes were used for the recording contact points around the eyes. Disposable electrode with low impedance functioning as a reference electrode is located on the midline of the forehead. The configuration of the electrodes is shown in chapter 7. One pair horizontally placed electrodes is to record the horizontal eye movements. To record the one eye horizontal movements, one electrode needs to be moved to the middle point of the two eyes. The EOG electrodes can easily be fixed in place without causing any discomfort to the subject. The subject can wear eyeglasses, spectacles and the EOG apparatus does not interfere significantly with the observer's visual field.

The electrooculography is usually recorded as a direct current (DC) signal because the movements of the eyes were relatively slow in both electrical and electrophysiological terms. The potential differences between the two electrodes was amplified and sent to the computer through the AD card with a $30Hz$ sample frequency. At the same time, the amplified signal was shown on the screen of an oscilloscope, as shown in chapter 7.

4.5 Experimental Results for EOG Eye Movement Detection

4.5.1 Health Research Ethics Approval

To do the experiment with human subject, we need to get the ethics approval. The protocol has been submitted to the review committee and the Health Ethics Board has reviewed the protocol for this project and found it to be acceptable within the limitations of human experimentation. The HERB has also reviewed and approved the patient information material and consent form, which were included in appendix.

Description of Research Procedures were stated as following:

The block diagram of the eye movement detection system was shown in figure 6.7. Configuration of the electrode setup was shown in figure 6.6. Two electrodes were placed on the skin to the outside of each eye. The reference electrode was placed on the lower forehead above the nose. The eye behaves like a dipole rotating through an inhomogeneous volume conductor (the head), the EOG being the d.c. signal that is measurable at the surface of the volume. The horizontally placed pair of electrodes will detect the signals with the angular deflection of the eye, which will be amplified and send to the computer through DAQ card. Whole experimental system set up The whole system was setup as shown in figure 4.12. EOG signal was detected by the system and the signal was sent to the micro controller through the interface. The micro controller uses the natural eye position signal to control the artificial eye movement to the corresponding position.

- Preparation

The subject was introduced to the present project, the apparatus being used, and the tasks to be completed.

- Electrode application

  Alcohol swab was used to clean the skin in the electrode locations. Fine sand paper was used to clear the skin and reduce surface offset potential. Silver/silver chloride disposable electrodes were then attached to the three locations around the head. Each electrode has electrode gel included, these are standard electrodes used clinically for electrical recording.

- Testing

  The testing protocol was a mainly tracking task. The subject was asked to focus on a specific target and then the signal was measured. The signal was filtered and fed to an A/D card for use by the micro controller.

- Task

  The subject was asked to stabilize his/her head. The subject he/she was asked to look to the left, right, and to the center. Then the subject was asked to move the eye horizontally. A calibration curve will be generated, and then the eye position signal will be used to move the artificial eyeball accordingly. The whole procedure will be recorded. Both eye position as measured by the target location and EOG signal will be recorded.

4.5.2 Sensor Placement

When using the EOG to detect the eye movement, it is important to know where to apply the electrodes. To detect the horizontal eye movement, one pair of electrodes was placed on the side of the eye, and the reference electrode was put

on the forehead. The question is if the two electrodes placed on the side of the eye has vertical offset, will it affect the result of the EOG. Experimental study has been carried out by trying different configurations of the electrodes. Three pairs of electrodes were placed on the side of the eye, as shown in the figure 4.4. The pair has no vertical offset with respect to the eye is called Middle pair. The upper one is called up pair and the lower pair is called down pair respectively.

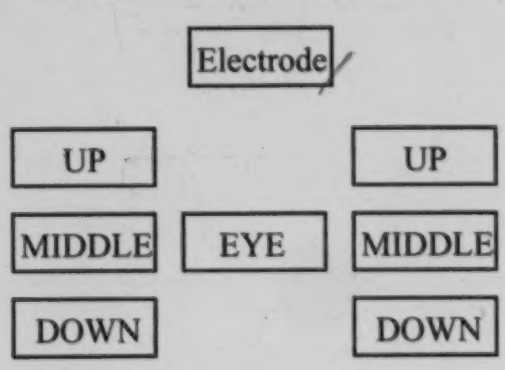

Figure 4.4: The Configurations of the Electrodes

For three pairs of electrodes, there were totally nine configuration sets, such as up-up, up-middle, up-down, middle-up, middle-middle, middle-down, down-up, down-middle, down-down. For each set of configuration, the subject was asked to fixate at center point throughout the test. The recorded data for each set was plotted in figure 4.5. It is straightforward that the middle-middle pair electrodes has the lowest drift by looking at the plot out in figure 4.5. It is verified by comparing the variance in table 4.1, which shows that the middle-middle pair has the lowest variance. From the experiment, it is also found out that the eye blink artifact shows up in the EOG signals. The eye blink signal does not corrupt the EOG signal, which uses the middle-middle pair, but corrupt all the rest of the sets. The eye blink signals were

the small spikes in the wave of the signal, which is easy to tell from each set data.

	UP	MIDDLE	DOWN
UP	0.2581	0.0810	0.0544
MIDDLE	0.5624	0.0038	0.0270
DOWN	0.1879	0.0470	0.0437

Table 4.1: The Variance of the Data from Each Set of Configuration

4.5.3 Two Eye and One Eye EOG Signal

Using the best configuration from the previous section, the two eye movement and one eye movement data were recorded. The recorded data were plotted in figure 4.6. The left panel depicts the two eye horizontal movement signals. The electrodes were placed close to the temple of each side of the head. The right panel shows the left eye horizontal movement signals. The reason for recording one eye movement signal is to find out the difference between the one eye horizontal movement signal and the two-eye horizontal movement signal. It is clear that the amplitude of the two-eye signal is almost twice as that of the one eye signal. These two figures show the smooth pursuit movement (from 1100 to 2000 in left side panel and from 400 to 1000 in right side panel) of the eye from left side to the right side and back to the left side.

The signal is close to linear, but d.c. drift is a problem. This is the drawback associated with the EOG, since it is subject to a slow shift in baseline electrical potentials. The drift is primarily caused by the polarization of electrodes.

The following steps are used to improve the signal quality by suppressing the drift:

- Preparation. The drift is usually caused by an accumulation of electrical charge in the recording electrodes, but it can be minimized, or even eliminated

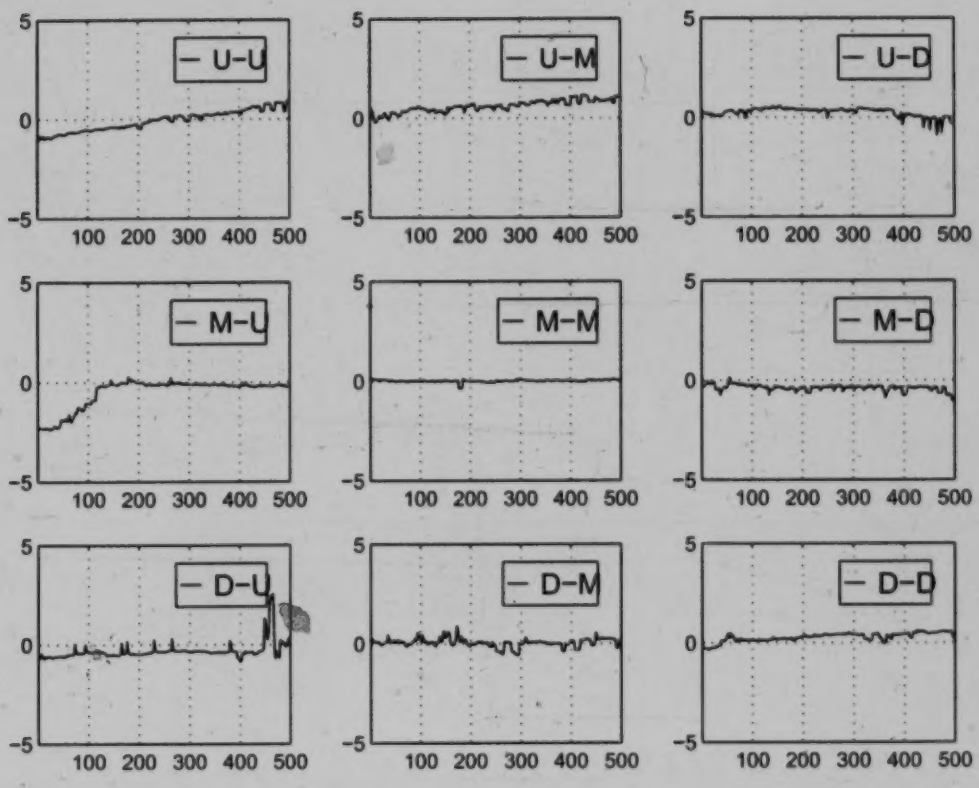

Figure 4.5: The Baseline of EOG to Detect Eye Movement with Different Electrode Configurations, u-up, D-down, M-middle (see figure 4.4). The subject was to asked to focus on a point at the center of the target

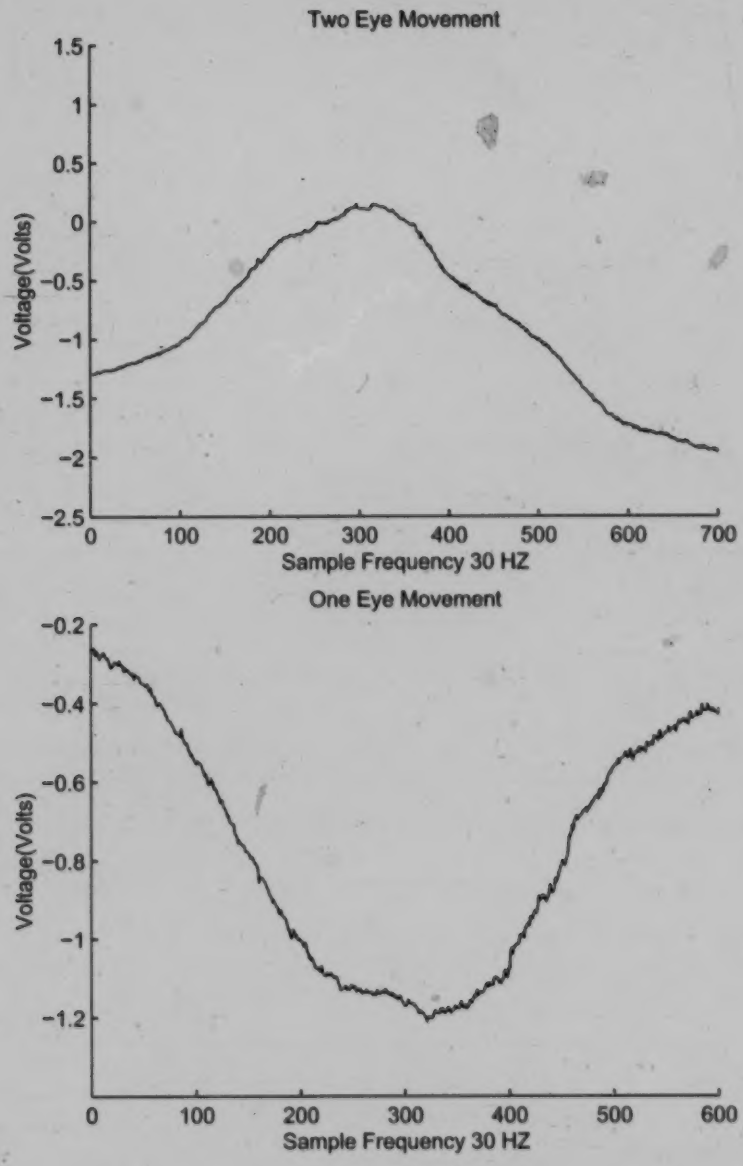

Figure 4.6: Using EOG to Detect One Eye (one electrode at nose and one at temple) and Two Eye Movement (electrodes at each temple). The subject moved his/her eye from one extreme to another and moved back

by several methods through recording contact area site preparation (i.e. mild skin abrasion, conductive paste).

- Polarization of the electrodes. Let the test subject settle for at least an hour or so.
- Filtering. Using a low-pass filter with the corner frequency set to some very low frequency around 10 Hz.

Using the methods above, low drift EOG signals can be obtained as shown in figure 4.7 to 4.9. The subject is required to direct his gaze from left to right and right to left very quickly. The experimental data of first subject is shown in top of figure 4.7. Drift can be observed from the EOG signal, possibly because the long leads were used in the experiment. After the short leads were used to replace the long leads, there was minor drift in the EOG signal of second subject's EOG signal (middle plot, figure 4.7). From the EOG signal of third subject (bottom plot, figure 4.7), we found the signal was bounded at bottom and top. The reason for this is that the amplifier gain was tuned a little bit high during the experiment, which is also happened in figure 4.8 and 4.9.

4.6 Experimental Study with the Eye Movement and Motor Control

EOG method was used to determine the natural eye position and use the signal to control the artificial eye movement. To find out the relationship between the output of the sensor and the eye deflection angle, a calibration set up is needed as shown in figure 4.10.

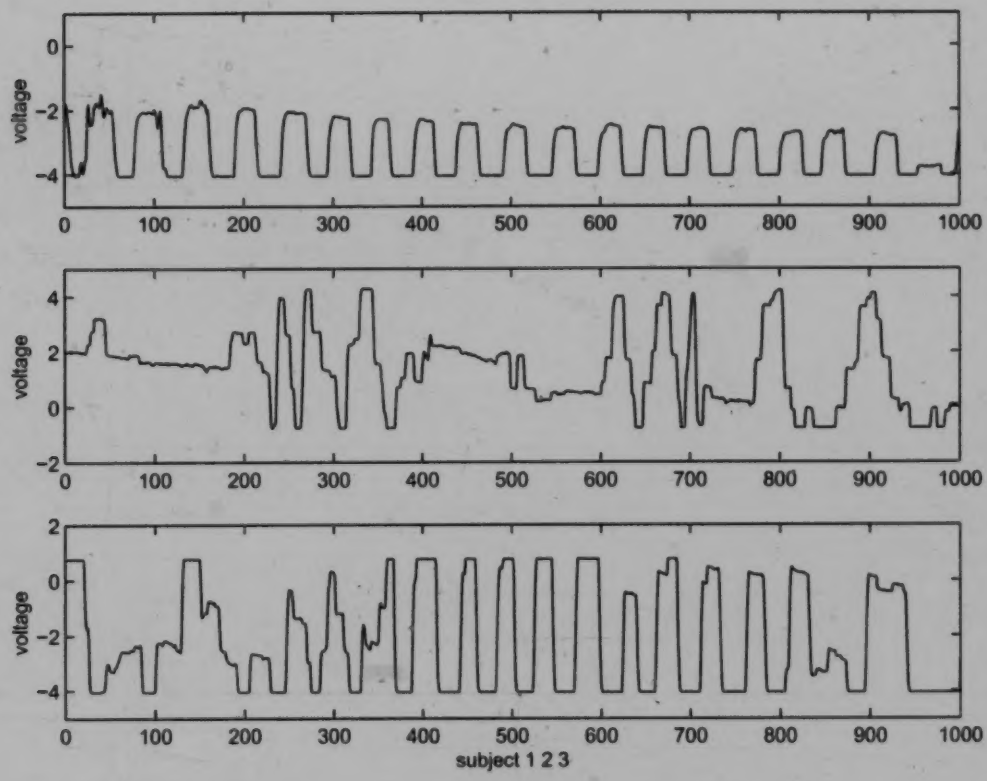

Figure 4.7: Experimental Study with Subject 1 2 3

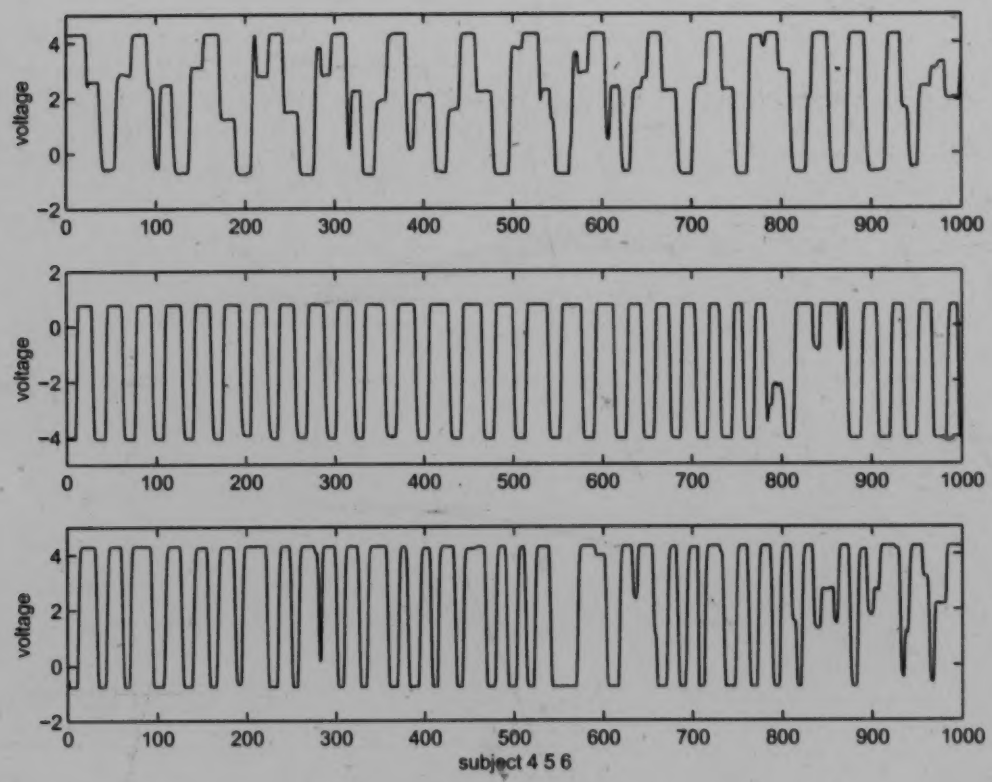

Figure 4.8: Experimental Study with Subject 4 5 6

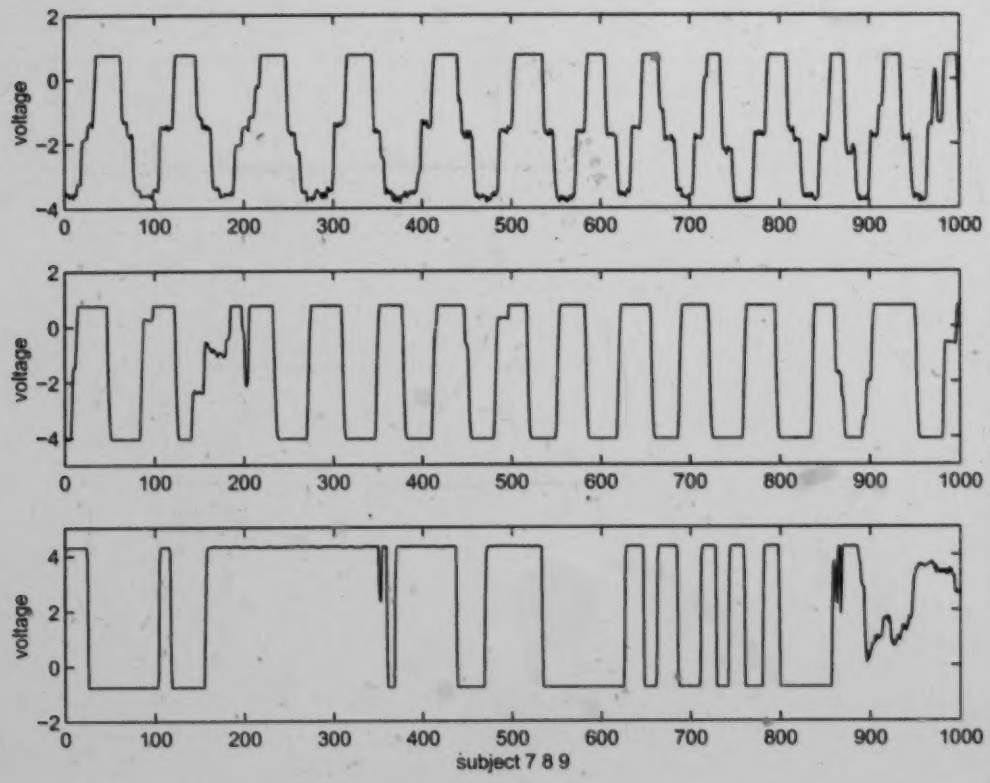

Figure 4.9: Experimental Study with Subject 7 8 9

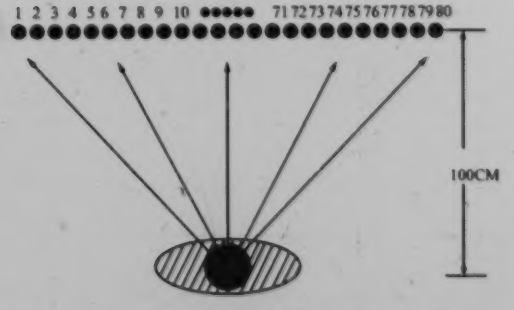

Figure 4.10: The Natural Eye Calibration Set Up

The subject was asked to stabilize his/her head in front of a board. The distance between the neighbor targets was constant. The distance between the subject and the board was set to one meter. The deflection angle of the subject's eye was determined from the distance between the start target dot and the end target dot. During the experiment, the subject was asked to look to the left, right, and to the center of the target board. Then the subject was asked to move his/her eye horizontally by looking at specific targets. Assume that the subject's left end vision was T_l, right end was T_r, and center T_c. The distance between the subject and the target board was L. Then the subject's eye deflection range is,

$$Range = \arctan(T_c - T_l)/L + \arctan(T_r - T_c)/L \tag{4.1}$$

The subject was asked to fixate at the left end target, and move the eye to the next target until he/she reaches the right end target. The corresponding voltage was recorded and a calibration curve will be generated, as shown in figure 4.11. The deflection range of the subject here is 102 degrees. The calibration curve is quite linear from minus 30 degrees to plus 40 degrees.

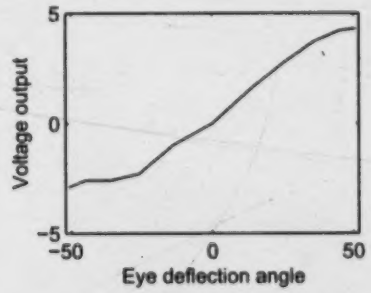

Figure 4.11: The Calibration Curve of EOG to Detect Eye Movement

After the calibration curve was obtained, the eye movement signal was fed to

the micro controller to control the artificial eye model, as shown in figure 4.12. The subject was asked to track the moving target with his/her eye. The eye position signal was fed to the controller to move the artificial eyeball so that it will have the same line of gaze as the natural eye. A pilot study has been carried out. The whole procedure was videotaped and promising results were obtained.

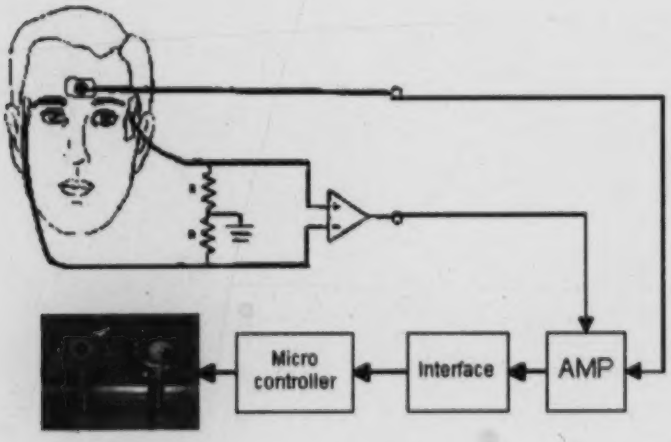

Figure 4.12: The Eye Movement Detection and Ocular System Set Up

4.7 Conclusions

This chapter describes the design of an assistive device, the Robotic Eye System, which can detect the natural eye movement and drive the artificial eye to follow the natural eye movement. This chapter proposes an EOG method to detect the eye movement. A lab prototype system has been designed and constructed, which performs the desired tasks very well. This approach needs to be further validated by further experiments. The next step is to refine the sensing elements of the device, improve the control algorithm, miniaturize the circuit design, and perform clinical test to validate the final design.

Chapter 5

Reliability of Multiple Sensors in Robotic Eye System

5.1 Introduction

The robotic eye system will be able to operate reliably and safely over prolonged periods of time, only if its sensors work properly. In our first generation of the robotic eye system, a linear infrared sensor array was used. Because the probability of success for each infrared sensor is different, determining the reliability of the entire sensory system based on the information from each sensor is very important. Adding more sensors will increase the reliability of the sensory system, however, the price will also increase. TO ensure satisfactory system reliability at reasonable cost is also very important for each system. So there is a trade off between the reliability of the system and the cost of the sensors used. This chapter describes an approach that uses several search algorithms to maximize the system reliability and, at the same time, minimize the sensor cost. The search algorithms utilized include tabu search,

genetic search, and simulated annealing. A new and improved search algorithm is also developed for this purpose [123]. The new algorithm is very efficient and can guarantee the optimal solution. Numeric examples are also included in this chapter. The algorithm developed here is expected to find its usefulness to improve reliability of the sensors in other multisensor robot systems.

5.2 Background

Multiple sensors are used for intelligent systems to deal with inaccuracy and uncertainty. During the past decade, computer technology has provided hardware with switch density as high as 10^6 per cubic centimeters which is approximately the neuron density in the human brain [124], but sensory system development lags far behind. For example, cameras have 10^6 pixel elements, but a human eyes have 250×10^6 pixel elements. To compensate for the lag in sensory technology development, multiple sensors are used in the system design, not only because of their information gathering capabilities, but also for their failsafe capability. Commonly used sensors for robotic systems include video cameras, range finders, sonar, and tactile and infrared sensors. Duplicate sensors can be employed for fault tolerance and they achieve tasks that cannot be performed by a single sensor. For these reasons, multiple sensors have attracted much research attention in recent years. When multiple sensors are used in a robotic system, the reliability of the sensor system as related to the probability of success of each individual sensor should be examined. For example, assume there are N independent sensors in the system, with each component having an identical probability of success p. Let $q = 1 - p$, the assumption of statistical independence allows us to use Bernoulli's law, which finds the probability of i out of N components

working at the same time as

$$\begin{pmatrix} N \\ i \end{pmatrix} p^i * q^{N-i} \tag{5.1}$$

If p is a function of time t, i.e. $p = p(t)$, then, then $q(t) = 1 - p(t)$ and, by using Bernoulli's law, the probability of i out of N components working at the same time t is:

$$\begin{pmatrix} N \\ i \end{pmatrix} p(t)^i q(t)^{N-i} \tag{5.2}$$

It is guaranteed that a system will function correctly as long as more than half (in

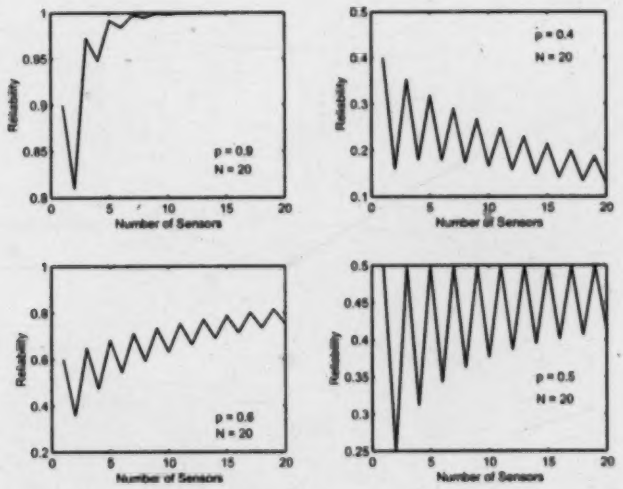

Figure 5.1: Relationship Between Number of Sensors and the Reliability

the case of one dimensional sensor fusion, which is exactly the case in our robotic eye system) or more than two-thirds (in the case of Byzantine Agreement) of the components function correctly [125, 126]. So the reliability of the system is the

summation of the terms in equation 3.1 with i varying from N to $[N/2]+1$. The maximum number of the sensors is set to 20, and the possibility of success of each sensor is set to 0.9, 0.6, 0.5, 0.4 respectively. It is easy to find out that for $p = 0.9$, only ten sensors will let the system have the possibility of success close to 1. For $p = 0.6$, the system reliability is increasing with respect to the number of the sensors, but not as fast as the curve of $p = 0.9$. For $p = 0.5$, the system reliability is oscillating with respect to the number of the sensors, the reliability is always less than the single sensor reliability, as shown in figure 5.1. It is interesting to see that for $p = 0.4$, the system reliability is decreasing with respect to the number of sensors. That means if we want to mount multiple sensors onto the system, and the reliability of each sensor has to be at least greater than 0.5, as otherwise, the reliability of the system will decrease with more sensors.

5.3 The Reliability Model of Multiple Types of Sensors

In the introduction, we considered only one type of sensor. In reality, there are usually many types of sensors used in a system. In what follows we first develop a reliability model for two types of sensors, and then extend it to the case of multiple types of sensors.

For a system with two types of sensors, assume that there are N_1 sensors in type one, and N_2 sensors in type two, respectively, and all sensors are independent of each other. For the same type of sensors, the probability of success is assumed to be the same. Let us assign p_1 and p_2 to type one and type two sensors as the

probability of success, respectively. Let $q_1 = 1 - p_1$, $q_2 = 1 - p_2$, and $N = N_1 + N_2$. The assumption of statistical independence allows us to use Bernoulli's law, which finds the probability of i_1 out of N components working at the same time as

$$\sum_{i_2=0}^{i1} \begin{pmatrix} N_1 \\ i_2 \end{pmatrix} {p_1}^{i_2} {q_1}^{N_1 - i_2} \begin{pmatrix} N_2 \\ i_1 - i_2 \end{pmatrix} p_2^{i_1 - i_2} * q_2^{N_2 - (i_1 - i_2)} \tag{5.3}$$

Let $r(i_1)$ denote the above equation and define

$$ben(p, n, i) = \begin{pmatrix} n \\ i \end{pmatrix} p^i * (1 - p)^{n-i} \tag{5.4}$$

then equation 5.3 can be rewritten as:

$$r(i_1) = \sum_{i_2=0}^{min(i1, N_2)} BEN_2(i_1, i_2)) \tag{5.5}$$

where

$$BEN_2(i_1, i_2) = ben(p_1, n_1, i_1) * ben(p_2, n_2, i_1 - i_2) \tag{5.6}$$

The reliability of the system is the summation of the terms in equation 5.5 with i_1 varying from N to $[N/2] + 1$. If D_2 denotes the reliability of the system, then

$$D_2 = \sum_{i_1=[N/2]+1}^{N} \sum_{i_2=0}^{min(i1, N_2)} ben(p_1, n_1, i_1) * ben(p_2, n_2, i_1 - i_2) \tag{5.7}$$

It is easy to extend the type of sensors from 1, 2, to m. Each type of sensors has N_i components, and the probability of success p_i.

Let $N = \sum_{i=1}^{m} N_i$, and the multiple variable Bernoulli term be $BEN_m(i_1, i_2, \ldots, i_m)$

$$BEN_m(i_1, i_2, \ldots, i_m) = (\prod_{j=i_2}^{i_m} ben(p_1, n_1, i)) * ben(p_m, n_m, i_1 - \sum_{k=i_2}^{i_m} i) \tag{5.8}$$

So the probability of i_1 out of N components working at the same time is

$$r(i_1) = \sum_{i_2=0}^{i1} \sum_{i_3=0}^{i1-i_2} \cdots \sum_{i_m=0}^{i1-\sum_{k=i_2}^{i_m} i} BEN_m(i_1, i_2, \ldots, i_m) \tag{5.9}$$

The reliability of this multiple type component system is the summation of the terms in equation 5.9 with i_1 varying from N to $[N/2]+1$. If D_m denotes the reliability of the system, then we have

$$D_m = \sum_{i_1=[N/2]+1}^{N} r(i_1) \tag{5.10}$$

5.3.1 Cost Constraints in Redundancy Systems

Multiple sensors are used for systems to increase reliability, however, they also raise the issue of cost, and there is a tradeoff between system cost and reliability. If the reliability and cost of each component are known, then an interest problem is to evaluate the reliability of the entire system subject to a cost constraint. The problem can be stated formally as follows

Assume there are m types of sensors in the system. The cost and reliability of the ith type sensor are c_i and p_i respectively. Let N_i be the sensor number for the ith type of sensor. The cost constrain in this case is given by

$$\sum_{i=1}^{m} N_i c_i <= Maximum\_Cost \tag{5.11}$$

and the problem is to determine the optimal combination of sensors such that the reliability of the system is maximized subject to the cost constraint in equation 5.11. Some heuristic approaches such as tabu search, genetic algorithms, and simulated annealing can be found in [125]. However, in general these methods cannot guarantee

that the solution is optimal. A robust and efficient method such as the quasi-Newton method can be used to solve this problem if the constraint is converted to a linear equality constraint. Here, in this chapter, we only discuss the three heuristic algorithms, and propose improved search algorithms for the problem.

5.3.2 Optimization Methods

- Tabu search

  Tabu search creates a list of nodes in the search space, which are visited by the search algorithm. These points then become "tabu" for the algorithm, where "tabu" means that these points are not revisited as long as they are on the list. This will allow the search algorithm to climb out of a shallow local minimal in the search process [127, 128].

- Genetic Algorithms

  Genetic algorithm attempts to apply the concept of "survival of the fittest" to optimization problems [129, 130]. Biological systems adapt themselves to fit into an ecological niche. The same evolutionary process will lead to series fit answers. This approach has been shown to be experimentally useful for solving optimization problems. Possible solutions to a problem are called chromosomes, which are grouped into gene pool. The next generation is formed via operations, known as crossover and mutation.

- Simulated annealing

Simulated annealing tries to find the optimal solution of an optimization problem in a process like the formation of cooling crystals [131, 132]. The idea is that the melted crystals will cool down to a minimal energy state. The strategy is as follows: Given a configuration of the elements of the system, randomly displace the elements, one at a time, by a small amount, and calculate the resulting change in energy, ΔE. If $\Delta E < 0$ then accept the displacement and use the resulting configuration as the starting point for the next generation. If $\Delta E > 0$ then the displacement is accepted with probability $p(\Delta E) = exp(-\Delta E/k_b T)$ where T is temperature and k_b is Boltzmann's constant.

For above three algorithms, each has its advantages and disadvantages. The tabu search is more sensitive to local minimum than the genetic algorithms, since it focuses on searching its very vicinity. It will quickly converge to local minimum and take a long time to climb out of the local minimum. Simulated annealing has the same drawbacks as the tabu search. The genetic algorithm does not look for a local minimum. None of the three algorithms can guarantee that the solution is a global minimum. Our improved algorithm guarantees the optimal solution without an exhaustive search. By studying the equation $\sum_{i=1}^{m} N_i c_i < Maximum\_cost$, we find there are a very large number of solutions. We need to minimize this solution space as far as possible. From the introduction section, it is easy to see that more sensors will result in a more reliable system. Inspired by this idea, we try to find the sets of N_i, so that the $cost = \sum_{i=1}^{m} N_i c_i$ is less than and closest to the $Maximum\_cost$. The optimal solution is guaranteed in these sets. Here is a numeric example. Assume that there are three types of sensors, their costs are [5 8 10], and the $Maximum\_cost = 50$. The whole solution space for $5N_1 + 8N_2 + 10N_3 < 50$ is shown on the right side of

figure 5.2, while the optimal solution space is shown on the left side of figure 5.2. The number of original sets is 100 and the number of optimal sets is 8. Thus the size of the solution space is greatly reduced.

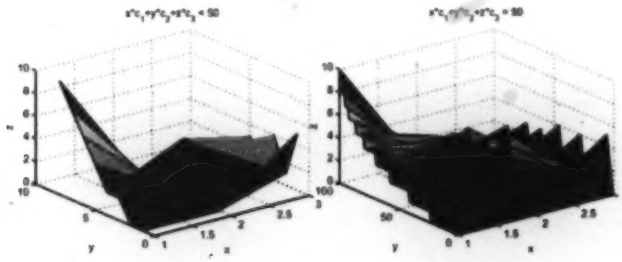

Figure 5.2: Three Types of Sensor Example

Here is a step-by-step description of the new proposed search method:

step1:	Sort cost vector $[c_1, c_2, \ldots, c_m]$ in ascending order.
step2:	Make the type $cc = [0, 0, \ldots, N_m]$, $N_m = int(Maximum\_cost/c_m)$ the start candidate.
step3:	Add cc to the optimal list.
step4:	Reduce N_m by 1, $maxprice = maxprice - c_m$, add cc to the optimal list.
step5:	Solve $[c_1, c_2, \ldots, c_{m-1}]$, maxprice problem .
step6:	Add result of step 5 to optimal list.
step7:	If $N_m \neq 0$, goto step 4.

Table 5.1: The New Search Method

The method is a recursive method. It always finds the configuration of the components so that the reliability is maximized with the price limit. Based on the above search method, the optimal list is much shorter than the original list. However, the optimal list will still be very large, if the number of the component type is very

large. Through experiment, it was found that if we use $averge = \sum N_i p_i / \sum N_i$ as a criteria, where p_i is the probability of success of each type, and then set the threshold as middle point of the average set, we will have a much reduced list, which will be called the final list.

Because the final list is very small, it is easy to calculate the reliability of each type from it and obtain the optimal value. The simulation results are included in the next section.

5.4 Numerical Experiment

Tables 5.2 to 5.4 give the results from the numerical example, which is based on reference [125]. Eleven possible component types are used to construct the sensor system. Table 5.2 shows the sensor cost and probability of success.

Table of sensor cost and possibility of success		
Sensor	Cost($)	Probability of Success
1	20	0.8333
2	10	0.6667
3	20	0.8617
4	5	0.6552
5	25	0.8911
6	15	0.7241
7	7	0.5882
8	8	0.7284
9	20	0.8750
10	6.8	0.6481
11	7	0.6452

Table 5.2: Table of Sensor Cost and Possibility of Success

Table 5.3 gives the best sensor configuration found by all three heuristics and the improved search method when cost limits of $58 and $52 are used. From these

two examples, we can see that only tabu search finds the single sensor configuration, although, it is not the best configuration. All the best configurations are the combination of the sensors.

	cost $ 52				cost $ 58			
S	Ta	Sa	Ga	new	Ta	Sa	Ga	New
1	0	0	0	0	0	0	0	0
2	0	0	0	0	0	0	0	0
3	0	0	0	0	0	0	0	0
4	1	0	0	0	0	0	0	0
5	0	0	0	0	0	2	1	2
6	0	0	0	0	0	0	0	0
7	0	0	0	0	0	0	0	0
8	3	1	1	1	7	1	1	1
9	1	2	2	2	0	0	1	0
10	0	0	0	0	0	0	0	0
11	0	0	0	0	0	0	0	0

Table 5.3: Sensor Configuration Under Cost Limit

Table 5.4 shows the differences among the methods. Our search method, which is labeled as "new" in the table, guarantees that the final solution is optimal. The results obtained using three heuristics are very close to optimal. In fact, the simulated annealing method also reaches optimal value in this case.

cost limit	algorithm	combination	cost	reliability
52	Ta	5	49.70	89%
52	Sa	3	49.40	92%
52	Ga	3	49.40	92%
52	New	3	49.40	92%
58	Ta	7	56.00	91%
58	Sa	3	58.00	94%
58	Ga	3	53.70	93%
58	New	3	58.00	94%

Table 5.4: Difference Among the Methods

Because the dimension of this problem is low, it is possible to plot the relationship between the reliability and the average probability of success for the space after ap-

plication of the improved search method. It is observed from figure 5.3 that the reliability of the system tends to be high when the average probability of success is high. Through a numerical experiment, we found that if we use the middle point as a threshold, we will always have the optimal configuration in the final list.

From table 5.5, we see that the new search method is very efficient. When the cost limit is 52, the solo configuration is $[2, 5, 2, 10, 2, 3, 7, 6, 2, 7, 7]$, and the number of configurations under the cost constraint is 4939200. After we apply the proposed search method, the number of configuration is reduced to 1599. Furthermore, the threshold method reduces the number to 87. This represents a reduction rate of 56772.

cost	Size of Solution Space	New	Threshold	Ratio
52	4939200	1599	87	56772
58	9461760	2768	371	25503

Table 5.5: Efficiency of the Method

Again, because the dimension is low for this case, the reliability of all the configurations can be calculated, and the relationship between the reliability and the average probability of success can be derived, as shown in figure 5.3.

We can use the following third-order polynomial to fit the data, here $\tilde{y}$ denotes the estimation of y;

$$\tilde{y} = ax^3 + bx^2 + cx + d \tag{5.12}$$

Using the LMS method, it is easy to find the coefficients for each case. The curve is shown in figure 5.4.

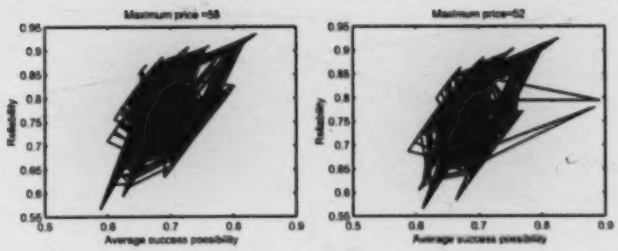

Figure 5.3: Relationship Between the Reliability and the Average Probability of Success

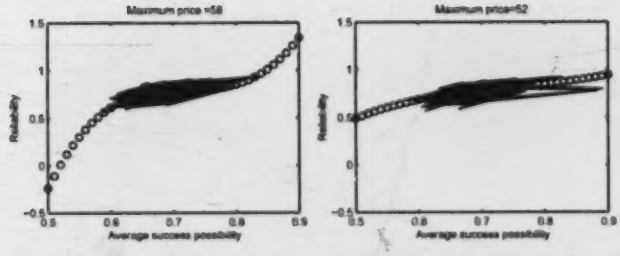

Figure 5.4: Linear Recursive Curve Fit

it is observed that the curves fit well to data in figure 5.4. In order to find the characteristics of the original data, we use the following model to describe the system.

$$y = \tilde{y} + e = ax^3 + bx^2 + cx + d + e \tag{5.13}$$

where e denotes the error between the original data and the fitted data. The distribution of the error can be obtained by a Q-Q plot [133], which can be generated in three steps as described below.

- 1. Arrange the errors obtained as $e_1, e_2, \ldots, e_N$, and their probability values $(1-1/2)/N$, $(2-1/2)/N$, ..., $(N-1/2)/N$;
- 2. Calculate the standard normal quantiles q_1, q_2, ..., q_N.
- 3. Plot the pairs of observations (q_i, e_i)

The correlation coefficient for the Q-Q plot is defined by

$$r_Q = \frac{\sum_{j=1}^{N}(e_j - \bar{e})(q_j - \bar{q})}{\sqrt{\sum_{j=1}^{N}(x_j - \bar{x})^2}\sqrt{\sum_{j=1}^{N}(q_j - \bar{q})^2}} \tag{5.14}$$

The Q-Q plot is shown in figure 5.5. From the correlation, we find that the error is close to a normal distribution.

5.5 Conclusion

In this chapter, a general formula is developed to derive to evaluate the reliability of the multiple sensor system. Several search methods are reviewed, and a new search method is developed for the problem addressed in Section 2. It is found that the three heuristics methods may be able to find a satisfactory configuration. Among

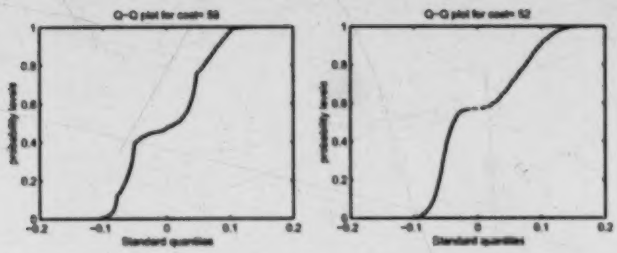

Figure 5.5: Q-Q Plot for Data in figure 3.4

these algorithms, the simulated annealing method may be able to find a satisfactory solution, which are as good as or better than that of the other two heuristics. However, none of these three heuristics is guaranteed to find the optimal configuration. Our new search method can find the optimal solution for this case. However, in this chapter, the assumptions used for the problem are too restrictive to allow generalization. It assumes that each component is independent, but in reality that may not be true. There are some approaches for this problem, such as PDOP [?]. These should also be considered in future research. The results from this chapter can be applied to the robotic eye system with the linear infrared sensor array. With the reliability of each sensor in the robotic eye system, the reliability of the robotic eye sensor system can be obtained easily. The approach can also find out the optimal solution for the number of the sensors can be used for the robotic eye system when the total cost of the sensor is given for the robotic eye system project. The application can be extended to any other multiple sensor robotic systems.

Chapter 6

Using Multivariate Statistical Sensor Fusion Techniques in Robotic Eye System

6.1 Introduction

To ensure the robustness of the robotic eye sensor system, multiple sensors are used to detect the eye movement. However, some sensors may fail and provide faulty data. In this chapter, multivariate statistical techniques are used to deal with sensor data monitoring, faulty sensor detection and isolation. In addition, principal component analysis is used to monitor the sensor data and detect the sensor failure, and incidence matrix is used to isolate the faulty sensor. We also study LMS and minimum variance methods for recovering the faulty sensor data. Simulation studies are included.

6.2 Background

Durrant Whyte [102] started the uncertainty modeling for multiple sensor systems in 1985. Gaussian distribution was assumed and Bayesian inference with minimum variance estimate was applied to fuse linearly structured multiple sensor systems. In 1990s, Centralized Kalman filter and decentralized Kalman filter were used for the sensor data fusion [102]. Many systems use the Kalman filter [103, 104, 105, 106] to explore the multiple sensor system. Luo [94, 96, 95] synchronized sensor information by a dynamic moving quadratic curve approximation and distance matrix. There are many other methods treat the uncertainty of the multiple sensor system, such as Dempster shafer rule [107], ellipse model [108], perception net [109], double bound test [110], and so on. The above sensor fusion method requires independence of sensor errors or closed form analytical expression for error densities. But in reality, independence of sensor errors can seldom be assured. Several methods such as triangulation based fusion [111] were proposed to overcome this problem. In this chapter, a statistical method is applied to explore the multiple sensor system.

Multivariate statistical method such as principal component analysis method has been used in chemical engineering for many years [112, 113, 114, 115, 116]. However, few papers have used this method in the field of robotics. Nowadays, robots are equipped with all kinds of sensors, such as video camera, range finder, sonar, tactile, and infrared sensors. In employing some of these sensors, sensor replication can be considered for fault tolerance. Because the sensor measurements are highly correlated under normal conditions, the availability of many sensors provides valuable redundancy for sensor fault detection and identification. The organization of the chapter is given as follows. Section 2 describes a principal component analysis approach to

monitoring the sensor data and detecting the fault sensor data. Section 3 presents a method for the fusion of sensor data. Sections 4 and 5 propose a method to detect and isolate the fault sensors. Two estimation techniques are presented in Section 6. Section 7 illustrates an application to an eye movement detection process. Finally, some conclusions are made in Section 8.

6.3 Principal Component Analysis

The principal components model of multivariate analysis accounts for the variance of a set of data by providing those combinations of correlated variables that maximize the variance of a weighted sum. The weights in the principal components associated with a vector of correlated attributes (or variables) are exactly the normalized latent vectors of the covariance matrix of the vector of attributes, and the latent roots of the covariance matrix are the variance of the principal components. PCA is concerned with the analysis of one block of data, and its goal is to form new orthogonal variables, which are linear components of the original variables. If the original variables are correlated, it is possible to summarize most of the variability in much lower dimension subspace.

Assume that we have a vector $X = [x_1, x_2, \ldots, x_{px}]$, and $\Sigma = var(X)$. Let $a = [a_1, a_2, \ldots, a_{px}]$ denote a px-variate vector of unknown weights for each of the components of X, and let c_1 denote the scalar

$$c_1 = a'X = \sum_{i=1}^{px} a_i x_i \tag{6.1}$$

where each weight a_i is a measure of the importance to be placed on component x_i. To maximize $var(c_1)$, note that $c_1 = a'X$, $var(c_1) = a'\Sigma a$. Thus the problem of

finding weight vector a that maximizes $var(c_1)$ is equivalent to the problem of solving the maximization problem

$$max(a'\Sigma a) \tag{6.2}$$

Subject to the constraints on a that $a'a = 1$. One approach to solving this constrained optimization problem is to use the associated Lagarian equation

$$t = a'\Sigma a - \lambda(a'a - 1) \tag{6.3}$$

where λ is a largarian multiplier, and maximize t using the constraint. Differentiating t with respect to a, and setting the result equal to zero yields

$$\frac{\partial t}{\partial a} = 2\Sigma a - 2\lambda a = 0 \tag{6.4}$$

that is

$$(\Sigma - \lambda I)a = 0 \tag{6.5}$$

Since $a \neq 0$, there will be a solution if

$$|\Sigma - \lambda I| = 0 \tag{6.6}$$

This means that, λ is the eigenvalue of Σ, and a is a normalized eigenvector of Σ. Since Σ is symmetric and positive semi definite matrix of $px \times px$, there are px values of λ that will satisfy the determinate equation. Let us assume that the eigenvalues of Σ are $\lambda_1 >= \lambda_2 >= \ldots >= \lambda_{px}$, $\lambda_{max} = max(\lambda_i) = \lambda_1$, and the eigenvectors are $(a_1, a_2, \ldots, a_{px})$ respectively. We will see that λ_{max} is selected as the λ. It is apparent that $\Sigma a = \lambda a$, premultiplied by a' gives

$$a'\Sigma a = \lambda a'a = \lambda = var(c_1) \tag{6.7}$$

To maximize $var(c_1)$, we take λ as the largest eigenvalue λ_1, i.e. $\lambda_{max} = \lambda_1$, and $a = a_1$. The scalar $c_1 = a_1'X$ is called the first principal component. Similarly, the i^{th} principal component of X is defined as $c_i = a_i'X$, where a_i is the ith normalized eigenvector so that $var(c_i) = \lambda_i$.

Explicitly we can write

$$\begin{aligned} c_1 &= a_{1,1}x_1 + a_{1,2}x_2 + \ldots + a_{1,px}x_{px} \\ c_2 &= a_{2,1}x_1 + a_{2,2}x_2 + \ldots + a_{2,px}x_{px} \\ &\vdots \\ c_{px} &= a_{px,1}x_1 + a_{px,2}x_2 + \ldots + a_{px,px}x_{px} \end{aligned} \tag{6.8}$$

or $C = AX$, where $C = [c_1, c_2, \ldots, c_{px}]$, $X = [x_1, x_2, \ldots, x_{px}]$, and $A = [a_1\ a_2\ \ldots\ a_{px}]$ with $A'A = I$. Pre-multiplying the above equation by A' gives $A'C = A'AX = X$. If we choose the first n principal component, X can be divided into two parts, first part the linear combination of the first n principal component, second part the error part, denoted as E. Then X can be expressed as follows:

$$X = \sum_{i=1}^{n} c_i a_i' + E = c_1 a_1' + c_2 a_2' + \ldots + c_n a_n' + E \tag{6.9}$$

Let $T = [c_1\ c_2\ \ldots\ c_n]$, and $P = [a_1\ a_2\ \ldots\ a_n]$, then

$$X = TP^T + E \tag{6.10}$$

When writing the above equation, we assumed that all the insignificant information in the data set is confined to error E. In this way, the dimension of X is reduced

from px to n, $n << px$. Matrix P is called the loading matrix, whose dimension is $px \times n$, and Matrix T is called the score matrix.

The residual matrix E can be further decomposed into $\tilde{T}\tilde{P}^T$. The decomposition is made so that $[T\ \tilde{T}]$ is orthogonal and $[P\ \tilde{P}]$ is orthonormal. The correlation matrix can be approximated as:

$$R \approx \frac{1}{n-1} x^T x \tag{6.11}$$

6.3.1 Identifying the Optimal Dimension n

Parameter n is a very important factor, because if n is too small, the error E will be very large. If the n is too large, the efficiency of dimension reduction is low. Determination of the value of n is a tradeoff that depends on how much information will be sacrificed. There are some rules:

- Retain those components whose eigenvalues are greater than one.
- Determine the dimension based on the fixed percentage of the cumulative variance explained.
- Plot out the variance versus the number of component, and find approximate value of n graphically.

No mater how the decision is made, some information will be lost. Hence the parsimony rule is the key factor.

6.3.2 Online Monitoring

The data collected during the normal operation of the system can be used to perform online monitoring. There are several tools for this purpose, these include

loading plot, score plot, and contribution plot.

- Loading plot

  Loading plot shows the relationship between the system variables. All the variables sharing the same information contents tend to cluster together. If abnormal data is collected, the clusters will change accordingly, thus using the loading plot can help find out the faulty data.

  (1) Loading plot can be used to identify the relationship between variables graphically,

  (2) Similar data tend to cluster together,

  (3) Loading plot can be used to detect abnormal sensor data.

- Score plot

  Score plot is used to indicate the relationship between various samples. Two similar samples with similar scores will lie close to each other in the score plot. The score plot is a tool to detect the abnormal system behavior. However, if no abnormal shift happens, only the correlation structure breaks down, and then the plot will not be able to detect the fault, but using contribution plot can detect this.

  (1) Score plot can be used to find out the relationship between variables graphically

  (2) Similar sample tend to cluster together

  (3) Score plot can be used to detect the abnormal sensor data.

- Contribution plot

  Using contribution plot can detect the abnormal data which the score plot

cannot detect. Contribution plot based on the value of squared prediction error (SPE), which is described as follows: Assume X_{new} is the new observation. Let $c_{new} = X_{new}A$, then a prediction of X_{new} is given by $\hat{X}_{new} = C_{new}P^T = X_{new}PP^T$. The error vector is given by $e_{new} = X_{new} - \hat{X}_{new}$, and SPE is denoted as $e'_{new}e_{new}$.

6.4 Sensor Fusion

Assume the system is linear with respect to its associated multiple inputs and multiple outputs, consider the input vector $u(t) = [u_1(t), u_2(t), \ldots, u_k(t)]^T$ and output vector $y(t) = [y_1(t), y_2(t), \ldots, y_m(t)]^T$. The correlation matrix between $u(t)$ and $y(t)$ can describe their relationship. The fusion can be divided into following three steps.

- Calibration

  Let the sensor operate under the normal situation, and record the sensor data of both the input and output simultaneously. Repeat the calibration procedure. The number of repeat should be so large that the expected square error is insignificant.

- Training

  Use the recorded a block of input and a block of the output data block, to derive the module for the system.

- Experiment

  During the real operation, feed the recorded sensor input data to the model. The output of the model is the desired output.

6.5 Sensor Fault Detection

When the PCA is applied to monitor the performance of process, the squared prediction error Q [117] is usually used. The Q statistic is given by:

$$Q_n = x^T(I - P_n P_n^T)x \tag{6.12}$$

where x is the new data to be monitored. The upper limit for the Q statistic is given by

$$Q_a = \theta_1 \left[\frac{c_a\sqrt{2\theta_2 h_0^2}}{\theta_1} + 1 + \frac{\theta_2 h_0(h_0 - 1)}{\theta_1^2} \right]^{\frac{1}{h_0}} \tag{6.13}$$

where c_a is the normal deviate corresponding to the upper $100(1-a)$th percentile,

$$\theta_k = \sum_{i=n+1}^{m} \lambda_i^k \tag{6.14}$$

and

$$h_0 = 1 - \frac{2\theta_1\theta_3}{3\theta_2^2} \tag{6.15}$$

6.6 Fault Sensor Isolation

By using the SPE, Sensor fault can be detected, but it cannot isolate the fault. Using the PCA model, the fault can be isolated [118, 121, 119, 120]

As shown in Section 2, the PCA model can be expressed as

$$X = TP^T + E = TP^T + \tilde{T}\tilde{P}^T = [T\ \tilde{T}][P\ \tilde{P}]^T \tag{6.16}$$

where $[T\ \tilde{T}]$ and $[P\ \tilde{P}]$ are orthonormal matrices. The dimension of P is the number of principal components used. The relationship between P and $\tilde{P}$ is

$$[P\ \tilde{P}][P\ \tilde{P}]^T = PP^T + \tilde{P}\tilde{P}^T = I \tag{6.17}$$

where I is the identity matrix. When the model is applied to the new data, the residual $e(t)$ is

$$\begin{aligned} e(t) &= x_{new}(t) - \hat{x_{new}}(t) \\ &= x_{new}(t) - PP^T x_{new}(t) \\ &= (I - PP^T)x_{new}(t) \\ &= \tilde{P}\tilde{P}^T x_{new}(t) \end{aligned} \tag{6.18}$$

Now assume $x_{new}(t) = x^0_{new}(t) + \Delta x_{new}(t)$, where $x^0_{new}(t)$ is true value, and the $\Delta x_{new}(t)$ is fault value. It is easy to find out that $\tilde{P}^T x^0_{new}(t) = 0$. thus we can dèfine the primary residual as $e(t) = \tilde{P}^T \Delta x_{new}(t)$. Using the primary residual, we can get the new residual $e^*(t) = We(t) = W\tilde{P}^T \Delta x_{new}(t)$ through a $px - n$ by $px - n$ transformation matrix W, so that the structure of $W\tilde{P}$ is isolable. If the ideal isolation structure is I_s, then we require

$$W_{(px-n,px-n)}\tilde{P}^T_{(px-n,px)} = I_{s(px-n,px)} \tag{6.19}$$

where $\tilde{P}^T$ can be obtained from the PCA model, I_s is predefined, and W can be determined from the above equation. Because the number of unknown variables are less than the number of linear equations, usually there will be no solution for W, but LMS method can be used to estimate an optimal W.

6.7 Error Data Recovering

6.7.1 LMS Method For The Sensor Data Estimation

When the sensor is used to explore the property of the object, the information is gathered as much as possible. Since the object's property is changing with respect to the time, higher sample rate need to be used to detect the object, so that the object property change becomes insignificant during one time interval of processing. In this way, the data obtained by each sensor is very smooth and can be approximated by a polynomial model. Typically a polynomial model can be expressed as:

$$f(t) = a_0 + a_1 t + a_2 t^2 + \ldots + a_n t^n \tag{6.20}$$

where t is time and $[a_0, a_1, \ldots, a_n]$ are coefficients. The least mean square error method can be used to determine the coefficients.

6.7.2 Minimum Error Variance Method

The unknown value is estimated by using a weighted linear combination of the available samples:

$$\hat{v} = \sum_{j=1}^{n} w_j v_j \tag{6.21}$$

The error r is defined as the difference between the estimated value and the true value

$$r_i = \hat{v_i} - v_i \tag{6.22}$$

v_i is the true value. Then the average error of k estimate is

$$m_r = \frac{1}{k}\sum_{i=1}^{k} r_i \tag{6.23}$$

Because v_i is not available, we cannot obtain $\hat{v}_i$ from above equation.

The error variance σ_R^2, can be written as

$$\sigma_R^2 = \frac{1}{k}\sum_{i=1}^{k}(r_i - m_r)^2 \tag{6.24}$$

$$= \frac{1}{k}\sum_{i=1}^{k}((\hat{v}_i - v_i) - (\frac{1}{k}\sum_{i=1}^{k}(\hat{v}_i - v_i)))^2 \tag{6.25}$$

Here $[v_1, v_2, \ldots, v_n]$ are the true values, $[\hat{v_1}, \hat{v_2}, \ldots, \hat{v_n}]$ are the corresponding estimates.

Because of the unknown v_i, σ_R^2, we cannot get $\hat{v}_i$, so the first step is to get σ_R^2.

Let us assume that some random noise is added to the data, so the error is also a random variable, since it is a weighted linear combination of other random variables. Now we compute

$$\hat{V}(X_0) = \sum_{i=1}^{n} w_i V(X_i) \tag{6.26}$$

$$R(x_0) = \hat{V}(X_0) - V(X_0) \tag{6.27}$$

$$var(R(x_0)) = cov(\hat{V}(X_0)\hat{V}(X_0)) \tag{6.28}$$

$$-2cov(\hat{V}(X_0)V(X_0)) + cov(V(X_0)V(X_0))$$

The first term of equation 6.11 is

$$cov(\hat{V}(X_0)\hat{V}(X_0)) = var(\sum_{i=1}^{n} w_i V_i) = \sum_{i=1}^{n}\sum_{j=1}^{n} w_i w_j \tilde{c_{ij}} \tag{6.29}$$

where $\tilde{c_{ij}} = cov(V_i V_j)$.

And the second term can be written as

$$\begin{aligned} & cov(\hat{V}(X_0)V(X_0)) \\ & = 2cov((\textstyle\sum_{i=1}^{n} w_i V_i)V_0) \\ & = 2E(\textstyle\sum_{i=1}^{n} w_i V_i V_0) - 2E(\textstyle\sum_{i=1}^{n} w_i V_i)E(V_0) \\ & = 2\textstyle\sum_{i=1}^{n} w_i \tilde{c_{i0}} \end{aligned} \tag{6.30}$$

By combining these three terms, we have the following equation:

$$\tilde{\sigma}_R^2 = \tilde{\sigma}^2 + \sum_{i=1}^{n}\sum_{j=1}^{n} w_i w_j \tilde{c_{ij}} - 2\sum_{i=1}^{n} w_i \tilde{c_{i0}} \tag{6.31}$$

Once $\tilde{\sigma}^2$ and all covariance $\tilde{c_{ij}}$ are computed, above equation becomes a function of $W_1, \ldots, W_n$, i.e.,

$$\tilde{\sigma}_R^2 = f(w_1, w_2, \ldots, w_n) \tag{6.32}$$

The minimization of $\tilde{\sigma}_R^2$ is accomplished by setting the n partial first derivatives of $\tilde{\sigma}_R^2$ with respect to W_i for $1 <= I <= n$ to zero.

$$\frac{\partial(\hat{\sigma}_R^2)}{\partial(w_1)} = 2\sum_{j=1}^{n} w_j \tilde{c_{1j}} - 2\tilde{c_{10}} = 0$$

$$\frac{\partial(\hat{\sigma}_R^2)}{\partial(w_2)} = 2\sum_{j=1}^{n} w_j \tilde{c_{2j}} - 2\tilde{c_{20}} = 0$$

$$\vdots \tag{6.33}$$

$$\frac{\partial(\hat{\sigma}_R^2)}{\partial(w_n)} = 2\sum_{j=1}^{n} w_j \tilde{c_{nj}} - 2\tilde{c_{n0}} = 0$$

Which yields

$$\sum_{j=1}^{n} w_j \tilde{c_{ij}} = \tilde{c_{i0}}, i = 1, 2, \ldots, n. \tag{6.34}$$

i.e.,

$$\begin{bmatrix} \tilde{c}_{11} & \cdots & \tilde{c}_{1n} \\ \vdots & \ddots & \vdots \\ \tilde{c}_{n1} & \cdots & \tilde{c}_{nn} \end{bmatrix} \begin{bmatrix} w_1 \\ w_2 \\ \vdots \\ w_n \end{bmatrix} = \begin{bmatrix} \tilde{c}_{10} \\ \tilde{c}_{20} \\ \vdots \\ \tilde{c}_{n0} \end{bmatrix} \tag{6.35}$$

Because the matrix in equation 6.35 is positive semi definite, this equation has one unique solution.

6.8 Application of the Eye Movement Detection

Multiple linear sensor arrays are used to detect the eye movement [122]. The infrared emitter mentioned in chapter 2 generates send out the infrared lights to illuminate the eye. The reflected lights are detected by a detector array. Because the

infrared sensor array is close to each other, the data among them are highly correlated. We can use the PCA model to examine the data, detect, isolate and recover from any sensor fault.

6.8.1 System Under Normal Operation

During the simulation, we use linear sensor array with seven sensor cells to detect the eye movement. So the data block will be $x_{n,m}$, where m=7 is the number of the sensor, and n is number of samples. Assume at first the data are all good. After analyzing the data, we obtain the correlation matrix and its eigenvalues in table 6.1

Number	1	2	3	4
Eigenvalue	5.1377	1.7647	0.0461	0.0254
Number	5	6	7	
Eigenvalue	0.0165	0.0090	0.0006	

Table 6.1: Eigenvalues of the Correlation Matrix

According to the rules discussed in Section 4.3.1 to identify the optimal dimension, since only λ_1, λ_2 are greater than 1, so the first principal component and the second principal component are chosen, and.

$$\frac{\lambda_1 + \lambda_2}{\sum_{i=1}^{7} \lambda_i} = 0.9861 \tag{6.36}$$

Shown in figure 6.1 are the two monitoring plots, namely the loading plot and the score plot, from which, it is easy to find out that the data tend to cluster together. The SPE test under normal operation region is shown in figure 6.2.

The residual space is given by

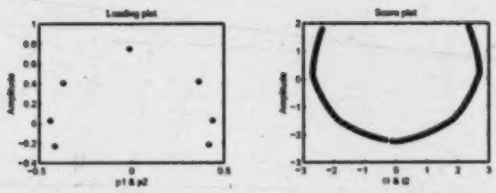

Figure 6.1: Loading and Score Plot for Normal System

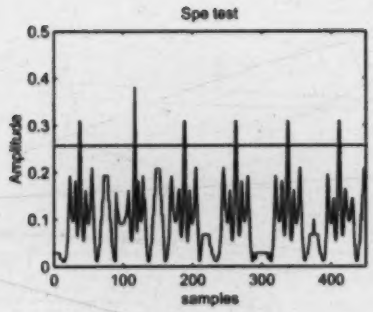

Figure 6.2: SPE Test

$$\begin{bmatrix} +0.5461 & -0.0628 & -0.2275 & +0.5743 & -0.2336 & -0.0322 & +0.5105 \\ -0.5538 & +0.3771 & +0.1891 & +0.0224 & -0.2065 & -0.3685 & +0.5800 \\ +0.0729 & +0.4049 & -0.5756 & +0.0152 & +0.5677 & -0.4150 & -0.0681 \\ -0.2712 & +0.4659 & -0.4135 & +0.2554 & -0.4117 & +0.4731 & -0.2828 \\ +0.3082 & +0.5286 & +0.3192 & -0.2161 & +0.3319 & +0.5231 & +0.3054 \end{bmatrix}$$

A desired structure is:

	ΔS_1	ΔS_2	ΔS_3	ΔS_4	ΔS_5	ΔS_6	ΔS_7
r_1	0	1	1	1	0	0	1
r_2	0	0	1	1	1	1	0
r_3	1	0	0	1	1	0	1
r_4	1	1	0	0	1	1	0
r_5	1	1	1	0	0	1	1

Table 6.2: Desired Isolation Structure

The transformation matrix W obtained by the LMS method is given by.

$$\begin{bmatrix} 0.6926 & 1.6870 & -0.3025 & -0.4958 & 1.4394 \\ -1.7949 & -0.2048 & -1.1247 & -1.2968 & 1.9376 \\ 0.2511 & -0.6942 & 0.6290 & -0.7724 & 0.7239 \\ 0.8839 & -1.9672 & 0.1670 & 0.5403 & 2.7962 \\ 1.3561 & 1.2824 & -1.1405 & -0.7973 & 2.7146 \end{bmatrix}$$

Which yields the transformed space

$$\begin{bmatrix} -0.0000 & +1.0000 & 1.0000 & -0.0067 & 0.0000 & 0.0000 & 1.9326 \\ +0.0000 & -0.0000 & 2.1716 & -1.8025 & 1.0000 & 1.0000 & 0.0000 \\ +1.0000 & -0.0000 & 0.0000 & -0.2154 & 1.0000 & 0.0000 & 0.1222 \\ +2.2996 & +1.0000 & 0.0000 & -0.0000 & 1.0000 & 2.3456 & 0.0000 \\ +1.0000 & +1.0000 & 1.7866 & +0.0000 & 0.0000 & 1.0000 & 2.5684 \end{bmatrix}$$

6.8.2 System With Sensor Fault

6.8.2.1 Simulation Results For Soft Sensor Failure

Soft sensor failure is referred to as sensors that are still working, however, the sensor data are corrupted with some noise. The amplitude of the sensor noise is usually very low. Since there are total seven sensors in the infrared sensor array, we divide the data into eight periods. For the first seven periods, we add the fault data to the sensor data, which is shown in following table 6.3. One means that fault has happened, 0 means no fault has happened.

Time	ΔS_1	ΔS_2	ΔS_3	ΔS_4	ΔS_5	ΔS_6	ΔS_7
$1 - -50$	1	0	0	0	0	0	0
$51 - 100$	0	1	0	0	0	0	0
$101 - 150$	0	0	1	0	0	0	0
$151 - 200$	0	0	0	1	0	0	0
$201 - 250$	0	0	0	0	1	0	0
$251 - 300$	0	0	0	0	0	1	0
$301 - 350$	0	0	0	0	0	0	1
$351 - 450$	0	0	0	0	0	0	0

Table 6.3: Structure of the Faulty Sensors

Figure 6.3 is the plot of loading and score plot. Because of the fault data, the data has transferred from original place to other place. It is easy to find out from figure 6.4, that the sensor data has fault from the beginning to data sample 350. It is under normal operation after. Figure 6.5 shows the residual structure. The index at each moment reflects the faulty sensor. For example, from data 0-50, first sensor fault, the index should be [00111], which is exactly shown in figure 6.5.

6.8.2.2 Simulation Results for Hard Sensor Failure

Hard sensor failure means that the sensor does not work at all. Usually in electronics it can be defined as the stuck-at sensor failure, where the sensor is stuck

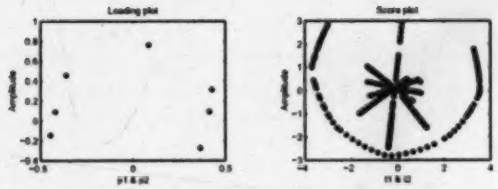

Figure 6.3: Loading and Score Plot Under Sensor Fault

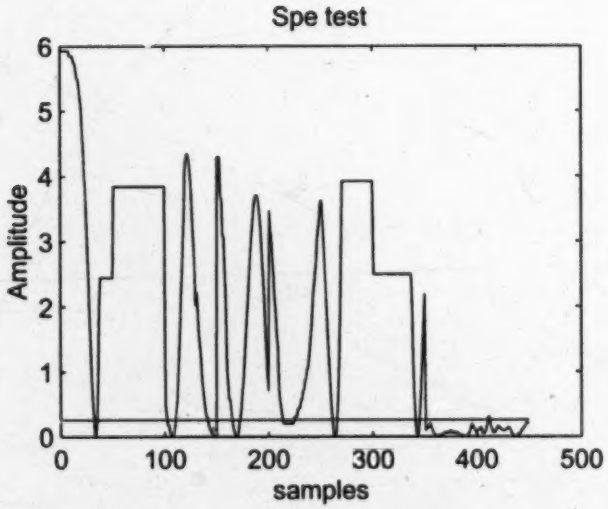

Figure 6.4: SPE Test Under Sensor Fault

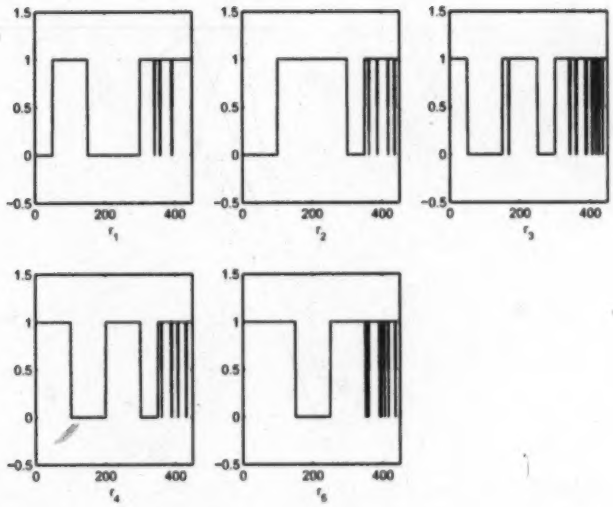

Figure 6.5: Use Residual Structure to Isolate the Fault

at one extreme of its signal range. In practice, this is likely to be an open (stuck-at 0) sensor or a short circuited (stuck-at 1) sensor. Figure 6.6 shows SPE test under the hard sensor failure when each sensor is stuck at extreme value. The residual structure is same as the soft sensor failure. From the simulation, it is found that the sensor fault can be isolated. In this chapter we assume only one sensor is fault at one time.

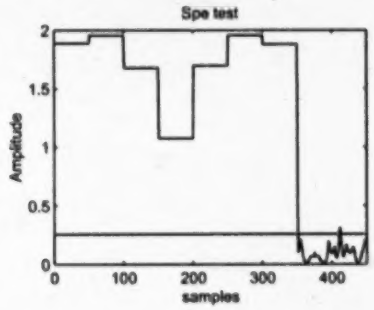

Figure 6.6: SPE Test Under Hard Sensor Failure

6.8.3 Fault Sensor Recovery

When the fault happens, it needs to be isolated and recovered. Previous sections addressed the isolation problem when a sensor fault appears. This section will address the recovery problem. If the sensor data is not changing rapidly during the operation, the faulty data is simply replaced by the previous data. But when the data is changing quickly, some estimation methods need to be used to handle the problem. In this section, two methods are presented for estimation. Method 1 is a minimum variance method and method 2 is a LMS method. As shown in table 6.4, the first row shows the noise level, which is the percentage of the maximum value of the signal. The second and the third rows show the average error between the measurement and the estimation in percentage for method 1 and method 2, respectively. From the table, we

can observe that when the noise level is low, method 2 performs better than method 1. But the performance of method 2 degrades as the noise level becomes higher, and eventually method 1 becomes a preferred choice. So when we operate the system, we can combine these two methods together to confront the different noise environment.

Noise %	0	1.56	3.12	3.90	7.81	9.76
Method 1	8.88	9.98	9.18	9.23	10.25	11.42
Method 2	0.91	3.86	6.55	8.02	15.91	20.35

Table 6.4: Comparison Between Two Methods

6.9 Conclusion

A principal component analysis technique was presented which enables a system to detect faulty external sensors. The approach has been applied to eye movement detection and verified by simulation with soft sensor failure and hard sensor failure using infrared linear arrays. Two sensor fault recovery methods are also explored and compared with each other through simulation.

This approach does not require the assumption that the individual sensor statements are independent. It not only extends the types of the sensor used, but also makes the approach flexible in terms of the number of the sensors used.

Simultaneous multiple sensor failure detection is not covered in this chapter. The possibility of the simultaneous sensor failure is very low; still it will have worse effect on the system than the single sensor failure. Further works will concentrate on detecting the simultaneous multiple sensor failure.

Chapter 7

Using FIR Median Hybrid Filters on Study of Eye Movements in Robotic Eye System

7.1 Introduction

This chapter describes an approach of using FIR Median Hybrid Filters for analysis of eye movements in the Robotic Eye System. In the Robotic Eye System's second model, the real eye movement is detected using the biomedical electrodes. However, the bio-signal is corrupted with the eye blink artifact. Using the FIR hybrid Filter, eye blink artifact can be removed from the eye movement signal.

The background of the project is described first. From the review of the eye movement methods, the electro-oculogram (EOG) to determine the eye position is used. The FIR Median Hybrid Filter is studied in the chapter. Its properties are explored with examples. Finally the filter is used to deal the real eye blink corrupted

EOG signal. Examples are given of analysis procedure for eye tracking or a random moving target. The method proved to be highly reliable.

7.2 Background

The loss of an eye results in a shocking deformity. A person with one eye missing, through various reasons, may suffer severely psychologically as well as physically. These problems frequently concern the re-constructive surgeons, who want to create the artificial eye. The purpose of our project is to develop an ocular system to let the artificial eye have the same natural movement. To provide the artificial eye with the same functionality as the muscles, the artificial eye was mounted onto a tiny small servomotor. The aim of the present project is to sense the natural eye movement in the horizontal direction only and then to control the motor to drive the artificial eyeball to move correspondingly and naturally, matching the horizontal movement of the natural eye. Eye movement methods were extensively reviewed to find the suitable sensing method for this project. The sensor should be small, easy to mount, not invasive and not obstruction of the vision of the real eye. EOG method is one of the most suitable methods that can be used for the project. As a classic eye movement method, EOG is extensively used for many applications, such as detection of the rapid eye movement in infants [136], determination of the eye position in fast jet flight [147], and in the development of a fish eye VR system [135]. There are many techniques used to analysis the EOG signal, such as kalman filter [137], conventional and matched filtering method [139], non linear eye movement detection method [145].

The EOG signal is always corrupted by the eye blink signal, which is of high amplitude with a short half-wave lasting approximately 0.2 seconds [145]. The ad-

dressed problem can be solved using the Median filter, which has been previously applied to biological signal processing, mainly to situations in which the mean value of the signal abruptly changes.

This chapter mainly talks about using different kinds median filter to process the EOG signal [146].

Median filtering, first introduced in 1971, is a rather well-understood nonlinear data smoothing technique useful for noise suppression [134, 138, 142, 141, 140]. Median filters are used in many signal processing applications [143] and in image processing [144] due to their good edge preserving ability combined with moderate noise attenuation on flat regions. Median filter is better than classical smoothing procedure in certain situations, their advantages are:

- Median filters preserve sharp edges, whereas linear low-pass filtering blurs such edges.
- Median filters are very efficient for smoothing of spiky noise.

In noise free situations an ideal edge is preserved completely, the property cannot be achieved with any other linear low-pass filter. However, in noisy conditions also the median filters lose their ability to preserve sharp edges, so improved FIR Median Hybrid filter is used instead.

The rest of the chapter is organized as follows. In section 2, median filter and improved median filter are given and their characteristic is explored. In section 3, the properties of the median filters are explored. Numeric examples are included. The method is used to process EOG data in section 4, last section concludes the chapter.

7.3 Median Filters and Improved Median Filters

7.3.1 Median Filters

The median of n numbers x_1, x_2, ..., x_n is, for n odd, the middle number in size. It can be written in form:

$$Median(x_1, x_2, \ldots, x_n) \tag{7.1}$$

A median filter of size n on a sequence is for n odd defined through

$$y_i = Median(x_i) = Median(x_{i-v}, \ldots, x_i, \ldots, x_{i+v}), \tag{7.2}$$

where $v = (n-1)/2$, median filters are known to preserve sharp change in signals, which, in many cases, happened in biomedical and communication signals. However, one of the disadvantages of the median filters are the fact that sinusoidal waveforms are distorted in the process, another disadvantage is that the median filters lose its properties in noise conditions. To solve this problem, Hybrid filter is introduced.

7.3.2 FIR Median Hybrid Filter

The FIR Median hybrid (FMH) filters consist of few linear FIR sub filters and the median operation taken over the outputs of the substructures. All kinds of FIR filters can be used as substructures. The general form of the hybrid filter is defined by

$$y(n) = Median(f_1(x(n)), f_2(x(n)), \ldots, f_m(x(n)))), \tag{7.3}$$

Where f_1, f_2, ..., f_m are linear FIR filters, which work on the input signals. The block diagram of the general structure of the FMH filter is shown in figure 7.1.

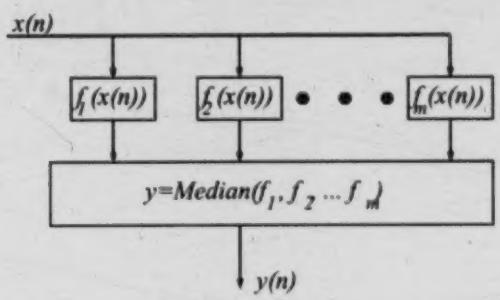

Figure 7.1: General Structure of the FMH Filter

7.3.3 Least Square Optimal Approach

When the sensor is used to explore the property of the object, the information obtained must be maximized. The object's property is changing with respect to time. A higher sample rate will be used to detect the object, so that the object property change is insignificant during the time interval. In this way, the data for each sensor is very smooth and can be approximated by a polynomial equation. We are given a collection of data $\{z(t_1), z(t_2), \ldots, z(t_n)\}$, that are noisy measurements of a process, which is estimated by a polynomial equation and can be expressed as follows:

$$y = a_0 + a_1 * t + a_2 * t^2 + \ldots + a_n * t^n \tag{7.4}$$

t is time, $[a_0, a_1, \ldots, a_n]$ are unkown coefficients. Measurements are of

$$z(t_k) = y_k + v_k \tag{7.5}$$

Where v_k is observation error, with variance ${\sigma_k}^2$ We let the estimate be

$$\hat{y}_k = \hat{a}_0 + \hat{a}_1 * t + \hat{a}_2 * t^2 + \ldots + \hat{a}_n * t^n \tag{7.6}$$

Assume the observation error zero mean and uncorrelated with each other, and have the variance ${\sigma_k}^2$, or the covariance matrix

$$R = diag\{{\sigma_1}^2, \ldots, {\sigma_{n+1}}^2\} \tag{7.7}$$

Residual is designed as

$$r_k = z_k - \hat{y}_k = (y_k - \hat{y}_k) + v_k \tag{7.8}$$

The mode is shown in figure 7.2.

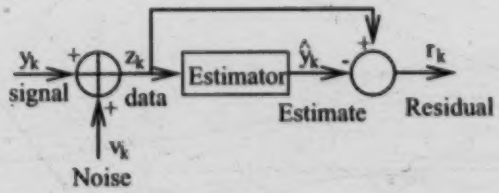

Figure 7.2: The Block Diagram of the Estimator

The least-square estimation problem may be stated: Determine $\{\hat{a}_k\}$ to minimize the sum of the squared weight residuals

$$J = \sum_{k=1}^{n} (r_k/\sigma_k)^2 \tag{7.9}$$

We can find $\{\hat{a}_k\}$by setting

$$\frac{\partial J}{\partial(\{\hat{a}_k\})} = 0 \tag{7.10}$$

Once we get $\{\hat{a}_k\}$, we get the model signal, then by plugging the next time internal, we will be able to estimate the next step signal.

7.3.4 Residual Smoothing

For small white noise, a method called residual smoothing can filter it out. Assume that the x variables are generated by a signal-plus-noise model

$$x_i = s_i + n_i \tag{7.11}$$

Where the signal s_i varies slowly compared with the noise n_i. Median filtering gives an estimate of s_i

$$y_i = Median(x_i) \approx s_i \tag{7.12}$$

Thus the residuals

$$\hat{n}_i = x_i - Median(x_i) \approx n_i \tag{7.13}$$

Gives the estimates of the noise variables. Further median filtering of the residuals could reduce the noise further

$$z_i = Median(\hat{n}_i) \approx 0 \tag{7.14}$$

Addition of y_i and z_i now gives a hopefully good estimate of s_i,

$$\hat{s}_i = y_i + z_i = Median(x_i) + Median[x_i - Median(x_i)] \tag{7.15}$$

Simulation results show that using above equation can achieve better results than using equation 6.12.

7.3.5 Linear-nonlinear Combinational Filters

A new class of linear-nonlinear combinational filter is developed in this chapter. It will be able to restore the biomedical signal not only from the impulsive noise, but also from the Gaussian noise. Figure 7.3 shows the structure of the linear-nonlinear combinational filter. It consists two parts. The least square optimal filters are used in the first layer to remove the noise. The median filter is used in the second layer to preserve the edge and remove the impulses. The better performance was achieved by using the following structured filter. It can remove the impulse noise, preserve the edge, and filter out the white noise.

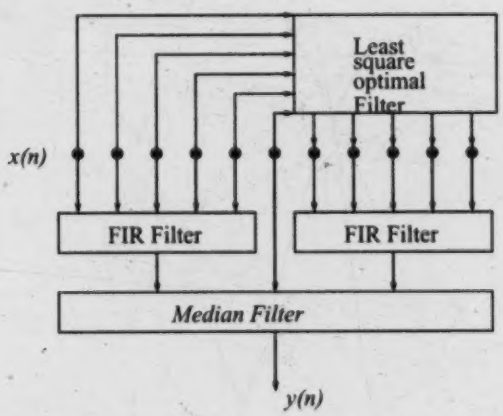

Figure 7.3: Linear-Nonlinear Combinational Filters

7.4 Properties of the Median Filters

The noise attenuation properties of all the types of median filters are explored in this section. Because the median filters are nonlinear, this complicates the mathematical analysis of their performance. It is not possible to separate signal effects and noise effects as simply as for linear filter. So we start from the easiest case.

Assume the input signal has the probability density and distribution functions of $f(x)$ and $F(x)$ respectively. The length of the filter window is $N = 2k + 1$. The probability density of

$$y = Median(x_{i-k}, \ldots, x_i, \ldots, x_{i+k}),$$

is given by

$$f_m(y) = n \begin{pmatrix} n-1 \\ (n-1)/2 \end{pmatrix} f(y) F(y)^{(n-1)/2} [1 - F(y)]^{(n-1)/2} \tag{7.16}$$

Let us consider an input signal consisting of a polynomial signal corrupted by white noise. In the figure 7.3, the median is taken over three values. $x_l(n)$, $x(n)$, and $x_r(n)$. Assume their density functions are $f_l(x)$, $f(x)$, and $f_r(x)$, and distribution functions are $F_l(x)$, $F(x)$, and $F_r(x)$ respectively. Then the output density function becomes

$$\begin{aligned} f_{out}(y) &= f(y)(F_l(y) + F_r(y) - 2F_l(y)F_r(y)) \\ &= f_l(y)(F(y) + F_r(y) - 2F(y)F_r(y)) \\ &= f_r(y)(F_l(y) + F(y) - 2F_l(y)F(y)) \end{aligned} \tag{7.17}$$

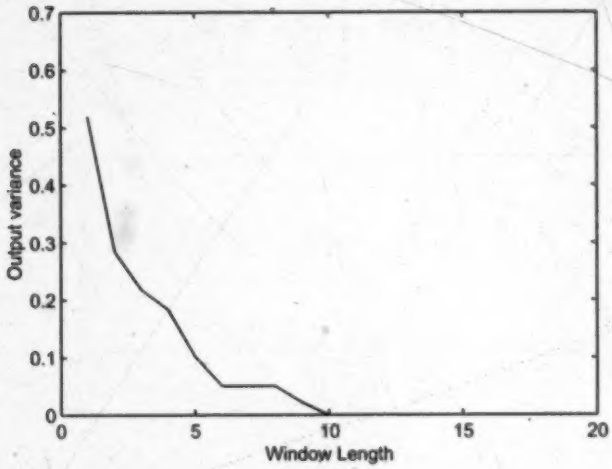

Figure 7.4: Output Variance Versus Filter Window Length

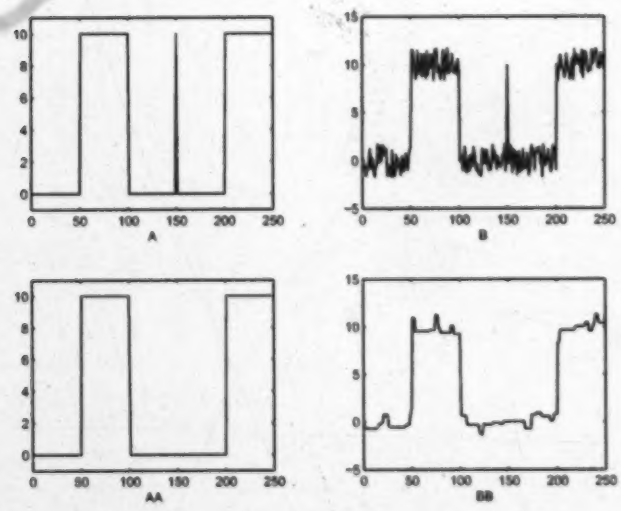

Figure 7.5: Use Linear-Nonlinear Combinational Filters to Filter the Signal with and without Noise

Numeric examples are shown in figure 7.4 and figure 7.5 respectively. In figure 7.4, the input is a zero mean unit variance Gaussian noise. Different window length of the median filter is used to process the input, and the variance of the output is obtained. From the simulation, it is easy to find out that with shorter window length, the output noise becomes larger. A numeric example is given in figure 7.5. Input signals are shown in A without noise and B with white noise. Both signals have the spike, which should be removed. Picture AA and BB are the corresponding processing results. For the signal without noise, the spike is wiped out, and the signal is totally restored. For the second input with white noise corrupted, the spike is also removed, some very small spike happened somewhere else, which is related to the window length.

7.5 Experimental Study with the EOG

7.5.1 Using EOG to Detect the Eye Horizontal Movement

To measure the eye movement, we detected the EOG signal. Two small (6-8mm in diameter) Ag/AgCl electrodes were used for the recording. One electrode was placed on the skin outside each eye. A low impedance disposable electrode is located on the midline of the forehead and functioned as a reference electrode. The configuration of the electrodes is shown in figure 7.6. One pair of horizontally placed electrodes is to record the horizontal eye movements. The potential difference between the two electrodes is amplified and sent to the computer through the AD card with a $30Hz$ sample frequency. At the same time, the amplified signal is shown on the screen of an oscilloscope, as shown in figure 7.7.

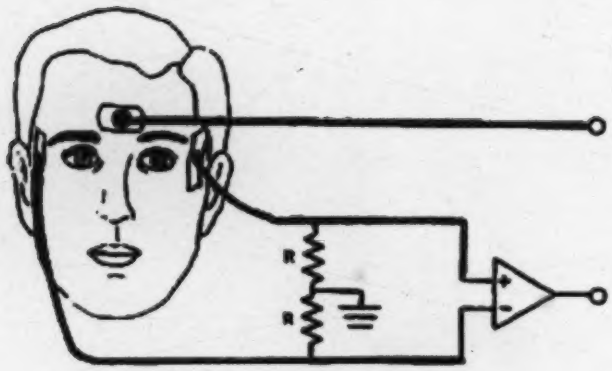

Figure 7.6: Electrode Configuration

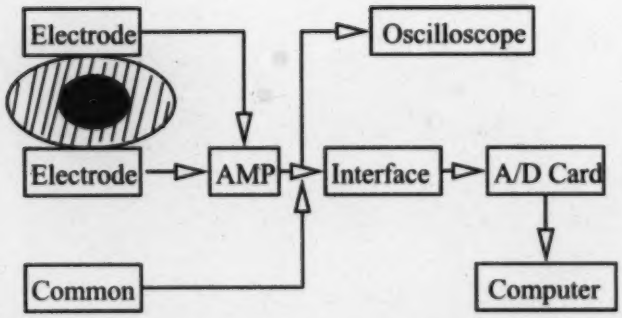

Figure 7.7: The Block Diagram of EOG Based Eye Movement Detection System

7.5.2 Using the Median Filter to Remove the Eye Blink from the Corrupted Signal

The overall performance of the EOG detection system was good. The subject was asked to sit still and quiet to prevent the EMG and other artifacts from entering the EOG channel. During the experiment, the subject was asked to look at the center first, and intentionally blinked his/her eye. Then the subject randomly moved his/her eye. The EOG signal will be recorded. As shown in figure 7.8, the upper part is the eye blink corrupted EOG signal. It is apparent that two eye blinks happened during the recording period. The filter can remove the eye blink and recover the eye movement signal, as shown in the lower part of the figure.

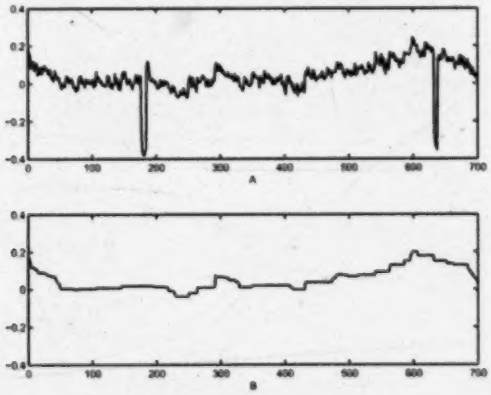

Figure 7.8: Using the Median Filter to Remove the Eye Blink

7.6 Conclusion

In this chapter, an improved median filter was described. It can remove the eye blink signal from the EOG signal. Compared to the regular linear FIR filter, this

method works better under white noise and preserves the edges very well. To realize the method in real time, this approach needs to be validated by hardware design. The filter can be built into the micro controller of the robotic eye system as the processor before the controller control the artificial eye to move.

Chapter 8

Fundamental Study of Robotic Motion Control for Robotic Eye System

This chapter addresses several techniques to control the robot manipulator under the uncertainty model, which can be applied to the Robotic Eye System.

First a neural network is proposed to control the robot to follow the generated path. This network model is able to compensate the structured and unstructured dynamic uncertainties of the robot by using both on-line and off-line training. PD control, computed torque control, and adaptive control with and without exact model are used to control the robot and compared with the proposed method. The simulation study on a 2-d.o.f planar robot is included, which can be applied to the robotic eye system.

8.1 Introduction

To reach a specific target, the robot should follow the trajectory with controller. There are lots of studies of the control aspects of a robot [153, 151]. An ideal robot control system is difficult to achieve. There are environment noise, modeling error and faults which will effect the robot system as shown in figure 8.1).

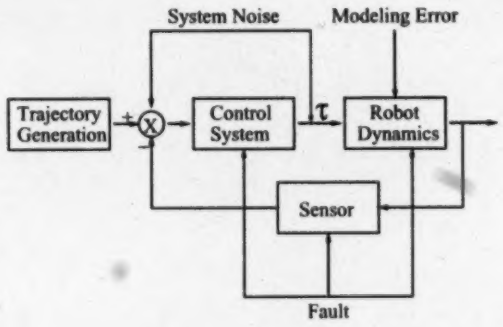

Figure 8.1: A Typical Robot Control System with Uncertainties

It is difficult to control the robot under uncertainties. Classic PD controller doesn't require the model of the robot, however, it needs the large actuation to achieve precise control. Computed torque controller needs the exact model to have good performance. Adaptive controller can deal with the robot under uncertainty model. There are lots of studies of robot control under uncertainties using neural networks [148, 149]. Meng [150] proposed efficient neural network architecture for identification and adaptive control of unknown robot dynamics. These controllers can achieve precise control and compensate partially unknown manipulator dynamics, but it needs the online estimation of the robot dynamics.

This chapter begins with a proposed neural network, which can control and compensate partially unknown manipulator dynamics. The results of the simulation

were presented and the control algorithms were compared with each other. The chapter concludes with the discussion and further considerations

8.2 Partially Unknown Robot Manipulator Control

A one-layered feed forward neural network is designed for motion control of robot manipulators.

8.2.1 Model for Motion Control of Robot Manipulators

The dynamics of an n d.o.f rigid robot manipulator can be described by

$$M(q)\ddot{q} + c(q,\dot{q}) * \dot{q} + G(q) = \tau \tag{8.1}$$

Where τ is the vector of joint torques; q, $\dot{q}$, and $\ddot{q}$ are the joint position, velocity and acceleration, respectively; M, C and G represent the mass, velocity and gravity terms, respectively. Equation (8.1) can also be expressed as [150]

$$M\ddot{q} + C * \dot{q} + G = Y(q,\dot{q},\ddot{q}_r) * \Theta = \tau \tag{8.2}$$

Where $Y \in R^{n \times r}$ is a coefficient matrix consisting of known function of q, $\dot{q}$, and $\ddot{q}$, which is called manipulator regressor, and $\Theta \in R^{r \times 1}$ is a vector consisting of known and unknown robot dynamic parameters. The control law is assigned as

$$\tau = Y(q,\dot{q},\ddot{q}_r) * \hat{\Theta} - Ks \tag{8.3}$$

Where $\dot{q}_r = \dot{q}_d - \Lambda * e$, $s = \dot{q} - q_r$, $e = q - q_d$ and K and Λ are a constant matrices (for more detail, see Meng, [150]). Variable $\hat{\Theta}$ can be expressed as

$$\hat{\Theta} = \bar{\Theta} + \Delta\Theta \tag{8.4}$$

Where $\bar{\Theta}$ is obtained by an off-line learning process using a recursive error back propagation process [152]. $\Delta\Theta$ is updated using an on-line learning process,

$$\Delta\dot{\Theta} = -\Gamma Y^T s \tag{8.5}$$

Where $\Gamma > 0$ is a constant matrix Choosing a Lyapunov function

$$v = \frac{1}{2}(s^T M s + (\hat{\Theta} - \Theta)^T \Gamma^{-1}(\hat{\Theta} - \Theta)) \tag{8.6}$$

It is proved that the position and velocity tracking error converge to zero [150]. The off-line training process can be expressed as

$$Y = WX \tag{8.7}$$

Where $Y \rightarrow \tau$, $X \rightarrow Y(q, \dot{q}, \ddot{q}_r)$ and $W \rightarrow \Theta$.

The weight W is updated by

$$W_m = W_{m-1} + (1 - X^T{}_m P_{M-1} X_m)^{-1}(Y_m - W_{m-1} X_m) X_m{}^T P_{m-1} \tag{8.8}$$

The variable P is updated by

$$P_m = P_{m-1} + (1 - X^T{}_m P_{M-1} X_m)^{-1} P_{m-1} X_m) X_m{}^T P_{m-1} \tag{8.9}$$

Where $X_m = [X_{m-1}, X_m]$, $Y_m = [Y_{m-1}, Y_m]$. For details, see [152].

8.3 Simulation Study

8.3.1 Trajectory Generation

For simplification without losing generalization, a two-degree of freedom (d.o.f) planar robot is used for simulation study. The length of the two links is chosen as $1m$

and the point mass of each link is $2k_g$ and $1k_g$ respectively. The desired trajectory is an ellipse with the horizontal axis length $1.5m$ and the vertical axis $1m$ respectively. Using inverse kinematics, the joint space $[\theta\ \dot{\theta}\ \ddot{\theta}]$ of the robot tracking the whole ellipse is obtained. The trajectories of the robot in joint space and Cartesian space are shown in figure 8.2

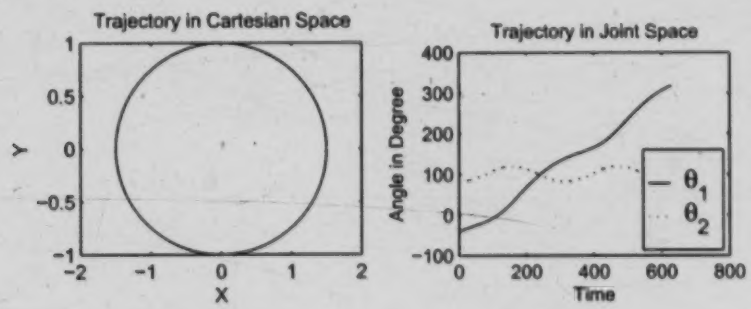

Figure 8.2: Cartesian Space and Joint Space

8.3.2 Using the Proposed Neural Network Controller to Control the Robot Under Uncertainty

Using proposed neural network architecture; several computer simulations have been done with motion control of robot manipulators. To control the robot to follow the generated trajectory shown in the left panel of figure 8.2, the desired velocity and acceleration of the desired trajectory are obtained by using the inverse Jacobian and the derivative of the inverse Jacobian. Then, the neural network is trained off-line using the recursive error back propagation process. The weights are referred to the manipulator regressor is given by

$$\theta^T = [m_2 l_1 l_2\ \ m_2 {l_2}^2\ \ m_2 l_2\ \ (m_1 + m_2) l_1\ \ (m_1 + m_2) {l_1}^2] \tag{8.10}$$

The true value of m_1 and m_2 are 2 and 1 respectively, the true value of l_1 and l_2 are 1 respectively. The initial of θ^T is chosen randomly. After three steps, the final error is less than 10^{-6}. After learning, the manipulator regressor is [1.00 1.00 1.00 3.00 3.00], and the true values is [1 1 1 3 3], which is exactly the same with the trained results as shown in figure 8.3.

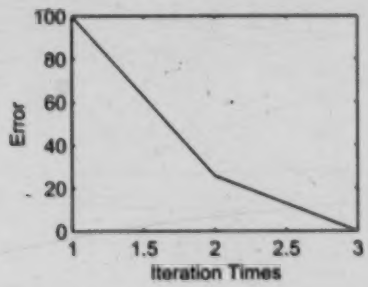

Figure 8.3: The Error Dynamics of Off-Line Training

Then the weight obtained via off-line training process is used as the initial values for the adaptive on-line training whose learning algorithm is described in (8.7-8.9). The initial position, velocity and acceleration is chosen 95% of the desired initial values, respectively. In addition, a disturbance $[1\ 1]^T$ is added to the model. The dynamics of the trajectory in workspace is shown in the left panel of figure 8.4. The right panel of figure 8.4 shows the error dynamics of two joint angles. The steady-state error of θ_1, θ_2 are -0.1600^o and 0.0337^o, respectively. It shows that proposed model could follow the generated trajectory very well.

8.3.3 The Comparison of Joint Dynamics With Other Controller

To see how well the proposed model performs, several other control approaches, such as PD controller, computed torque controller and adaptive controller are used

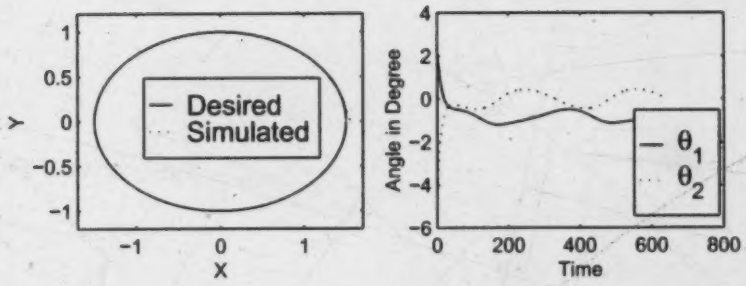

Figure 8.4: The Trajectory and Error Dynamics Using Neural Network Controller. The Left Panel Shows the Simulated Trajectory in Comparison with the Desired Trajectory. The Error Dynamics is shown in the Right Panel.

to control the robot to follow the desired trajectory.

First, a PD controller is used. Figure 8.5 shows the error dynamics of the joint angles. Various gains are tried to test the PD controller, and when $Kp = 200$ and $kv = 10$, the controller can achieve a better result. The steady state error of the joint angles θ_1, θ_2 are 7.5256^o and 2.7662^o, respectively.

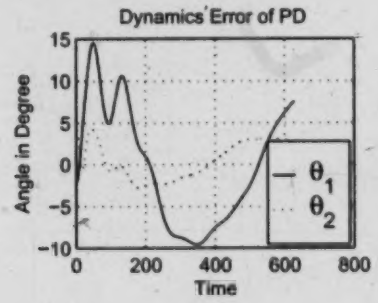

Figure 8.5: The Error Dynamics of Joint Angles Using a PD Controller

Then, computed controller with and without exact robot configuration model is used. The left panel of figure 8.6 shows the error dynamics of joint angles using computed torque controller with exact model. The steady state error of the joint angle θ_1, θ_2 are -0.1913^o and -0.3656^o, respectively. This result is better than that using a PD controller, but is not as good as the proposed model. Using a computed torque controller with model mismatch by multiplying a constant 0.4 to $M(\theta)$ matrix, the error dynamics of the joint angles is shown in the right panel of figure 8.6. The steady state error of joint angles θ_1, θ_2 are -0.4831^o and -0.9453^o, respectively.

Finally, an adaptive controller is used to control the robot to follow the trajectory shown the left panel of figure 8.7. The adaptive controller uses the compute torque control and takes advantage of the manipulator regressor of the robot dynamics. There is a model mismatch; the initial value of m_1 and m_2 are set as 0.8 and 0.4

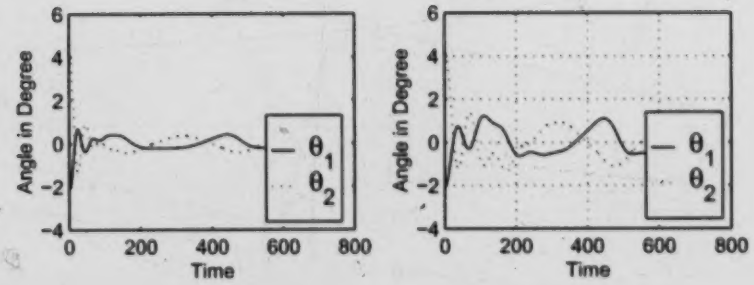

Figure 8.6: The Error Dynamics of Joint Angles Using a Computed Torque Controller with Exact Model (Left Panel) and Model Mismatch (Right Panel).

respectively. The true value of m_1 and m_2 are 2 and 1 respectively. The steady state error of the joint angles θ_1, θ_2 are -0.1036^o and -0.1363^o respectively. The results of the adaptive controller are better than the PD controller and computed torque model, and is as good as the proposed model.

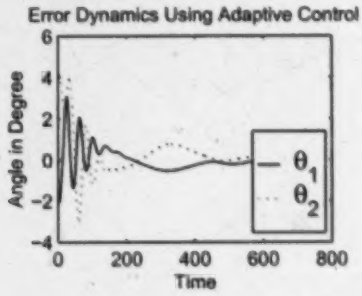

Figure 8.7: The Error Dynamics of Joint Angles Using an Adaptive Controller

8.4 Conclusion

The proposed neural network controller takes advantage of the manipulator regressor and the recursive error back propagation learning algorithm, it can dynamically control the robot to follow a desired trajectory. For only three steps of iteration, the error goes to less than $1.0e^{-6}$. In addition, the on-line learning process will guarantee that the tracking position and velocity errors will converge to zero although initially there may exists a model mismatch. The proposed models can be built into the micro controller of the Robotic Eye System, so that the system can adaptively control the artificial eye movement under the uncertainty of the model of the model of the artificial eye system.

Chapter 9

Conclusion and Future Work

In this chapter, the results obtained in this thesis will be summarized in the conclusion section. Then the future work related to our study will be outlined.

9.1 Conclusion

In this thesis, several aspects of the eye movement detection and motor control were investigated. The results obtained in Chapters 2, 3, 4, 5, 6, 7, 8 can be summarized as follows.

- An autonomous ocular motor system was developed and the simulation resulted are included. The fusion method is proposed for eye movement detection. First the eye movement is recorded and stored as sensed data space. Then during the experiment, the eye movement signal is obtained through the sensor array and through the matching rule and the eye position is obtained. The experimental system set up, fusion technologies, and preliminary results are included for the first generation model.

- A neural network based approach for sensor fusion was developed for the multiple sensor fusion. An artificial neural network can learn the characteristics of a non-linear, non-modeled system through training samples. Then during the real application, the sensor signal can be used to feed the network and obtain the desired output.

- Newly developed intelligent sensor and control system was developed. This was the second-generation model of the robotic eye project, which comprises biomedical electrodes and a micro controller. The system is intended to provide a rehabilitation ocular implant device that could be useful to some people with ocular implant. With the proposed device, the ocular implant can have the same natural movement as the normal eye. The basis for this system is the use of bioelectrical signals from the user's body. The authors are investigating the use of Electrooculogram. The system can acquire the dynamical eye orientation, which is sent to the micro controller to control the artificial eye to have the same orientation. Bioelectrical sensor, micro servomotor, and artificial eye modal were setup to investigate the eye movement detection and control methods. The pilot study has demonstrated its potential for clinical applications.

- A new approach that uses search algorithms to maximize system reliability and minimize the sensor cost was achieved. Compare with tabu search, genetic search, and simulated annealing, this new approach is very efficient and can guarantee the optimal solution. Numeric examples are included.

- Principal component analysis was used to monitor the sensor data and detect the sensor failure for the first generation sensor model. Incidence matrix was

used to isolate the fault sensor. LMS and minimum variance methods were used to recover the fault sensor data. Simulation studies were also included in the chapter.

- A new approach of using FIR Median Hybrid Filters for analysis of eye tracking movements was described. The program can filter out the eye blink artifact from the eye movement signal. Because the eye blink artifact is always corrupted in the EOG signal, it must be filtered out for the purpose of our project. The FIR Median Hybrid Filter was studied and its properties were explored with examples. Finally the filter was used to deal the real eye blink corrupted EOG signal. Examples were given of analysis procedure for eye tracking or a random moving target. The method proved to be highly reliable.

- Several techniques to control the robot manipulator under the uncertainty model and sensor failure were addresses. First a neural network was proposed to control the robot to follow the generated path. This network model was able to compensate the structured and unstructured dynamic uncertainties of the robot by using both on-line and off-line training. PD controller computed torque controller and adaptive controller with and without exact model were used to control the robot and compared with the proposed method. Second a residual generator for detection and isolation of the senor failure was designed. Assume one fault a time, the proposed method could detect and isolate the fault sensor. The simulation study based on a 2-d.o.f planar robot was included.

9.2 Future Work

The work presented in this thesis can only be considered preliminary, since many challenging and possibly more important problems have not been touched in this thesis. In this section, a number of problems will be proposed as the future directions.

- Circuit minimization is very important in the design of this robotic eye system. Because the whole system, the motor, the artificial eyeball and the micro controller will be integrated into the size of the eye pit volume, it is critical to find the tiny and powerful and energy efficient motor for the system. The controller not only should be small, but also shall be able to process the sensor signal and control the motor to drive the eyeball to move simultaneously with the real eye. The further directions in this project are search for the smaller motor, trying out smaller size controller and necessary component, and integrate them into a small size system.

- The energy is very important issue in the further design of the robotic eye system. The motor used to drive the eyeball will consume lots of power, so low power design technique [154, 187, 180, 178] has to be incorporated into the system. Search for high power, rechargeable and smaller size battery is an approach. In this case, the whole system should be very easily removable. There are many high technical rechargeable solutions [172, 158, 183, 177, 163, 160, 159, 179, 162, 185, 175, 176, 157, 181, 186, 169], such as infrared charge and microwave charge, which may be taken into consideration.

- Sensor is always the key to the success. Although the second generation

of the system can detect the eye movement and control the motor to drive the artificial eye to move accordingly, the robustness, the stability of the system needs to be further tested and improved. Further direction of the eye movement detection may be the residual signal of the injury eye socket, and other multisensor fusion techniques. Multiple sensor fusion technique can be used to prevent the sensor failure and recover the faulty data.

Bibliography

[1] Jianjun Gu; Max Meng; Garry Faulkner and Al Cook. Movement control system design for an artificial eye implant. In Proceedings of the IEEE International Conference on Systems, Man and Cybernetics, pages 3735–3740. IEEE, 1998.

[2] Jianjun Gu; Max Meng; Al Cook and Garry Faulkner. A novel sensing and control system of artificial eye-implant. In Proceedings of 14th World Congress of International Federation of Automatic Control (IFAC'99), pages 43–46. IEEE, 1999.

[3] Xie Xangdong Sudhakar Raghavan Zhuang Hanqi. Real-time eye feature tracking from a video image sequence using kalman filter. IEEE Transactions on Systems, Man and Cybernetics, 25(12):1568–1577, 1994.

[4] Laurence R. Young. Methods and designs:survey of eye movement recording methods. Behavior Research Methods and Instrumentation, 7(5):597–429, 1975.

[5] Laurence R. Young. looking around: 35 years of oculomotor modeling. Annals of Biomedical Engineering, 23:456–466, 1995.

[6] Carpenter R. H. S. Movements of the eyes. Behavior Research Methods and Instrumentation, 1977.

[7] D. A. Smith. Calibration and testing of an eye movement measurement system for use with cerebral palsied subjects. In Thesis, master of science in Biomedical Engineering. California State University, 1993.

[8] Tomlinson R.D.; Cheung R.; Blakeman A. Naso-occipital vestibulo-ocular reflex responses in normal subjects. IEEE Engineering in Medicine and Biology Magazine, 19(2):43–47, 2000.

[9] Yuan W.; Semmlow J.L.; Munoz P. The influence of prediction on vergence eye movements. In Proceedings of the IEEE 24th Annual Northeast Bioengineering Conference, volume 4, pages 56–57. IEEE, 1999.

[10] Sharkey P.M.; Murray D.W. Feasibility of using eye tracking to increase resolution for visual telepresence. In 1997 IEEE International Conference on Systems, Man, and Cybernetics, volume 2, pages 1078–1083. IEEE, 1997.

[11] Minho Lee; Sang-Woo Ban; Jun-Ki Cho; Chang-Jin Seo; Soon Ki Jung. Modeling of saccadic movements using neural networks. In International Joint Conference on Neural Networks, volume 4, pages 2386–2389. IEEE, 1999.

[12] Yoshimatsu H.; Yamada M. High dimensional chaos of miniature eye movements. In Proceedings of the Annual International Conference of the IEEE Engineering in Medicine and Biology Society, volume 13, pages 1513–1515. IEEE, 1991.

[13] Kiyoshi Hoshino. One dimensional stochastic models for spontaneous and burst blink. IEEE International Workshop on Robot and Human Communication, pages 229–231, 1996.

[14] Iwata Kazuaki; Moriwaki Toshimichi; Kawano Tsuneo; Mizoi Yasuhiko Fujiwara-Satoshi. Evaluation of eye movement in target tracking. Mem Fac Eng Kobe Univ, 1(26):31–40, 1980.

[15] Ebisawa-Yoshinobu; Minamitani-Haruyuki; Inagaki-Tatsuya; Ohmori-Masachika; Takase-Moriichiro. Stability of saccadic eye movements depending upon attention in tracking a moving target. In IEEE Engineering in Medicine and Biology Society Annual Conference, pages 707–709. IEEE, 1988.

[16] Horii Ken; Ishii Hideo; Tomoda Yasuyuki. Retinal image method to obtain limiting velocity of smooth pursuit eye movement. In Technol Rep Kansai Univ, pages 151–158. IEEE, 1987.

[17] Buizza A; Schmid R. Influence of smooth pursuit dynamics on eye tracking:a mathematical approach. Med Biol Eng Comput, 27(6):617–622, 1980.

[18] Shuichi Ojima and Sumio Yano. Evaluation of 2d and 3d images using eye movement, head movement and body sway. In Proceedings of SPIE The International Society for Optical Engineering, volume 2411, pages 262–270. IEEE, 1995.

[19] Chan F.H.Y.; Yong-Sheng Yang; Lam F.K.; Yuan-Ting Zhang; Parker P.A. Fuzzy emg classification for prosthesis control. IEEE Transactions on Rehabilitation Engineering, 8(3):305–311, 2000.

[20] Semyonov P.A. Microcomputer eog-system for ophthalmology. In Proceedings of the Twelfth Annual International Conference of the IEEE Engineering in Medicine and Biology Society, volume 1, page 918. IEEE, 1990.

[21] Semyonov P.A. Optimized unjoined linear approximation and its application for eog biosignal processing. In Proceedings of the Twelfth Annual International Conference of the IEEE Engineering in Medicine and Biology Society, volume 1, pages 779–780. IEEE, 1990.

[22] Jerrold M. Shapiro; J.E. Cantonnet; S.S. Heighinian. Eye position measurement from the surface recorded electroretinogram. In IEEE Eng in Med and Biol Soc Ann Conf, pages 40–44. IEEE, 1979.

[23] Semyonov P.A.; Kondakov S.A. Erg-biosignals modeling and adaptive pattern filtering. In Proceedings of the Annual International Conference of the IEEE Engineering in Medicine and Biology Society, volume 1, pages 371–372. IEEE, 1991.

[24] Lipoth L.L.; Hafez H.M.; Goubran R.A. Electroretinographical (erg) based classification of eye diseases. In Proceedings of the Annual International Conference of the IEEE Engineering in Medicine and Biology Society, volume 1, pages 1417–1418. IEEE, 1991.

[25] Semyonov P.A.; Protzak A.M.; Kondakov S.A.; Pervyshev V.I.; Rudneva M.A. Automatic erg-vep biosignals processing system for ophthalmology. In Proceedings of the Twelfth Annual International Conference of the IEEE Engineering in Medicine and Biology Society, volume 1, pages 881–882. IEEE, 1990.

[26] Monster A Willem; Chan Hing C; O' Connor David. Long term trends in human eye blink rate. Biotelem Patient Monit, 5(4):206–222, 1978.

[27] Gut R.; Moschytz G.S. High-precision emg signal decomposition using communication techniques. IEEE Transactions on Signal Processing, 48(9):2487–2494, 2000.

[28] Rahal M.; Winter J.; Taylor J.; Donaldson N. An improved configuration for the reduction of emg in electrode cuff recordings: a theoretical approach. IEEE Transactions on Biomedical Engineering, 47(9):1281–1284, 2000.

[29] Yuancheng Deng; Wolf W.; Schnell R.; Appel U. New aspects to event-synchronous cancellation of ecg interference: an application of the method in diaphragmatic emg signals. IEEE Transactions on Biomedical Engineering, 47(9):1177–1184, 2000.

[30] Martin Robert J; Harris Michael G. Instrumentation amplifier for the measurement of eye position. Midwest Symposium on Circuits and Systems, 1:17–19, 1984.

[31] J. Tichon; J.M. Toulotte; H. De Rop; G. Trehou; Y. Carnol; P. Lardinois. Eye position sensor used to command a bllissymbolic communicator. In Annual Conference of the IEEE Engineering in Medicine and Biology Society, volume 13, page 1706. IEEE, 1991.

[32] Ron Remmel. An electromegnetic eye movement monitor with one arc second resolution. In Annual Conference of the IEEE Engineering in Medicine and Biology Society, volume 13, pages 1696–1699. IEEE, 1991.

[33] Tetsutani Nobuji; Omura Katsuyuki; Kishino Fumio. Study on a stereoscopic display system employing eye position tracking for multi viewers. In Proceedings of SPIE The International Society for Optical Engineering, volume 2177, pages 135–142. IEEE, 1994.

[34] Podoleanu A.G.; Dobre G.M.; Webb D.J.; Jackson D.A. Fiberised set-up for retinal imaging of the living eye using low coherence interferometry. In IEE Colloquium on Biomedical Applications of Photonics, volume 12, pages 1 5. IEEE, 1997.

[35] Johnson D C; Drouin D M; Drake A D. Two dimensional fiber-optic eye position sensor for tracking and point-of-gaze measurements. In Bioengineering, Proceedings of the Northeast Conference, pages 12–14. IEEE, 1988.

[36] Allen Dean Drake David Michael Drouin. A two dimensional fiber optic eye position sensors. In Ninth Annual Conference of the Engineering in Medicine and Biology Society, pages 1829–1830. IEEE, 1987.

[37] Allen Dean Drake David Michael Drouin. A fiber optic eye position sensor. In Proceedings of the Northeast Conference, pages 181–184. IEEE, 1987.

[38] Robinson Richard M; Thomas Melvin L; Wetzel Paul A. Eye tracker development on the fiber optic helmet mounted display. In Proceedings of SPIE The International Society for Optical Engineering, volume 1116, pages 102–108. IEEE, 1989.

[39] Eadie A.S. Improved method of measuring eye movements using limbus reflection. Medical and Biological Engineering and Computing, 33(1):107–112, 1995.

[40] Reulen J. P. H.; Marcus J. T.; Koops D; de Vries F.R.; Tiesinga G.; Boshuizen K.; Bos J. E. Precise recording of eye movement: The iris technique part. Med Biol Eng Comput, 26(1):20–26, 1988.

[41] K. Matsuoka. Generalization of the differential measurement and its applications to an eye position sensor. In IMeko Symp. on measurement and estimation Bressanone, pages 102–108. IEEE, 1984.

[42] Yoshinobu Ebisawa and Ken ichi Suzu. Focal attentional level while tracking a smoothly moving target influences saccadic dynamics. Medical and Biological Engineering and Computing, pages 107–112, 1997.

[43] Terdiman Joseph; Sun Fuchuan; Stark Lawrence. Sampling or quantization in saccadic eye movement control. In Proc. 1988, IEEE Int Conf Syst Man Cybern, volume 1, pages 294–296. IEEE, 1988.

[44] Brandt Stephan A; Stark Lawrence W; Hacisalihzade Selim; Allen John; Tharp-Gregg. Experimental evidence for scanpath eye movements during visual imagery. In Proceedings of the Annual Conference on Engineering in Medicine and Biology, volume 11, pages 278–179. IEEE, 1989.

[45] Yamada M; Fukuda T; Hirota M. Development of an eye-movement analyser possessing functions for wireless transmission and autocalibration. Medical and Biological Engineering and Computing, 28(4):317–324, 1990.

[46] Razdan Rikki; Kielar Alan. Eye slaved pointing system for teleoperator control. In Proceedings of SPIE The International Society for Optical Engineering, volume 1388, pages 361–371. IEEE, 1991.

[47] Hanqi Zhuang Raghavan Sudhakar and Xangdong Xie. Automatic extraction of eye features from facial images. In Proceedings of the Annual Conference on Engineering in Medicine and Biology, volume 13, pages 1702–1703. IEEE, 1991.

[48] Denise C.R. Benel and Jr Donald Ottens. Use of an eye tracking system in the usability laboratory. In Proceedings of the Human Factors society 35 th annual meeting, pages 461–465. IEEE, 1991.

[49] J.D. Enderle L.S. Baczkowski and E.J. Engelken. Digitally calibrated eye movement measurement system. In Proceedings of the Human Factors society 35 th annual meeting, pages 161–165. IEEE, 1991.

[50] Myers Glenn A; Wiemann Bradley T; Carlson Stephen G. Measuring eye movements using the shape of the pupil. In Proceedings of the Annual Conference on Engineering in Medicine and Biology, volume 13, pages 1694–1695. IEEE, 1991.

[51] Sauter D; Martin B J; Di Renzo N; Vomscheid C. Analysis of eye tracking movements using innovations generated by a kalman filter. Medical and Biological Engineering and Computing, 29(1):63–69, 1991.

[52] K. J. Sung and D.J. Anderson. A video eye tracking system based on a statistical algorithm. In Midwest Symposium on Circuits and Systems, pages 438–441. IEEE, 1993.

[53] Andrew Gee and Roberto Cipolla. Estimating the gaze from a single view of a face. In Proceedings International Conference on Pattern Recognition, volume 1, pages 758–759. IEEE, 1994.

[54] Andrew Gee and Roberto Cipolla. Determining the gaze of faces in images. Image and Vision Computing, 12(10):758–759, 1994.

[55] Colombo C; Del Bimbo A; De Magistris S. Human computer interaction based on eye movement tracking. In Computer Architectures for Machine Perception, Proceedings (CAMP). 1995, pages 258–263. IEEE, 1995.

[56] Iwamoto Kazuyo; Tanie Kazuo. Binocular head mounted display with eye movement tracking function: -development of the prototype and its application. In IEEE International Conference on Intelligent Robots and Systems, volume 1, pages 354–359. IEEE, 1996.

[57] Hutchinson T.E. White K. P. and Carley J. M. Spatially dynamic calibration of an eye-tracking system. IEEE Transactions on system, Man, and Cybernetic, 23(4):1162–1168, 1993.

[58] Kyung S. Park and Kyung T. Lee. Eye controlled human/computer interface using the line of sight and the intentional blink. Computers of Industrial Engineering, 30(3):463–473, 1996.

[59] Funada M.F.; Ninomija S.P.; Suzuki S.; Idogawa K.; Yazu Y.; Ide H. On an image processing of eye blinking to monitor awakening levels of human beings. In Proceedings of the 19th Annual International Conference of the IEEE Engineering in Medicine and Biology Society, volume 3, pages 966–967. IEEE, 1997.

[60] Esaki S.; Ebisawa Y.; Sugioka A.; Konishi M. Quick menu selection using eye blink for eye-slaved nonverbal communicator with video-based eye-gaze detection. In Proceedings of the 19th Annual International Conference of the IEEE Engineering in Medicine and Biology Society, volume 5, pages 2322–2325. IEEE, 1997.

[61] Yano K.; Ishihara K.; Makikawa M.; Kusuoka H. Detection of eye blinking from video camera with dynamic roi fixation. In 1999 IEEE International Conference on Systems, Man, and Cybernetics, volume 6, pages 335–339. IEEE, 1999.

[62] Hussein Khorram Jose Sellek, Wunnava Subbarao. Non invasive bio sensing for the eye blinking and head movement. In Tenth Annual Conference of the IEEE Engineering in Medicine and Biology Society, volume 13, pages 801–802. IEEE, 1988.

[63] Stern John A;Skelly June J. Eye blink and workload considerations. In Proceedings of the Human Factors Society, volume 2, pages 942–944. IEEE, 1984.

[64] B. Piccoli; M. Braga; P. L. Zambelli and A. Bergamaschi. Viewing distance variation and related ophthalomogical changes in office activities with and without vdus. Ergonomics, 39(5):719–728, 1996.

[65] Vincent Victor J; Subbarao Wunnava. Software for an expert system for human fatigue analysis. In IEEE Engineering in Medicine and Biology Society Annual Conference, volume 13, pages 1402–1403. IEEE, 1988.

[66] Kazuhiko; Mizuno; Morimichi; Yamamoto Shin Nakano, Tomoaki; Sugiyama. Blink measurement by image processing and application to detection of driver's drowsiness. Terebijon Gakkaishi/Journal of the Institute of Television Engineers of Japan, 50(12):1949–1956, 1996.

[67] I. Tock, D; Craw. Tracking and measuring drivers' eyes. Image and Vision Computing, 14(8):541–547, 1996.

[68] Ogawa Kenji; Shimotani Mitsuo. Drowsiness detection system. Mitsubishi Electric Advance, 78:13–16, 1997.

[69] Sanjay Gupta and Harvinder Singh. Prepocessing eeg signals for direct human system interface. In IEEE International Joint Symposia on Intelligence and Systems, pages 32–37. IEEE, 1988.

[70] Varner J.L.; Rohrbaughz J.W.; Sirevaag E.J.; Packingham K.; Stern J.A. Time-frequency signal analysis applied to eeg signals associated with eye blinks. In Proceedings of the 19th Annual International Conference of the IEEE Engineering in Medicine and Biology Society, volume 3, pages 1013–1014. IEEE, 1997.

[71] Phillips G N; Bibles L D; Currie D E; Toepperwien C L. Pneumatic pressure switch for communication. Rehabilitation Engineering Society of North America, pages 265–267, 1985.

[72] Murphy Robert A; Basili Annamaria. Developing the user system interface for a communications system for als patients: the results. Designing for Diversity Proceedings of the Human Factors and Ergonomics Society, 2:1034, 1993.

[73] M.Takagi; K. Mohri; M. Katoh and S. Yoshino. Magnet displacement sensor using magneto inductive elements for sensing eyelid movement. IEEE Transaction Journal on Magnetics in Japan, 9(2):103–104, 1994.

[74] Matthias Bonacker Wolfgang Jaschinski and Edwald Alshuth. Accommodation, convergence, pupil diameter and eye blinks at a crt display flickering near fusion limit. Ergonomics, 39(1):152–164, 1996.

[75] O. Martin and L. Clodius. The history of the artificial eye. Annals of Plastic Surgery, 3(2):168–171, 1979.

[76] Ponnavaillo M.; Kumar V.P. The artificial eye. IEEE Potentials, 18(5):33–35, 2000.

[77] R.W. Dagnelie, G.; Massof. Toward an artificial eye. IEEE Spectrum, 33(5):20–29, 1996.

[78] Guy G. Massry and John B. Holds. Coralline hydroxyapatite spheres as secondary orbital implants in anophthalmos. Ophthalmology, pages 161–166, 1995.

[79] Carol L. Shields A. Sheilds and Patrick De Potter. Hydroxyapatite orbital implant after enucleation experience with 200 cases. In Mayo Clinic Proceedings, volume 68, pages 1191–1195. IEEE, 1993.

[80] LiaoHongfei Chen Qiangjuan, Yi Jinglin and Wan lageng. Clinical application of a new mobile integrated orbital implant. Chin J ophthalmol, 32(3):182–184, 1996.

[81] James H. Schwartz Eric R. Kandel and Thomas M. Jessell. The ocular motor system. In Essentials of Neural Science and Behavior, pages 660–677, 1995.

[82] Ren C. Luo and M. G. Kay. Multisensor integration and fusion in intelligent systems. IEEE Trans. on Systems, Man, and Cybernetics, 19(5):901–931, 1989.

[83] Ren C. Luo and Kuo L. Su. A review of high-level multisensor fusion: Approaches and applications. In Proc. of the IEEE Int. Conf. on Multisensor Fusion and Integration for Intelligent Systems, pages 25–31. IEEE, 1999.

[84] Jay K. Hackett and M. Shah. Multisensor fusion: A perspective. In Proc. of the Int. Conf. on Robotics and Automation, pages 1324–1330. IEEE, 1990.

[85] J. Gu; M. Meng and A. Cook. Motion control of robot manipulators under sensor failure. In Proc. of World Congress on Intelligent Control and Automation, pages 73–78. IEEE, 2000.

[86] G. Kamberova; R. Mandelbaum and M. Mintz. Statistical decision theory for mobile robotics: Theory and application. In Proc. of the 1996 IEEE/SICE/RSJ Int. Conf. on Multisensor Fusion and Integration for Intelligent Systems, pages 17–24. IEEE, 1996.

[87] G. Rajive Joshi and Arthur C. Sanderson. Multisensor fusion and unknown statistics. In Int. Conf. on Robotics and Automation, pages 2670–2677. IEEE, 1995.

[88] G. Chen. Application of neural networks in target tracking data fusion. IEEE Trans. on Aerospace and Electronic Systems, 30(1):281–287, 1994.

[89] S. G. Goodridge; M. G. Kay and Ren C. Luo. Multi-layered fuzzy behavior fusion for real-time reactive control of systems with multiple sensors. IEEE Trans. on Industrial Electronics, 43(3):387–394, 1996.

[90] J. Tu and S. Xu. Application of knowledge-based system in multisensor data fusion. In Proc. of the World Congress on Intelligent Control and Automation, pages 351–354. IEEE, 2000.

[91] J. Tan; N. Xi; and W. Kang. The role of sensing in motion stability of mobile robots. In Proc. of the 1999 IEEE Int. Conf. on Multisensor Fusion and Integration for Intelligent Systems, pages 62–66. IEEE, 1999.

[92] J. A. benediktsson; P. H. Swain and O. K. Ersoy. Neural network approaches versus statistical methods in classification of multisource remote sensing data. IEEE Trans. on Geoscience and Remote Sensing, 28(4):540–552, 1990.

[93] Jianjun Gu; Max Meng; Al Cook and Garry Faulkner. A study on natural movement of artificial eye implant. Robotics and Autonomous System, 32(2):153–161, 2000.

[94] Min Hsiung Ren C. Luo and Ralph S. Scherp. Multi-sensor based intelligent robot system. In IECON'86, pages 238–243. IEEE, 1986.

[95] Min Hsiung Lin Ren C. Luo and Ralph S. Scherp. Dynamic multi-sensor data fusion system for intelligent robotics. In Journal of the 1988 International Conference on Robotics and Automation, pages 386–396. IEEE, 1988.

[96] Ren C. Luo and Min Hsiung Lin. Robot multi-sensor fusion and integration: Optimum estimation of fused sensor data. In Proceedings of the 1988 International Conference on Robotics and Automation, pages 1076–1081. IEEE, 1988.

[97] Pinckers A. Cuypers MH. Aandekerk AL. The eog in best's disease and dominant cystoid macular dystrophy. Ophthalmic Genetics, 17(3):103–108, 1996.

[98] Prim Espada MP. De Diego Sastre JI. de Sarria Lucas MJ. Eog findings in patients with multiple sclerosis. Acta Otorrinolaringologica Espanola, 47(1):29–31, 1996.

[99] J. K. Choudhury R. Bhattacharya, T. K. Basak. Design and development of electro-oculograph. Journal of Instrument Engineering India Part EL, 70(5):166–168, 1989.

[100] Patmore David W and Knapp R Benjamin. Toward an eog-based eye tracker for computer control. In Annual ACM Conference on Assistive Technologies, pages 197–203. IEEE, 1998.

[101] Viveash Jacqueline P; Belyavin AJ; Bigmore D; Clarkson Geoffreyy J; Mccarthy GW; Rumbold DA; Stott JR. Determination of eye position in fast jet flight. In Proceedings of SPIE, the international society for optical Engineering, pages 120–125. IEEE, 1994.

[102] B.Y.S Rao H. F. Durrant-Whyte and H. Hu. Toward a fully decentralized architecture for multi-sensor. In Proceedings of the 1990 International Conference on Robotics and Automation, pages 1331–1336. IEEE, 1990.

[103] Toshiharu Mukai and Masatoshi Ishikawa. An active sensing method using estimated errors for multi sensor fusion systems. IEEE Transactions on Industrial Electronics, 43(3):380–385, 1996.

[104] Pierrick Grandjean. 3d modeling of indoor scenes by fusion of noisy range and stereo data. In Proceedings of the 1989 International Conference on Robotics and Automation, pages 681–687. IEEE, 1989.

[105] J. D. Tardos J. Neiral, J. Horn and G. Schmidt. Multi sensor mobile robot localization. In Proceedings of the 1997 International Conference on Robotics and Automation, pages 673–679. IEEE, 1997.

[106] S. Emura and S. Tachi. On design of sequential sensor fusion system. In Proceedings of the 1998 International Conference on Robotics and Automation, pages 3400–3406. IEEE, 1998.

[107] Billur Barshan Birsel Ayrulu and Simukai W. Utete. Target identification with multiple logical sonars using evendential reasoning and simple majority voting. In Proceedings of the 1997 International Conference on Robotics and Automation, pages 2063–2068. IEEE, 1997.

[108] Yoshihiko Nakamura and Yingti Xu. Geometrical fusion method for multi-sensor robotic systems. In Proceedings of the 1989 International Conference on Robotics and Automation, pages 668–673. IEEE, 1989.

[109] Sukhan Lee and Sookwang Ro. Uncertainty self management with perception net based geometric data fusion. In Proceedings of the 1997 International Conference on Robotics and Automation, pages 2075–2081. IEEE, 1997.

[110] Helen C. Shen Xiao-gang Wang and Wen han Qian. A hypothesis testing method for multi-sensory data fusion. In Proceedings of the 1998 International Conference on Robotics and Automation, pages 3407–3412. IEEE, 1998.

[111] P. Jenesfelt O. Wijk and H. I. Christensen. Triangulation based fusion of ultrasonic sensor data. In Proceedings of the 1998 International Conference on Robotics and Automation, pages 3419–3424. IEEE, 1998.

[112] John F. MacGregor James V. Kresta and Thomas E. Marlin. Multivariate statistical monitoring of process operating performance. The Canadian Journal of Chemical Engineering, 69:35–47, 1991.

[113] Eyle H. Ungar Richard D. De Veaux and Jonathon M. Vinson. Statistical approaches to fault analysis in multivariate process control. In Proceedings of the American Control Conference, pages 1274–1278. IEEE, 1994.

[114] Robert H. Storer Wenfu Ku. Disturbance detection and isolation by dynamic principle component analysis. Chemometrics and intelligent laboratory systems, 1:179–176, 1995.

[115] Ricardo Dunia S. Joe Qin Thomas F. Edgar and Thomas J. McAvoy. Identification of faulty sensors using principle component analysis. AICHE Journal, 42:2797–2812, 1996.

[116] Conny Wikstrom Christer Albano Lennart Eriksson and Hakan Friden. Multivariate process and quality monitoring applied to an electrolysis process. Chemometrics and intelligent laboratory systems, 42:221–231, 1998.

[117] J. E. Jackson and G. Mudholkar. Control procedures for residuals associated with principle component analysis. Technometrics, 21(1):341–349, 1979.

[118] J. Gertler and D. Singer. A new structural framework for parity equation-based failure detection and isolation. Automatica, 2(1):381–389, 1990.

[119] Janos Gertler. Survey of model based failure detection and isolation in complex plants. IEEE Control systems magazine, pages 3–11, 1988.

[120] Janos Gertler, Weihua Li, and T. McAvoy. Isolation enhanced principle component analysis. AIChE Journal, 45(1):323–334, 1999.

[121] J. Gertler and D. Singer. Augmented models for statistical fault isolation in complex systems. In Proceedings of the 1985 American Control Conference, pages 317–322. IEEE, 1985.

[122] J. Gu and M. Meng A. Cook M. G. Faulkner. Sensing and control system for ocular implant. In Proceedings of the 1999 IEEE Canadian Conference on Electrical and Computer Engineering, pages 1408–1412. IEEE, 1999.

[123] Jianjun Gu; Max Meng; Al Cook. The reliability of multiple sensor robot system. In 2000 international conference of the IEEE Industrial Electronics Society, volume 1, 2000.

[124] Julius T. Tou and Jens G. Balchen. Highly redundant sensing in robotic system. In Highly Redundant Sensing in Robotic System, volume 2, pages 1–60, 1994.

[125] R. R. Brooks and S. S. Iyengar. Maxmizing multi_sensor system dependability. In Proceedings of the 1996 IEEE/SICE/RSJ International Conference on Multi sensor Fusion and Integration for Intelligent Systems, volume 1, pages 1–8. IEEE, 1996.

[126] Brooks R.R.; Iyengar S.S.; Rai S. Minimizing cost of redundant sensor-systems with non-monotone and monotone search algorithms. In 1997 Proceedings, Annual Reliability annd Maintainability Symposium, volume 2, pages 307–313, 1997.

[127] F. Glover. Tabu thresholding: Improved search by nomonotonic techniques. ORSA Journal on Computing, 7(4):426–442, 1996.

[128] A.J. Gallego, R.A.; Romero R. Monticelli. Tabu search algorithm for network synthesis. IEEE Transactions on Power Systems, 2000.

[129] J.C. Bean. Genetic algorithms and random keys for sequencing and optimization. ORSA Journal on Computing, 6(2):154–160, 1994.

[130] Hughes E.J.; Leyland M. Using multiple genetic algorithms to generate radar point-scatterer models. IEEE Transactions on Evolutionary Computation, 4(2):147–163, 2000.

[131] P.J.M. Van; Laarhoven and E.H.L. Arts. Simulated annealing: Theory and applications. D. Reidel Publishing Corporation, 1987.

[132] ; Altiparmak F.; Dengiz B. Alabas C. The optimization of number of kanbans with genetic algorithms, simulated annealing and tabu search. In Proceedings of the 2000 Congress on Evolutionary Computation, volume 1, pages 580–585, 2000.

[133] Richard A. Johnson and Dean W. Wichern. Applied multivariate statistical analysis. In Applied Multivariate Statistical Analysis, volume 2, pages 122–160, 1988.

[134] Spiros Fotopoulos Jukka Neejarvi, Alpo Varri and Yrjo Neuvo. Weighted fmh filters. Signal Processing, 31:181–190, 1993.

[135] Tohru Yagi Yoshiki Uchikawa Yoshiaki Kuno. Development of a fish-eye vr system with human visual functioning and biological signals. In Proceedings of the 1996 IEEE/SICE/RSJ International Conference on Multisensor Fusion and Integration for Intelligent Systems, volume 1, pages 389–394. IEEE, 1996.

[136] Barschdorff D. and Gerhardt D. Rapid eye movement detection in infants using a neural network. In 18th Annual International Conference of the IEEE Engineering in Medicine and Biology Society, volume 1, pages 935–936. IEEE, 1996.

[137] N. Di Renzo D. Sauter, B.J. Martin and C. Vomscheid. Analysis of eye tracking movements using innovations generated by a kalman filter. Medical and biological Engineering and Computing, pages 63–69, 1991.

[138] Neal C. Gallagher and Gary L. Wise. A theatrical analysis of the properties of median filters. IEEE Transactions on Acoustics, Speech, and Signal Processing, ASSP-29(6):1134–1140, 1981.

[139] G.M. Hatzilabrou; N. Greenberg; R.J. Sclabassi; T. Carroll; R.D. Guthrie; and Mark S. Scher. A comparison of conventional and matched filtering techniques for rapid eye movement detection of the newborn. IEEE Transactions on Biomedical Engineering, 41(10):990–995, 1994.

[140] Richard A. Haddad and Thomas W. Parsons. Digital signal proceeding: Theory, applications, and hardware. In Computer Science Press. An imprint of W.H. Freeman and Company New York, 1991.

[141] Pekka Heinonen and Yrjo Neuvo. Median type filters with linear predictive substructures. In ICASSP: Proceedings/Sponsored by the Institute of Electrical and Electronics Engineers, Acoustics, pages 956–959. IEEE, 1987.

[142] Pekka Heinonen and Yrjo Neuvo. Fir-median hybrid filters with predictive fir substructures. IEEE Transactions on Acoustics, Speech, and Signal Processing, 36(6):892–899, 1988.

[143] Risto Wichman; Jaakko T. Astola; Pekka J. Heinonen and Yrjo A. Neuro. Fir median hybrid filters with excellent transient response in noisy conditions. IEEE Transactions on Acoustics, speech and Signal Processing, 38(12):892–899, 1990.

[144] Bing Zeng Hongbing Zhou and Yrjo Neuro. Weight fir median hybrid filters for image processing. In China 1991 International Conference on Circuits and Systems, volume 1, pages 793–796. IEEE, 1991.

[145] Alpo Varri; Kari Hirvonen; Veikko Hahhinen; Joel Hasan; Pekka Loula. Nonlinear eye movement detection method for drowsiness studies. International Journal of Bio-Medical Computing, 43:227–242, 1996.

[146] Jianjun Gu; Max Meng; Al Cook and Garry Faulkner. Analysis of eye tracking movements using fir median hybrid filters. In 2000 Eye Tracking Research and Applications Symposium, volume 1. IEEE, 2000.

[147] Jp Viveash; Aj Belyavin; Dj Bigmore; Gj Clarkson; Gw Mccarthy; Da Rumbold and Jrr Stott. Determination of eye position in fast jet flight. In SPIE, volume 2218, pages 78–81. IEEE, 1994.

[148] L. Jin and M. Gupta. Dynamic feedback control of unknown nonlinear systems using dynamic neural networks. In IEEE 1995 Intl. Conf. on Systems, Man and Cybernetics, pages 1261–1266. IEEE, 1995.

[149] A. R. S. R. K. S. and A. O. H. Adaptive neural network for identification and tracking control of a robotic manipulator. In IEEE 1995 Intl. Conf. on Systems, Man and Cybernetics, pages 601–609. IEEE, 1995.

[150] M. Meng. Application of an efficient neural network to identification and adaptive control of unknown robot dynamics. International Journal of Intelligent Control and Systems, 1(4):459–468, 1993.

[151] M. Meng. An enhanced computed-torque control scheme for robot manipulator with a neuro-compensator. In IEEE 1995 Intl. Conf. on Systems, Man and Cybernetics, pages 61–66. IEEE, 1995.

[152] K. N. and V. A. Efficient learning algorithms for neural networks. IEEE Transaction on System, Man and Cybernetics, 23(3):1372–1383, 1993.

[153] W. S. Lu and M. Meng. Regressor formulation of robot dynamics: computation and applications. IEEE Transaction on Robotics and Automation, pages 323–333, 1993.

[154] Mahapatra N.R.; Garimella S.V.; Takeen A. Efficient techniques based on gate triggering for designing static cmos ics with very low glitch power dissipation. In The 2000 IEEE International Symposium on Circuits and Systems, volume 28, pages 537–540. IEEE, 2000.

[155] LiXing Yuan Aiqun Wang, Nanning Zheng and Xiaodong Fu. Multiplicative inhibitory velocity detector (mivd) and multi_velocity motion detection neural network model. In Proceedings of the 1996 IEEE/SICE/RSJ International Conference on Multi sensor Fusion and Integration for Intelligent Systems, pages 476–483. IEEE, 1996.

[156] L. Y. Alfred. Eye movements and vision. Institute for Information transmission Academy of Science of the USSR, page 19, 1967.

[157] Ghahary A.; Cho B.H. Design of transcutaneous energy transmission system using a series resonant converter. IEEE Transactions on Power Electronics, 7(2):261–269, 1992.

[158] Gyu Bum Joun; Cho B.H. An energy transmission system for an artificial heart using leakage inductance compensation of transcutaneous transformer. IEEE Transactions on Power Electronics, 13(6):1013–1022, 1998.

[159] Joung G.B.; Cho B.H. An energy transmission system for an artificial heart using leakage inductance compensation of transcutaneous transformer. In 27th Annual IEEE Power Electronics Specialists Conference, volume 1, pages 898–904. IEEE, 1996.

[160] Kim C.G.; Cho B.H. Transcutaneous energy transmission with double tuned duty cycle control. In Proceedings of the 31st Intersociety Energy Conversion Engineering Conference, volume 1, pages 587–591. IEEE, 1996.

[161] Dukki Chung and Francis L. Merat. Neural network based sensor array signal processing. In Proceedings of the 1996 IEEE/SICE/RSJ International Conference on Multi sensor Fusion and Integration for Intelligent Systems, pages 757–764. IEEE, 1996.

[162] Matsuki H. Energy transfer system utilizing amorphous wires for implantable medical devices. IEEE Transactions on Magnetics, 31(2):1276–1282, 1995.

[163] Matsuki H.; Yamakata Y.; Chubachi N.; Nitta S.-I.; Hashimoto H. Transcutaneous dc-dc converter for totally implantable artificial heart using synchronous rectifier. IEEE Transactions on Magnetics, 32(5):5118–5120, 1996.

[164] Jay K. Hackett and Mubarak Shah. Multi-sensor fusion: A perspective. In Proceedings of the 1990 International Conference on Robotics & Automation, pages 1324–1330. IEEE, 1990.

[165] Kwon S.H.; Kim H.C. Eog-based glasses-type wireless mouse for the disabled. In Proceedings of the First Joint BMES/EMBS Conference, volume 1, page 592. IEEE, 1999.

[166] Al Cook Jianjun Gu, Max Meng and Garry Faulkner. Micro sensor based eye movement detection and neural network based sensor fusion and fault detection and recovery. In 2000 IEEE Canadian Conference on Electrical and Computer Engineering, pages 151–156. IEEE, 2000.

[167] Al Cook Jianjun Gu, Max Meng and Garry Faulkner. A study of the identification of the natural eye movement and the control of an ocular implant. In Third Asian Control Conference, pages 628–633. IEEE, 2000.

[168] Kuo-Chih Jung-Jae Chao and Lain-Wen Jang. Uncertain information fusion using belief measure and its application to signal classification. In Proceedings of the 1996 IEEE/SICE/RSJ International Conference on Multi sensor Fusion and Integration for Intelligent Systems, pages 151–157. IEEE, 1996.

[169] Inoue T.; Nishimura T.H.; Saito M.; Naka ka M. A transcutaneous energy transmission system for an artificial organ by using a novel resonant converter. In IEEE International Conference on Systems Engineering, volume 1, pages 294–297. IEEE, 1992.

[170] Harouna Kabre. On the active perception of speech by robots. In Proceedings of the 1996 IEEE/SICE/RSJ International Conference on Multi sensor Fusion and Integration for Intelligent Systems, pages 765–774. IEEE, 1996.

[171] Sukhan Lee. Sensor fusion and planning with perception-action network. In Proceedings of the 1996 IEEE/SICE/RSJ International Conference on Multi sensor Fusion and Integration for Intelligent Systems, pages 687–696. IEEE, 1996.

[172] Foo Chek Fok; Tseng King Jet; Zhao Lingyin. New structure transcutaneous transformer for totally implantable artificial heart system. Electronics Letters, 35(2):107–108, 1999.

[173] Thomas D. Garvey; Gohn D. Lowrance; and Martin A. Fischler. An inference technique for integrating knowledge from disparate sources. In Proceedings of the 7th International Joint Conference on Artificial Intelligence, pages 319–325. IEEE, 1981.

[174] Shih-Chung Chen; Tzu-Tung Tsai; Ching-Hsing Luo. Portable clinical eog instrument system. In Proceedings of the First Joint BMES/EMBS Conference, volume 2, page 858. IEEE, 1999.

[175] Nishimura T.H.; Eguchi T.; Hirachi K.; Maejima Y.; Kuwana K.; Saito M. A large air gap flat transformer for a transcutaneous energy transmission system. In 25th Annual IEEE Power Electronics Specialists Conference, volume 2, pages 1323–1329. IEEE, 1994.

[176] Nishimura T.H.; Hirachi K.; Maejima Y.; Kuwana K.; Saito M. Characteristics of a novel energy transmission for a rechargeable cardiac pacemaker by using a resonant dc-dc converter. In Proceedings of the IECON'93., International Conference on Industrial Electronics, Control, and Instrumentation, volume 2, pages 875–880. IEEE, 1993.

[177] S. Matsuki H.; Ofuji K.; Chubachi N.; Nitta. Signal transmission for implantable medical devices using figure-of-eight coils. IEEE Transactions on Magnetics, 32(5):5121–5123, 1996.

[178] Khellah M.M.; Elmasry M.I. Low voltage low power cmos design techniques for deep submicron ics. In 1999 IEEE International Solid-State Circuits Conference, volume 1, pages 286–287. IEEE, 1999.

[179] Matsuki H.; Yamakata Y.; Jinguji N.; Nitta S.; Hoshimiya N.; Chubachi N. Energy transferring system reducing temperature rise for implantable power consuming devices. In 18th Annual International Conference of the IEEE in Medicine and Biology Society, volume 1, pages 185–186. IEEE, 1997.

[180] Banna S.R.; Chan P.C.H.; Chan M.; Fung S.K.H.; Ko P.K. Fully depleted cmos/soi device design guidelines for low-power applications. IEEE Transactions on Electron Devices, 46(4):754–761, 2000.

[181] Geselowtiz D.B.; Hoang Q.T.N.; Gaumond R.P. The effects of metals on a transcutaneous energy transmission system. IEEE Transactions on Biomedical Engineering, 39(9):928–934, 1992.

[182] Tigges P.K.; Kathmann N.; Engel R.R. Semiautomated extraction of decision relevant features from a raw data based artificial neural network demonstrated by the problem of saccade detection in eog recordings of smooth pursuit eye movements. In Proceedings of the 1995 IEEE Neural Networks for Signal Processing, volume 3, pages 465–474. IEEE, 1995.

[183] S.; Masuzawa T.; Tatsumi E.; Taenaka Y.; Takano H. Shiba K.; Shu E.; Koshiji K.; Tsukahara K.; Tsuchimoto K.; Ohu-Mi, T.; Nakamura T.; Endo. Efficiency improvement and in vivo estimation of externally-coupled transcutaneous energy transmission system for a totally implantable artificial heart. In Proceedings of the 19th Annual International Conference of the IEEE in Medicine and Biology Society, volume 6, pages 2503–2505. IEEE, 1997.

[184] Shushtarian S.M. Early diagnosis of choloroquine toxicity on human visual system using electrooculogram (eog). In Proceedings of the 14th Conference of the Biomedical Engineering Society of India, volume 3, pages 103–104. IEEE, 1995.

[185] Matsuki H.; Matsuzaki T.; Satoh T. Simulations of temperature rise on transcutaneous energy transmission by non-contact energy transmitting coils. IEEE Transactions on Magnetics, 29(6):3334–3336, 1993.

[186] Matsuki H.; Shiiki M.; Murakami K.; Yamaoto T. Investigation of coil geometry for transcutaneous energy transmission for artificial heart. IEEE Transactions on Magnetics, 28(5):2406–2408, 1992.

[187] Liqiong Wei; Roy K.; De V.K. Low voltage low power cmos design techniques for deep submicron ics. In Thirteenth International Conference on VLSI Design, volume 28, pages 24–29. IEEE, 2000.

[188] Peter Wide and Dimiter Driankov. A fuzzy approach to multi-sensor data fusion for quality profile. In Proceedings of the 1996 IEEE/SICE/RSJ International Conference on Multi sensor Fusion and Integration for Intelligent Systems, pages 215–221. IEEE, 1996.

[189] Enrico Pagello Xiao-Gang Wang, Wen-Han Qian and Ren-Qing Pei. On the uncertainty and ignorance of statistical decision and evidence combination. In Proceedings of the 1996 IEEE/SICE/RSJ International Conference on Multi sensor Fusion and Integration for Intelligent Systems, pages 166–173. IEEE, 1996.

[190] Kuno Y.; Yagi T.; Uchikawa Y. Development of eye pointer with free head-motion [eog-based system]. In Proceedings of the 20th Annual International Conference of the IEEE Engineering in Medicine and Biology Society, volume 4, pages 1750–1752. IEEE, 1998.

[191] Yong-Jian Zheng and Bir Bhanu. Adaptive object detection from multi sensor data. In Proceedings of the 1996 IEEE/SICE/RSJ International Conference on Multi sensor Fusion and Integration for Intelligent Systems, pages 633–640. IEEE, 1996.

Appendix A

HREB A ___
HREB B ___

HEALTH RESEARCH ETHICS BOARD
REQUEST FOR ETHICS REVIEW

**NOTE: This form has been designed to be used by researchers in a wide variety of fields. Some questions may not be pertinent for this particular project. It is extremely important to read the information and follow the instructions found in the Guidelines for Researchers. Please refer to the guidelines for all the submission information.

Section A:
General information.

A1. Title of Project:
Design, sensing and control of an artificial eye-implant for natural eye movement

A2. Name of Principal Investigator: Jianjun Gu

Title(s): Ph. D. Candidate

Department / Program: Department of Electrical and Computer Engineering

Mailing address for ethics information: 238 Civil/Electrical Engineering Building

Telephone: (780) 492-4875 Fax: (780) 492-1811 E-Mail: Jason@nyquist.ee.ualberta.ca

Signature: _____ Date: _____

A3. Name of Co-Investigator: (Required for Students, Residents, Visiting Scholars, etc.)

Name: Dr. Cook

Title(s): Professor and Dean, Faculty of Rehabilitation Medicine
Department/Program: Faculty of Rehabilitation Medicine
Mailing address:

Al Cook
Faculty of Rehabilitation Medicine
University of Alberta
3-48 Corbett Hall
Edmonton, AB T6G 2G4

Telephone: (780) 492-5991 Fax: (780) 492-1626 E-Mail: Al.Cook@ualberta.ca

Signature: _____ Date: _____

Name: Dr. Max Meng

Title(s): Associate Professor and Director, Department of Electrical and Computer Engineering

Department/Program: Department of Electrical and Computer Engineering

Mailing address:

Department of Electrical and Computer Engineering
University of Alberta
Edmonton, Alberta
Canada T6G 2G7

Telephone: (780) 492-5917 Fax: (780) 492-1811 E-Mail: Max.Meng@Ualberta.Ca

Signature: _____ Date: _____

A4. Authorizing Signatures: (For U of A staff, must be signed by Department Chair or Associate Dean, Research. For CHA or Caritas staff, must be signed by administrative supervisor of Principal Investigator.)

I support the implementation of this project.

_____ _____
(Signature) (Date)

_____ _____
(Name: Please print) (Title)

A5. Co-Investigator(s) / Thesis Committee:

Name	Department / Program	Telephone
1. Dr. Al Cook	Faculty of Rehabilitation Medicine	492-5991
2. Dr. Max Meng	Dept. of Electrical and computer Eng.	492-5917

3. Dr. Tongwen Chen	Dept. of Electrical and computer Eng.	492-3940
4. Dr. Faulkner	Dept. of Mechanical Engineering	492-3446

A6. Expedited review:

If the study procedures are **limited** to any of the following, please check the appropriate box. (See guidelines page 7)

___ examination of patient or medical or institutional records
___ secondary analysis of data
___ use of biological specimens normally discarded
___ collection of blood and urine specimens
___ modification of previously approved protocol
*specify title and approval date:

A7. Which one of the following best describes the type of investigation proposed? Check more than one if appropriate.

___ clinical trial
___ multi-centre trial
_x_ pilot study
___ drug study
_x_ technology assessment / development
___ qualitative study
___ epidemiological study
___ sequel to previously approved project
___ first application in humans
___ other (specify):

A8. Where will the research be conducted? (Note that administrative approval is required to carry out research in any Capital Health or Caritas facility):

___ Capital Health Site (specify):

___ Caritas Site (specify):

_x_ U of A Site (specify): Department of Electrical Engineering, Room 557 ART lab

___ Other (specify):

Funding/Budget

A9. How is the proposal funded?

_x_ funding approved (specify source): the overall projects was funded from May 1997 to Sept. 1998. No current funding.

___ funding request pending (specify source):

___ no external funding required

A10. Are any of the investigators involved in this study receiving any direct personal remuneration or other personal or family financial benefits (either direct or indirect) for taking part in this investigations? (See guidelines, page 7)

___ yes If yes, append a letter detailing these activities to the Chair of the appropriate review committee.

_x_ no

Attach a budget summary. Note that the summary must include details of investigator payments and recruitment incentives (if present).

Additional Documentation

A11. If any of the following applies to this study, attach the appropriate letters of approval / support. (See Guidelines page 8)

Health Protection Branch or other Canadian federal agency approval:

_x_ Not applicable
___ Attached
___ Pending

Radiation Safety Committee Approval (required for all studies involving radioisotopes and non-routine X-rays):

_x_ Not applicable
___ Attached
___ Pending

Electromechanical or Biohazardous Materials Safety Approval:

___ Not applicable
___ Attached
_x_ Pending

Section B:
Details of Project
{Note that spaces have been minimized in this electronic version of the form. Use "cut and paste" to add information. Do **NOT** indicate that the board should "see attached".}

Description of the Project

B1. Provide a clear statement of purpose and objectives of the project.

The aim of this project is to let the anophthalmic patient have a natural movement of his artificial eye. The loss of an eye can be solved by the ocular implant. The artificial eye can be made like the real eye. But the problem is that it is static, and doesn't have the natural movement. Present study is to design a small automatic control system to let the artificial eye has the same natural movement as the real eye.

B2. State hypotheses and / or research questions.

1) How to detect the real eye movement?
2) How to use the real eye position signal to control the artificial eye movement?
3) How to design the miniaturized control system?

B3. Briefly summarize past human and/or animal research, which has led to this project.
(1 page maximum, 12-point font)

A person with one eye missing, through various reasons, may suffer severely psychologically as well as physically.

Figure. 1. The patient has his lost eye replaced

Patients with such defects may withdraw from society. The prosthesis has been created to replace the lost eye, as shown in figure 1. The prosthesis is an artificial eye, which appears natural. But it

is static. The purpose of this paper is to develop an ocular system to help this kind of patient, so that the real eye and the artificial eye can have the same natural movement.

The first step is to get the signal from the real eye. The artificial eye is mounted on a small servomotor. The control algorithm is to get the movement signal from the real eye and use it to control the artificial eye.

For eye movement sensing, the following methods are used: electrodes, magnetic induction, optical sensing, photoelectric methods and infrared oculography, and video Imaging.

There are many methods that don't measure the mechanical movement of the eyeball itself, rather they measure the induced potential, which cause the eye movement; These include the electro-oculography signal sensing, electroretinogram signal sensing, and electromyogram sensing, etc. The resolution of these methods is around 1 degree.

Fiber optic eye position sensing enables both horizontal and vertical eye positions to be determined with respect to a pair of eyeglass frames placed on a subject (Drouin and Drake, 1987).

The imaging lenses are mounted on a pair of eyeglass frames around the field of vision. This allows normal eye movement and unobstructed vision. The optical sensors detect light reflected from left and right of the iris and send this light through optical fibers to remote detectors. The instrument can achieve accuracy of better than half a degree in the horizontal direction and three degree in the vertical direction.

Nakano and others measured eye blink by image processing and application to detect the driver's drowsiness (Nakano, et al., 1996).

Tock and Craw described a computer vision system for tracking the eyes of a car driver in order to measure the eyelid separation (Tock and Craw, 1996).

Sanjay and Harvinder concentrated on real-time removal of eye-blink and eyeball movement artifacts from the forehead EEG recordings (Sanjay, et al., 1996).

Eadie used an improved limbus reflection method to measure eye movements (Eadie, 1995). Eadie used a new technique, which involved illuminating the limbus with infrared radiation and measuring the difference in the reflected radiation as the eye moved. Practical realizations employ a pair of emitter/detector systems directed at opposite sides of the eye and amplify the difference between the detected signals as the eye moves. The use of a pair of emitter/detectors has been shown to improve the linearity of the system. The methods above can detect the eye movement, but the system is large and complex, it can't be used in small system. The following methods from Japan researchers provide the idea to use the small device and get the signal from the real eye.

There were also some simple devices used infrared sensors to detect the eye blink, although the speed might be slow and the precision might be low, the device was simple and easy to use. From all the methods and systems and devices, a suitable method can be found to design a small eye movement detection and control system.

References

Drouin D. and A. Drake (1987) A two-dimensional fiber optic eye position sensors In: Ninth Annual Conference of the Engineering in Medicine and Biology Society. pp1829-1830

Eadie, A.S (1995). Improved method of measuring eye movements using limbus reflection In: Medical & Biological Engineering & Computing. Vol. 33, pp. 107-112

Nakano, T., K. Sugiyama, M. Mizuno, and S.Yamamoto (1996). Blink measurement by image processing and application to detection of driver's drowsiness In: Terebijon Gakkaishi Journal of the Institute of Television Engineers of Japan. Vol. 50, pp. 1949-1956

Sanjay G. and S. Singh (1996). Pre-processing EEG Signals for direct Human System Interface In: IEEE International Joint Symposia on Intelligence and Systems, PP. 32-37.

Takagi M., K. Mohri, M. Katoh and S. Yoshino (1994). Magnet displacement Sensor Using Magneto Inductive Elements for Sensing Eyelid Movement In: IEEE Transaction Journal on Magnetics in Japan, Vol. 9.

Tock, D. and I. Craw (1996). Tracking and measuring drivers' eyes In: Image and Vision Computing. Vol.14, pp. 541-547

Young, L. (1975). Methods and designs: Survey of eye movement recording methods In: *behavior Research Methods & Instrumentation.* Vol. 7(5) pp.397-429.

Description of Sample/Population.

B4. Describe the numbers and type(s) of subjects to be included. If appropriate, specify number of subjects in each study group. Provide a rationale for the sample size and include sample size calculations where appropriate.

This experimental study tries to find out that the subject without oculormotor disabilities can have their eye movement detected by the EOG and IR method, and the signal can be used to control the artificial eyeball movement. The number is temporarily set between 10 and 20. The subjects will have no known oculomotor disabilities. They will all be able to understand the tasks.

B5. List any subject inclusion/exclusion criteria.

The only criterion is that the subject should have at least one natural eye.

B6. Will subjects be recruited who are -

Under 18 years of age	[ ] yes	[x] no
Cognitively impaired	[ ] yes	[x] no
Residing in institutions (e.g. prison, extended care facility)	[ ] yes	[x] no
Students	[x] yes	[ ] no

Employees of researcher(s)' organization	[x] yes	[ ] no
In emergency or life-threatening situations	[ ] yes	[x] no
Have language barriers (eg. illiterate, not English-speaking, dysphasic)	[ ] yes	[x] no
In another country	[ ] yes	[x] no

Description of Research Procedures

B7. Provide a summary of the design and procedures of the research. Include details of any specific manipulations/interventions and measures: quantity, type and route of administration of drugs or radiation; operations; tests; use of devices that are prototypic or altered from those in clinical use; time commitment for subjects; method of data analysis.
(Maximum 2 pages using 12-point font. Append questionnaires, interview protocols, if applicable.)

- **Use EOG (Electrooculography) to detect the eye horizontal movement**

1) System set up

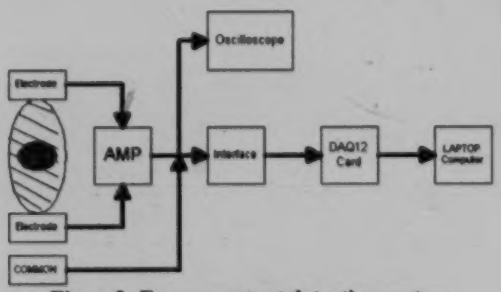

Figure2: Eye movement detection system

Above is the block diagram of the eye movement detection system.

2) Configuration of the electrode setup is shown in figure 3

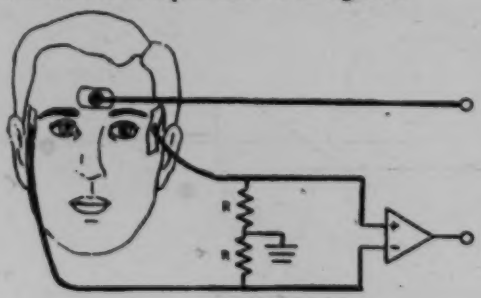

Figure 3: Electrode configuration

As shown in the figure3, two electrodes are placed on the skin to the outside of each eye. The reference electrode is placed on the lower forehead above the nose. The eye behaves like a dipole rotating through an inhomogeneous volume conductor (the head), the EOG being the d.c. signal that is measurable at the surface of the volume. The horizontally placed pair of electrodes will detect the signals with the angular deflection of the eye, which will be amplified and send to the computer through DAQ card.

3) Whole experimental system set up

The whole system is setup as shown in figure4. EOG signal is detected by the system and the signal is sent to the micro controller through the interface. The micro controller uses the natural eye position signal to control the artificial eye movement to the corresponding position.

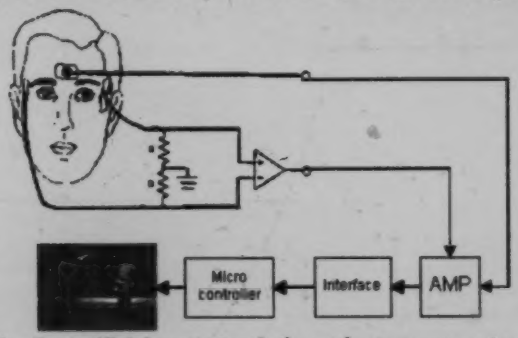

Figure 4: Use the artificial eye to track the real eye movement system set up

4) Protocol

1. Preparation

The subject is introduced to the present project, the apparatus being used, and the tasks to be completed.

2. Electrode application

Alcohol swab is used to clean the skin in the electrode locations. Fine sand paper is used to clear the skin and reduce surface offset potential. Silver/silver chloride disposable electrodes are then attached to the three locations around the head. Each electrode has electrode gel included, these are standard electrodes used clinically for electrical recording.

3. Testing

The testing protocol is a mainly tracking task. The subject is asked to focus on a specific target and then the signal is measured. The signal is filtered and fed to an A/D card for use by the micro controller.

5) Task

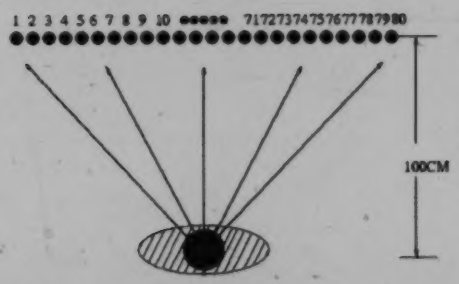

The subject is asked to stabilize his/her head. The subject he/she is asked to look to the left, right, and to the center. Then the subject is asked to move the eye horizontally. A calibration curve will be generated, and then the eye position signal will be used to move the artificial eyeball accordingly. The whole procedure will be recorded. Both eye position as measured by the target location and EOG signal will be recorded.

- **Use Infrared array to detect the eye horizontal movement**

1) The emitter and the detectors are mounted to the frame of the eyeglasses that subject will wear. The emitter sends out the infrared light to illuminate the eye. The reflected infrared light is detected by the detector array. As shown in figure 5, the detector array is fixed so the position of the detector is fixed. The reflected light will change according to the eye position. The reflected light signal is converted to a digital signal and transferred to the micro controller. Through sensor fusion algorithm, the eye position can be acquired
2)

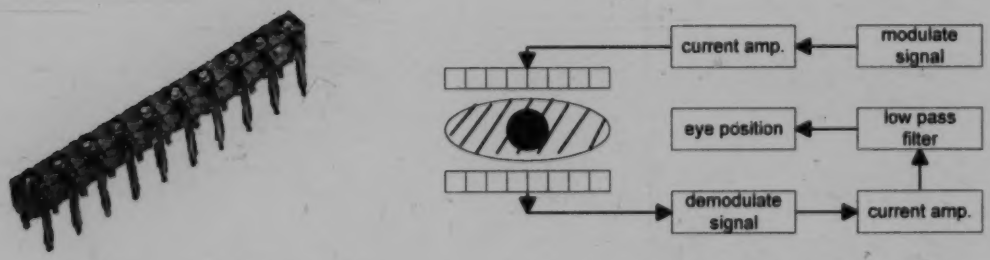

Fig. 5. Infrared emitter array (left panel) and eye position acquisition block diagram (right panel)

2) Protocol

Protocol is similar to EOG experiment. The subject wears the eyeglass with the infrared array instead of the electrodes.

B8. Which treatments or procedures are additional to those required for standard patient care?

Infrared measurement of eye position is not commonly used clinically, however, IR measurements are used in some other ophthalmology. EOG measurements of eye position are routinely used.

B9. If the procedures include a blind, under what conditions will the code be broken and what provisions have been made for this? Who will have the code?

NA

Obtaining Consent

B10. Clearly detail who will be recruiting subjects and obtaining consent, and the procedures for doing this. If appropriate, specify whether subjects will be randomly assigned to groups before or after consent has been attained.

Subjects will recruited at the U of A and Glenrose hospital. Recruitment will be via announcement at posted in electrical engineering and Glenrose hospital. U of A student volunteers will be recruited by contact with department directors.

B11. Attach a copy of consent form(s), information sheets and all recruitment notices, letters or advertisements. (See Appendix A of Guidelines. Use of standard Consent is highly recommended.)

B12. Specify methods for dealing with groups identified in #B6. If the subjects are not able/competent to give fully informed consent, who will consent on their behalf?

Potential subjects will not be contacted directly.

B13. What is the reading level of the Information Letter?
What is the reading level of the Consent Form?
Grade 7.
(For most populations, the target level is Grade 8. See Appendix A of Guidelines for information on calculating reading level. The Standard Consent Template is Grade 7.)
What steps have been taken to make the consent form and subject information documents comprehensible to the person giving consent? (Please include a statement on how the reading level was determined, i.e.: level was determined using Word Perfect 6.0)

B14. If subjects will be offered compensation for participating in the research, provide details.

Specify the amount, what the compensation is for, and how payment will be determined for subjects who do not complete the study.

Only volunteers will be recruited.

B15. Do any of the procedures include the use of deception or partial disclosure of information to subjects?

[ ] yes — Provide rationale for deception or partial disclosure. Describe the procedures for (a) debriefing the subjects and (b) giving them a second opportunity to consent to participate after debriefing.

[x] no

Risks and Benefits

B16. What are the benefits of the proposed research for the subject and / or for scientific knowledge in general?

The subjects who have two normal eyes will not receive any benefits. Patients who lost one of their eyes will receive great benefit from this automatic control device designed to provide more natural appearance prosthesis.

B17. What adverse effects may result from the research? (Include risks, discomfort, incapacity, psychological risks, and any reported side effects of procedure or drug.) How will adverse effects be dealt with?

There is no possibility of electrical shock, since we will use battery power.
For the IR eye measurement, there are four level of risks pecified by William A. Hyman, Gerald E. Miller, and Joseph S. Neigut [1]. These are:

Class	power
1	<0.1mw
2	>class 1 but <= 1mw
3	> class 2 but <=5mw
4	> class 3 but <=0.5w
5	>0.5w

The emission level for this experiment is calculated as follows:

Emitter energy = E_e = 0.5 mw/cm^2 (from the manufactured specification sheet)
Sensitivity area = A_s=0.17 mm^2 . (from the manufactured specification sheet)
Therefore the total energy efficient with the area is

$E_{total} = 0.5\ mw * 0.17 * 10^{-4} = 8.5 * 10^{-5}\ mw.$
Which is below the lowest level of risk specified by William A. Hyman, Gerald E. Miller, and Joseph S. Neigut.

References

[1] William A. Hyman, Gerald E. Miller, and Joseph S. Neigut. (1992) Laser diode for head pointing and environmental control In: RESNA international'92. pp377-379

Privacy and Confidentiality

B18. What steps will be taken to respect privacy of subjects and protect confidential data?
The principal investigator or faculty supervisor will retain all data for a period of seven years after the project is complete.

B19. Identify any agencies or individuals who will have access to confidential data now or in the future.

B20. Do you anticipate secondary analysis of these data? (Note that secondary analysis requires further research ethics approval.)

___ Yes
_x_ No

CONSENT FORM

Part 1:

Title of Project: Design, sensing and control of an artificial eye-implant for natural eye movement

Principal Investigator(s): Jianjun Gu phone number(s): (780) 492-4875

Part 2:

During this experiment, three electrodes will be put on the three locations of the head. The subject is required to keep his/her head steady and move his/her eye according to the instruction of the principal investigator. To prevent electrical shock, we are using battery power.

We have calculated the infrared levels to be safe.

Do you understand that you have been asked to be in a research study?	Yes	No
Have you read and received a copy of the attached Information Sheet?	Yes	No
Do you understand the benefits and risks involved in taking part in this research study?	Yes	No
Have you had an opportunity to ask questions and discuss this study?	Yes	No
Do you understand that you are free to refuse to participate or withdraw from the study at any time? You do not have to give a reason and it will not affect your care. *(Use wording appropriate to your subject group)*	Yes	No
Has the issue of confidentiality been explained to you? Do you understand who will have access to your records?	Yes	No
Do you want the investigator(s) to inform your family doctor that you are participating in this research study? If so, please provide your doctor's name: _____ *(N.B. This question is optional).*	Yes	No

This study was explained to me by: _____

I agree to take part in this study.

_____	_____	_____
Signature of Research Participant	Date	Witness
_____		_____
Printed Name		Printed Name

I believe that the person signing this form understands what is involved in the study and voluntarily agrees to participate.

_____	_____
Signature of Investigator or Designee	Date

Information Sheet

Title of Project:

Design, sensing and control of an artificial eye-implant for natural eye movement

Name of Principal Investigator:

Name: Jianjun Gu
Title(s): Ph. D. Candidate
Department / Program: Department of Electrical and Computer Engineering
Mailing address for ethics information: 238 Civil/Electrical Engineering Building
Telephone: (780) 492-4875 Fax: (780) 492-1811 E-Mail: Jason@nyquist.ee.ualberta.ca

Name of Co-Investigators

Name: Dr. Cook
Title(s): Professor and Dean, Faculty of Rehabilitation Medicine
Department/Program: Faculty of Rehabilitation Medicine
Mailing address:

Al Cook
Faculty of Rehabilitation Medicine
University of Alberta
3-48 Corbett Hall
Edmonton, AB T6G 2G4

Telephone: (780) 492-5991 Fax: (780) 492-1626 E-Mail: Al.Cook@ualberta.ca

Name: Dr. Max Meng
Title(s): Associate Professor and Director, Electrical and Computer Engineering
Department/Program: Department of Electrical and Computer Engineering
Mailing address:

Department of Electrical and Computer Engineering
University of Alberta
Edmonton, Alberta
Canada T6G 2G7

Telephone: (780) 492-5917 Fax: (780) 492-1811 E-Mail: Max.Meng@Ualberta.Ca

Statement of purpose and objectives of the project.

The aim of this project is to let the anophthalmic patient have a natural movement of his artificial eye. The loss of an eye can be solved by the ocular implant. The artificial eye can be made like the real eye. But the problem is that it is static, and doesn't have the natural movement. Present study is to design a small automatic control system to let the artificial eye has the same natural movement as the real eye.

Risk of the experiment.

During this experiment, three electrodes will be put on the three locations of the head. The subject is required to keep his/her head steady and move his/her eye according to the instruction of the principal investigator. To prevent electrical shock, we are using battery power.
We have calculated the infrared levels to be safe.

Privacy of subjects and protect confidential data

The principal investigator or faculty supervisor will retain all data for a period of seven years after the project is complete. The name of the subject, private information of the subject and the data of the subject will not be released without the permission of the subject.
The subject can withdraw from the experiment anytime without any reason, and stop to be a volunteer.

Protocol

1. Preparation

The subject is introduced to the present project, the apparatus being used, and the tasks to be completed.

2. Electrode application

Alcohol swab is used to clean the skin in the electrode locations. Fine sand paper is used to clear the skin and reduce surface offset potential. Silver/silver chloride disposable electrodes are then attached to the three locations around the head. Each electrode has electrode gel included, these are standard electrodes used clinically for electrical recording.

3. Testing

The testing protocol is a mainly tracking task. The subject is asked to focus on a specific target and then the signal is measured. The signal is filtered and fed to an A/D card for use by the micro controller.

4. Task

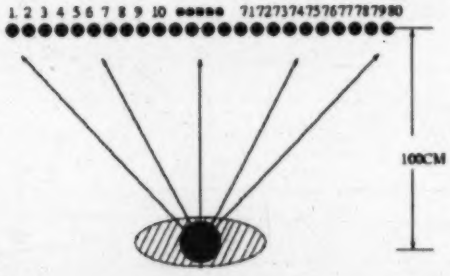

The subject is asked to stabilize his/her head. The subject he/she is asked to look to the left, right, and to the center. Then the subject is asked to move the eye horizontally. A calibration curve will be generated, and then the eye position signal will be used to move the artificial eyeball accordingly. The whole procedure will be recorded. Both eye position as measured by the target location and EOG signal will be recorded.

5 The emitter and the detectors are mounted to the frame of the eyeglasses that subject will wear. The emitter sends out the infrared light to illuminate the eye. The reflected infrared light is detected by the detector array. The detector array is fixed so the position of the detector is fixed. The reflected light will change according to the eye position. The reflected light signal is converted to a digital signal and transferred to the micro controller. Through sensor fusion algorithm, the eye position can be acquired

Protocol is similar to EOG experiment. The subject wears the eyeglass with the infrared array instead of the electrodes.

Volunteer Wanted

In

Electrical and Computer Engineering

Title of Project:

Design, sensing and control of an artificial eye-implant for natural eye movement

Statement of purpose and objectives of the project.

The aim of this project is to let the anophthalmic patient have a natural movement of his artificial eye. The loss of an eye can be solved by the ocular implant. The artificial eye can be made like the real eye. But the problem is that it is static, and doesn't have the natural movement. Present study is to design a small automatic control system to let the artificial eye has the same natural movement as the real eye.

Risk of the experiment.

During this experiment, three electrodes will be put on the three locations of the head. The subject is required to keep his/her head steady and move his/her eye according to the instruction of the principal investigator. To prevent electrical shock, we are using battery power.
We have calculated the infrared levels to be safe.

Contact information:

Name: Dr. Max Meng
Telephone: (780) 492-5917 Fax: (780) 492-1811 E-Mail: Max.Meng@Ualberta.Ca
Name: Dr. Cook
Telephone: (780) 492-5991 Fax: (780) 492-1626 E-Mail: Al.Cook@ualberta.ca
Name: Jianjun Gu
Telephone: (780) 492-4875 Fax: (780) 492-1811 E-Mail: Jason@nyquist.ee.ualberta.ca

Volunteer Wanted

In

Glenrose Rehabilitation hospital

Title of Project:

Design, sensing and control of an artificial eye-implant for natural eye movement

Statement of purpose and objectives of the project.

The aim of this project is to let the anophthalmic patient have a natural movement of his artificial eye. The loss of an eye can be solved by the ocular implant. The artificial eye can be made like the real eye. But the problem is that it is static, and doesn't have the natural movement. Present study is to design a small automatic control system to let the artificial eye has the same natural movement as the real eye.

Risk of the experiment.

During this experiment, three electrodes will be put on the three locations of the head. The subject is required to keep his/her head steady and move his/her eye according to the instruction of the principal investigator. To prevent electrical shock, we are using battery power.
We have calculated the infrared levels to be safe.

Contact information:

Name: Dr. Max Meng
Telephone: (780) 492-5917 Fax: (780) 492-1811 E-Mail: Max.Meng@Ualberta.Ca
Name: Dr. Cook
Telephone: (780) 492-5991 Fax: (780) 492-1626 E-Mail: Al.Cook@ualberta.ca
Name: Jianjun Gu
Telephone: (780) 492-4875 Fax: (780) 492-1811 E-Mail: Jason@nyquist.ee.ualberta.ca